EVALUATION OF ANTIDIABETIC ACTIVITY OF THE WATER AND ETHYL ACETATE FRACTIONS FROM *WITHANIA COAGULANS* FRUITS AND THE MECHANISM UNDERLYING THEIR HYPOGLYCEMIC EFFECTS

Siriporn Riyajan

A Thesis Submitted in Partial Fulfillment of the Requirements for the Degree of Doctor of Philosophy in Biomedical Sciences

Suranaree University of Technology

Academic Year 2018

การประเมินฤทธิ์ต้านเบาหวานของสารสกัดชั้นน้ำและชั้นเอทธิลอะซีเตท ที่สกัดจากผล *Withania coagulans* และกลไกการออกฤทธิ์ในการลดระดับน้ำตาลในเลือด

นางสาวศิริพร ริยะจันทร์

วิทยานิพนธ์นี้เป็นส่วนหนึ่งของการศึกษาตามหลักสูตรปริญญาวิทยาศาสตรดุษฎีบัณฑิต
สาขาวิชาชีวเวชศาสตร์
มหาวิทยาลัยเทคโนโลยีสุรนารี
ปีการศึกษา 2561

EVALUATION OF ANTIDIABETIC ACTIVITY OF THE WATER AND ETHYL ACETATE FRACTIONS FROM *WITHANIA COAGULANS* FRUITS AND THE MECHANISM UNDERLYING THEIR HYPOGLYCEMIC EFFECTS

Suranaree University of Technology has approved this thesis submitted in partial fulfillment of the requirements for the Degree of Doctor of Philosophy.

Thesis Examining Committee

Rungrudee Srisawat
(Asst. Prof. Dr. Rungrudee Srisawat)
Chairperson

(Assoc. Prof. Dr. Nuannoi Chudapongse)
Member (Thesis Advisor)

(Asst. Prof. Dr. Naruwan Saowakon)
Member

Jarinyaporn Naowaboot
(Asst. Prof. Dr. Jarinyaporn Naowaboot)
Member

Oratai Weeranantanapan
(Dr. Oratai Weeranantanapan)
Member

(Assoc. Prof. Capt. Dr. Kontorn Chamniprasart)
Vice Rector for Academic Affair and Internationalization

(Assoc. Prof. Dr. Worawat Meevasana)
Dean of Institute of Science

ศิริพร ริยะจันทร์ : การประเมินฤทธิ์ต้านเบาหวานของสารสกัดชั้นน้ำและชั้นเอทธิลอะซีเตทที่สกัดจากผล *Withania coagulans* และกลไกการออกฤทธิ์ในการลดระดับน้ำตาลในเลือด (EVALUATION OF ANTIDIABETIC ACTIVITY OF THE WATER AND ETHYL ACETATE FRACTIONS FROM *WITHANIA COAGULANS* FRUITS AND THE MECHANISM UNDERLYING THEIR HYPOGLYCEMIC EFFECTS). อาจารย์ที่ปรึกษา : รองศาสตราจารย์ ดร.นวลน้อย จูฑะพงษ์, 117 หน้า.

Withania coagulans เป็นยาแผนโบราณของประเทศอินเดีย ถูกนำมาใช้ในทางการแพทย์อายุรเวชพื้นเมืองเพื่อรักษาโรคเบาหวาน มีการศึกษารายงานฤทธิ์ต้านเบาหวานในหลอดทดลองและในสัตว์ทดลองของสารสกัดหยาบซึ่งมีสารประกอบจำนวนมากจากพืช *W. coagulans* อย่างไรก็ตามกลไกการออกฤทธิ์ต้านเบาหวานของพืชชนิดนี้มีการศึกษาและตรวจสอบเฉพาะกลไกการยับยั้งการทำงานของเอนไซม์แอลฟากลูโคซิเดสเท่านั้น ในการศึกษานี้จึงใช้สารสกัดชั้นเอทธิลอะซีเตทและชั้นน้ำที่สกัดจากผลของพืช *W. coagulans* มาทำการทดสอบเพื่อลดจำนวนชนิดของสารประกอบที่อาจจะเป็นสารออกฤทธิ์ของพืชลง โดยได้ทำการตรวจสอบองค์ประกอบทางเคมี ความเป็นพิษ ฤทธิ์ต้านโรคเบาหวานและสารประกอบในสารสกัดที่สามารถดูดซึมได้ ผลจาก HPLC-MS แสดงให้เห็นว่าสารสกัดชั้นเอทธิลอะซีเตทมีจำนวนชนิดของสารที่เป็นองค์ประกอบทางเคมีมากกว่าสารสกัดชั้นน้ำ จากโครมาโตแกรมของ HPLC พบว่าสารสกัดทั้งสองมีแท่งกราฟที่มีมวลเท่ากัน คือ ที่ 471 และ 453 โดยมีความเป็นไปได้ที่อาจจะเป็นสาร 17β-Hydroxywithanolide K หรือ Withanolide F สำหรับมวล 471 และ Coagulin C สำหรับมวลที่ 453 ผลการทดสอบความเป็นพิษในเซลล์แสดงให้เห็นว่าสารสกัดชั้นน้ำมีความเป็นพิษต่อเซลล์ HepG-2 น้อยกว่า แต่อย่างไรก็ตามเมื่อทำการศึกษาความเป็นพิษของสารสกัดชั้นเอทธิลอะซีเตทและชั้นน้ำในหนูปกติ แสดงให้เห็นว่าสารสกัดทั้งสองที่ความเข้มข้น 50 มิลลิกรัมต่อกิโลกรัมน้ำหนักตัวไม่ได้ก่อให้เกิดความเป็นพิษใด ๆ โดยเฉพาะอย่างยิ่งความเป็นพิษต่อ ตับ ไต และตับอ่อน ฤทธิ์ที่ทำให้น้ำตาลในเลือดลดลงของหนูปกติถูกตรวจสอบโดยการทดสอบความทนทานต่อน้ำตาลกลูโคส (OGTT) ผลการทดลองพบว่าสารสกัดชั้นน้ำเพิ่มความทนทานต่อน้ำตาลกลูโคสอย่างมีนัยสำคัญทางสถิติ ($P<0.05$) จากผลศึกษาในหนูเบาหวานที่ถูกชักนำโดย alloxan พบว่าสารสกัดชั้นเอทธิลอะซีเตทลดน้ำตาลในเลือดได้เฉพาะวันที่ 5 ของการให้ยา แต่ไม่ลดลงในวันที่ 10 ขณะที่ระดับน้ำตาลในเลือดของหนูเบาหวานที่ได้รับสารสกัดชั้นน้ำมีการลดลงของระดับน้ำตาลในเลือดอย่างต่อเนื่องอย่างมีนัยสำคัญจนกระทั่งวันที่ 10 ของการทดลอง ผลการทดสอบฤทธิ์ยับยั้งการทำงานของเอนไซม์แอลฟากลูโคซิเดสพบว่ามีฤทธิ์เฉพาะในสารสกัดชั้นเอทธิลอะซีเตท ขณะที่ฤทธิ์กระตุ้นการหลั่งอินซูลินและฤทธิ์ยับยั้งการ

ดูดซึมกลูโคสถูกพบในสารสกัดทั้งสองชนิด จากผลการทดสอบการดูดซึมสารผ่านลำไส้โดยใช้ Caco-2 monolayer model และฤทธิ์การกระตุ้นการหลั่งอินซูลินชี้แนะว่า C1-C3 ที่มีมวล 471 และ 453 น่าจะเป็นสารออกฤทธิ์ที่ไปกระตุ้นการหลั่งอินซูลินเนื่องจากสารจะไปถึงบีต้าเซลล์ของตับอ่อนที่เป็นตำแหน่งที่ออกฤทธิ์จำเป็นจะต้องถูกดูดซึมจากทางเดินอาหารก่อน ในลำดับสุดท้าย จากผลการทดลองด้านความเป็นพิษและประสิทธิภาพในการป้องกันโรคเบาหวาน สารสกัดชั้นน้ำจึงถูกเลือกเพื่อนำมาพัฒนาระบบนำส่งยา เมื่อเปรียบเทียบตัวนำส่งยาที่ประกอบด้วยอนุภาคนาโนไคโตซานบรรจุสารสกัดชั้นน้ำ (Chnp+WF) อนุภาคนาโนไคโตซานที่บรรจุสารสกัดชั้นน้ำและเคลือบด้วยแป้งที่ย่อยง่าย (Chnp+SS+WF) และอนุภาคนาโนไคโตซานที่บรรจุสารสกัดชั้นน้ำและเคลือบด้วยแป้งที่ทนต่อการย่อย (Chnp+RS+WF) พบว่า Chnp+SS+WF เป็นระบบการนำส่งยาที่ดีที่สุด เนื่องจากสามารถเพิ่มระยะเวลาในการออกฤทธิ์ต้านโรคเบาหวานของสารสกัดชั้นน้ำในสัตว์ทดลองได้ ดังนั้นตัวพาขนาดนาโนที่ผลิตขึ้นนี้น่าจะสามารถนำไปใช้ในการห่อหุ้มสารสกัดจากพืชเพื่อใช้เป็นระบบนำส่งยาได้

สาขาวิชาปรีคลินิก ลายมือชื่อนักศึกษา ศิริพร วิยะดันตา

ปีการศึกษา 2561 ลายมือชื่ออาจารย์ที่ปรึกษา

SIRIPORN RIYAJAN : EVALUATION OF ANTIDIABETIC ACTIVITY OF THE WATER AND ETHYL ACETATE FRACTIONS FROM *WITHANIA COAGULANS* FRUITS AND THE MECHANISM UNDERLYING THEIR HYPOGLYCEMIC EFFECTS. THESIS ADVISOR : ASSOC. PROF. NUANNOI CHUDAPONGSE, Ph.D. 117 PP.

WITHANIA COAGULANS/ TOXICITY/ ANTIDIABETES/ α-GLUCOSIDASE/ INSULIN SECRETION/ GLUCOSE ABSORPTION/ INTESTINAL ABSORPTION/ CHITOSAN NANOPARTICLES.

Withania coagulans is a traditional medicine of India. It has been used in Ayurvedic and indigenous medicine to treat diabetic mellitus. *In vitro* and *in vivo* activities of crude extracts from *W. coagulans*, which contain many compounds have been reported. However, investigation of mechanism underlying its antidiabetic action was performed only in α-glucosidase inhibition. In this study, ethyl acetate and water fractions of *W. coagulans* fruits were used to narrow down the possible active ingredients of this plant. Evaluation of chemical composition, toxicity, antidiabetic action and absorbed compounds of the extracts were conducted in this study. The results from HPLC-MS showed more chemical components in EAF than in WF. HPLC chromatograms revealed that both fractions contained the same peaks at m/z 471 and 453, which could be 17β-Hydroxywithanolide K or Withanolide F for m/z 471 and Coagulin C for m/z at 453. The results from the cytotoxicity tests demonstrated that WF produced less toxic effect to HepG-2 cells. However, the toxicity studies of EAF and WF, which were evaluated in normal mice indicated that both fractions did not

induce any signs of toxicity especially to liver, kidney and pancreas at dose 50 mg/kg. The hypoglycemic activity was studied by oral glucose tolerant test (OGTT) in normal mice. It was found that WF significantly improved glucose tolerance similar to glibenclamide ($P<0.05$). From antidiabetic study in alloxan-induced diabetic mice, EAF showed a significant decrease in blood glucose level at day 5, but not at day 10. While, blood glucose level of diabetic mice treated with WF continuously declined and significantly decreased until day 10. The α-glucosidase inhibitory effect was presented only in EAF, while insulin secretion and inhibitory glucose absorption activities were shown in both of fractions. The results from intestinal absorption in Caco-2 monolayer model and insulin secretion experiment suggested that C1-C3 detected at m/z 471 and 453 may be responsible for insulin secretion activity because a chemical must be absorbed through gastrointestinal tract before reaching pancreatic β-cells, the site of action. Finally, based on the toxicity and antidiabetic efficiency, the WF was selected as a choice model for developing drug delivery system. Among chitosan nanoparticles loaded with water fraction (Chnp+WF), chitosan nanoparticles loaded with water fraction coated with soluble starch (Chnp+SS+WF) and chitosan nanoparticles loaded with water fraction coated with resistant starch (Chnp+RS+WF), the *in vivo* results indicated that (Chnp+RS+WF) was the best drug delivery system, as it extended duration of the antidiabetic effect of WF. Therefore, this synthesized nanocarriers may be used for encapsulate a plant extract as drug delivery system.

School of Preclinic Student's Signature Siriporn Riyajan

Academic Year 2018 Advisor' Signature

ACKNOWLEDGEMENTS

This thesis has been completed with the support and assistance from many people. I would like to express my sincere thanks to all the people who have directly or indirectly encouraged and helped me.

Firstly, I would like to thank my thesis advisor Assoc. Prof. Dr. Nuannoi Chudapongse who gave good advice and guidance to my thesis since the beginning until completion. Secondly, I would like to thank Dr. Oratai Weeranantanapan who gave good advice, especially on the parts of cell culture. Thirdly, I would like to thank my friends and my family for their encouragement. Finally, I would like to thank the Science Achievement Scholarship of Thailand (SAST) for the financial support.

Siriporn Riyajan

CONTENTS

Page

CONTENTS (Continued)

Page

CONTENTS (Continued)

Page

CONTENTS (Continued)

Page

CONTENTS (Continued)

Page

LIST OF TABLES

Table **Page**

LIST OF TABLES (Continued)

Table **Page**

LIST OF FIGURES

Figure **Page**

LIST OF FIGURES (Continued)

Figure **Page**

LIST OF ABBREVIATIONS

µg/ml	=	Microgram per milliliter
µg	=	Microgram
µl	=	Microliter
^{o}C	=	Degree Celsius
ALT	=	Alanine aminotransferase
AST	=	Aspartate aminotransferase
ATCC	=	The American Type Culture Collection
AUC	=	Area under the curve
BUN	=	Blood urea nitrogen
cm	=	Centimeter
DDP IV	=	Dipeptidyl peptidase IV
DI	=	Distilled water
DM	=	Diabetes mellitus
DPPH	=	2,2-diphenyl-l-picrylhydrazyl
DMEM	=	Dulbecco’s modified eagle’s medium
EAF	=	Ethyl acetate fraction
FBS	=	Fetal bovine serum
g/ml	=	Gram per milliliter
GLP-1	=	Glucagon-like peptide-1
Gli	=	Glibenclamide

LIST OF ABBREVIATIONS (Continued)

GLUT2	=	Glucose transporter 2
h	=	Hour
HepG2	=	Human hepatocarcinoma cell
HDL	=	High-density lipoprotein
IC_{50}	=	Inhibitory concentration at 50%
M	=	Molar
mg/dL	=	Milligram per deciliter
mg/kg	=	Milligram per kilogram
mg/ml	=	Milligram per milliliter
min	=	Minute
ml	=	Milliliter
mM	=	Millimolar
LDL	=	Low-density lipoprotein
MTT	=	3-(4,5-Dimethylthiazol-2-yl)-2,5-diphenyltetrazolium bromide
nm	=	Nanometer
OD	=	Optical density
OGTT	=	Oral glucose tolerance test
PBS	=	Phosphate buffer saline
PGO	=	Peroxidase-glucose oxidase
PNP-G	=	*p*-Nitrophenyl-α-D-glucopyranoside

LIST OF ABBREVIATIONS (Continued)

SEM	=	Standard error of mean
TDZ	=	Thiazolidinedione
U	=	Unit
UV	=	Ultraviolet
WF	=	Water fraction

CHAPTER I

INTRODUCTION

1.1 Rationale

Diabetes mellitus is a chronic metabolic disorder characterized by hyperglycemia resulting from reduction of insulin secretion and/or insulin resistance. This disease can be classified into 2 major types including Type 1 diabetes mellitus (T1DM) and Type 2 diabetes mellitus (T2DM). T1DM is caused by autoimmune beta-cell destruction. The damage of beta cells makes insulin production decrease. The prevalence of T1DM is about 5-10% of diabetic patients. In contrast, T2DM is caused by the reduction of insulin secretion and/or insulin resistance. The prevalence of T2DM is about 90-95% of all diabetic patients (American Diabetes Association, 2011; Bastaki, 2005). The prevalence of this disease for all age groups has been predicted to be double in 2020 (Shaw, Sicree, and Zimmet, 2010) and it is responsible for 5% of all deaths of the global population in each year (Joshi and Shrestha, 2010). Therefore, diabetes mellitus is a current major public health problem worldwide.

The patients with diabetes mellitus mostly die from various complications for example cardiovascular diseases, hypertension and nephropathy (American Diabetes Association, 2012; Schlienger, 2013). These complications can develop whenever normal blood glucose levels cannot be controlled for a long time. Currently, drugs are used primarily to prevent the complications, save life, alleviate symptoms and increase longevity (Bastaki, 2005). Many of hyperglycemia drugs have been

developed and used, such as insulin, insulin secretagogues, dipeptidyl peptidase IV (DPP IV) inhibitors, glucagon-like peptide-1 (GLP-1), insulin sensitizers, α-glucosidase inhibitors and sodium-glucose co-transporter-2 (SGLT-2) drugs (Bastaki, 2005; Chaudhury et al., 2017). However, these synthetic drugs show some serious side effects such as hypoglycemia, kidney complication, diarrhea, liver complication and urinary tract infection (Bastaki, 2005). The natural products from plants are searched as alternative medicines for the treatment of many diseases including diabetes mellitus (Gurjeet and Gloria, 2010; Wang et al., 2010) because they have been accepted to cause fewer side effects than synthetic chemicals (Blasa, Gennari, Angelino, and Ninfali, 2010; Wang et al., 2010). Moreover, they are not expensive and ease of availability in most areas (Gaddipati et al., 2004; Gautam et al., 2009; Thakur, Chauhan, Bhargava, and Dixit, 2009; Ven, Ranjekar, Ramassamy, and Deshpande, 2010).

Withania coagulans is an herb that belongs to the family Solanaceae. This plant is distributed in the Mediterranean region, Northern Africa and the Southwest of Asia. *W. coagulans* is known in several different names such as Vegetable Rennet, Indian Rennet, Indian-Cheese-Maker and Paneer. *W. coagulans* has been used in the traditional Indian system of medicine, called Ayurveda, for the treatment of diabetes mellitus (Gupta, 2012; Mishra, Dash, Mishra, and Gupta, 2013). Moreover, the plant extracts have been reported to possess many other pharmacological effects such as anticancer (Ahmad, Fatima, Srivastava, and Khan, 2017; Machin, Veleiro, Nicotra, Oberti, and Padron, 2010), antihyperlipidemia (Datta et al., 2013; Hemalatha, Wahi, Singh, and Chansouria, 2006), immunosuppressant (Huanga et al., 2009), wound healing (Prasad, Kumar, Patel, and Hemalatha, 2010), hepatoprotective (Budhiraja,

Garg, Sudhir, and Arora, 1986) and free radical scavenging (Hemalatha, Wahi, Singh, and Chansouria, 2004).

The antidiabetic property of the aqueous and alcoholic extracts of *W. coagulans* is reported in several *in vivo* models including normal rat, streptozotocin-induced, alloxan-induced and poloxamer-induced diabetic rats. It has been proposed that the antidiabetic activity of the extract is probably caused by its antioxidant activity and α-glucosidase activity (Agrawal et al., 2016; Hemalatha et al., 2004). However, the disadvantage of these previous studies was that the crude extracts which contained many compounds were used, therefore very high concentrations of the extracts up to 1 g/kg were needed to produce hypoglycemic effects in animals. Moreover, only α-glucosidase inhibitory activity (Agrawal et al., 2016) has been reported. It is worth to find more possible mechanism of actions which are account for the antidiabetic effect of *W. coagulans*.

In the present study, instead of crude extract, antidiabetic effects between the ethyl acetate and water fractions of *W. coagulans* fruits were investigated in alloxan-induced diabetes mice. Both *in vitro* and *in vivo* toxicities were investigated. Mechanism of actions underlying the antidiabetic activity, such as α-glucosidase inhibition, stimulation of insulin secretion and inhibitory effect on glucose absorption were elucidated. Moreover, to identify a possible active ingredient responsible for this antidiabetic activity, chemical compositions of each extract before and after passing through the Caco-2 cell monolayer were compared by HPLC-MS. At last, the water extract of *W. coagulans* fruits which appeared more effective and less toxic effect was suggest to use for developing a nanocarriers to improve its oral bioavailability.

Polysaccharide-coated nanoparticles loaded with the water fraction was designed and tested for antihyperglycemic activity *in vivo*.

The results obtained from this study will provide a safety profile and scientific rationale for the use of *W. coagulans* as an alternative medicine in the treatment of diabetic patients. The *in vitro* absorption data provide a useful information in term of an attempt to seek a new antidiabetic drug derived from this plant. Moreover, nanocarriers encapsulated with *W. coagulans* fruit extract was successfully developed and shown that it efficiently prolonged the antidiabetic action *in vivo*.

1.2 Research objectives

1. To determine the *in vitro* and *in vivo* toxicities of water and ethyl acetate fractions.
2. To examine antihyperglycemic action of the water and ethyl acetate fractions in alloxan-induced diabetic mice.
3. To investigate mechanism of action underlying the antidiabetic activity of the fractions on α-glucosidase activity, insulin secretion and glucose absorption.
4. To compare chemical compositions of the fractions before and after intestinal absorption in Caco-2 monolayer model.
5. To examine antihyperglycemic action of water fraction-loaded olysaccharide-coated nanoparticles in alloxan-induced diabetic mice.

1.3 Research hypothesis

The water and ethyl acetate fractions of *W. coagulans* fruits exhibit a different degree of activity. The water extract is more effective and less toxic than the ethyl

acetate fraction due to the different compositions. Both extracts produce α-glucosidase inhibitory activity, stimulate insulin secretion and enhance glucose absorption. The water extract-encapsulated nanocarriers reduce fasting blood glucose in tested animals with a sustained duration of action.

1.4 Scope and limitation of study

Both different extracts from of *W. coagulans* fruits containing several compounds were used in this study. The actual active ingredients which were responsible for antidiabetic action could not be definitely identified in this study.

CHAPTER II

LITERATURE REVIEW

2.1 *Withania coagulans*

Withania coagulans commonly known as Indian Cheese Maker, Vegetable Rennet and Paneer. It belongs to the family Solanaceae and it is distributed in the Mediterranean region and extends to Northern Africa and the Southwest of Asia such as Punjab, Gujarat, India, Iran, Pakistan and Afghanistan (Gupta, 2012; Mishra et al., 2013).

The feature of plant, flower and fruits of *W. coagulans* were shown in Figure 2.1. The leaves are lanceolate, entire, clothed with a persistent greyish tomentum on both sides. The flowers are dioecious and the flowering period is January to April. The berry is 6-8 cm in diameter, globose, smooth and sepals covers the fruit. The seeds are 2.5-3 mm in diameter, rounded and yellowish brown (Mishra et al., 2013).

W. coagulans is a traditional medicine of India. It is an important medicinal plant that has been used in Ayurvedic and indigenous medicine for more than 3,000 years (Gupta, 2012; Mishra et al., 2013). Many parts of *W. coagulans* were used in the prevention and treatment of various diseases. The berries are used as a blood purifier (Mishra et al., 2013). Fruits of *W. coagulans* are reported to be sedative, emetic, alterative, diuretic, dyspepsia, flatulent, liver complaints, asthma, biliousness, antihyperlipidemic (Datta et al., 2013; Hemalatha et al., 2006), immunosuppressive

(Huanga et al., 2009), wound healing (Prasad et al., 2010), hepatoprotective (Budhiraja et al., 1986), free radical scavenging (Hemalatha et al., 2004) and antidiabetic effects (Datta et al., 2013; Hemalatha et al., 2004; Jaiswal, Rai, and Watal, 2010; Shukla, Dikshit, Shukla, and Gambhir, 2012; Yasir, Shrivastava, Jain, and Das, 2012). Flowers of the plant were used in the treatment of diabetes (Bharti et al., 2012).

Figure 2.1 *Withania coagulans* growing in the field. (a) *Withania coagulans* plant, (b) *Withania coagulans* flowers and (c) *Withania coagulans* fruits (Ahmad et al., 2017; Gupta, 2012).

2.1.1 Phytoconstituents of *W. coagulans*

The phytochemicals present in plants are reported to be responsible for preventing disease and promoting health as show in Table 2.1. For *W. coagulans,* the phytochemical screening in many parts of this plant has been reported extensively. The seeds of plant shown consisted of free sugars and fatty oil. Carbohydrates, saponin, flavonoids, glycoside, steroids and oil are presented in both of methanolic and hydro alcoholic extracts of *W. coagulans* fruits (Mathur, Agrawal, and Shrivastava, 2013; Shendkar, Chaudhari, and Shendkar, 2014). In the part of *W. coagulans* berries, esterases, fatty oil, amino acids and alkaloids are presented as the main compounds (Mishra et al., 2013). Moreover, withanolide have been isolated from the whole plant of *W. coagulans*. The structure has been elucidated and studies by spectroscopic techniques. The biological activities of isolated compounds from *W. coagulans* are summarized in Table 2.2.

2.1.2 Antihyperglycemic effect of *W. coagulans*

Among many beneficial health effects, the antidiabetic property of *W. coagulans* is most significantly and extensively reported as shown in Table 2.3. Early studies of *W. coagulans* on streptozotocin induced diabetic rats have proven the ability of the both aqueous and alcoholic extracts to induce hypoglycemia in at dosages as high as 1g/kg and 750 mg/kg body weight of the rats, respectively (Hemalatha et al., 2004; Jaiswal et al., 2010). In the study conducted by Datta and colleagues (Datta et al., 2013), the hypoglycemic and hypolipidemic effects of the hydro-alcoholic extract of the fruits of *W. coagulans* were tested on rats in comparison to standard drugs–glipizide and atorvastatin, commonly used in the treatment of the above diseases. It was concluded from this study that the extract acts synergistically with the drug and could help lower

the doses of the drugs significantly. Also the histopathological evaluation of the pancreas of the streptozotocin-induced rats, showed a significant difference in the recovery of the beta cells of the untreated and *W. coagulans* extract treated animals (Datta et al., 2013). Loss of peripheral insulin sensitivity and hepatic insulin sensitivity are the most commonly observed forms of insulin resistance in type II diabetes. In the study conducted by Bharti and co-workers (Bharti et al., 2012) on Poloxamer-induced type 2 diabetic rats, it was shown that the aqueous extract of *W. coagulans* fruits could normalize hyperglycemia in rats. Another study has shown that the combined aqueous and organic extracts of *W. coagulans* fruits have higher antihyperglycemic effect on diabetic rats than those treated with metformin (Hoda et al., 2010). In an attempt to reduce the dosage of the extract significantly, Maurya et al. extracted a specific withanolide called coagulanolide from the plant *W.coagulans* and tested the antihyperglycemic and antihyperlipidemic properties of the isolated compound in doses comparable to standard drugs metformin and fenofibrate on streptozotocin-induced diabetic rats. Coagulanolide was found to be better than metformin at the same dosage (Maurya, Singh, and Srivastava, 2008). Although, the antidiabetic property of *W.coagulans* have been reported but the mechanism of action of antidiabetic activity of *W. coagulans* has been reported only α-glucosidase inhibitory and aldose reductase inhibitor activities (Agrawal et al., 2016) and probably by its antioxidant activities (Hemalatha et al., 2004).

Table 2.1 Biological functions of bioactive compounds (Maurya, Akanksha, and Jayendra, 2010; Saxena, Jyoti, Rajeev, Dharmendra, and Abhishek, 2013).

Phytoconstituents	Biological activity
Alkaloids	Antimicrobial, Antifungal
Phenolic	Antioxidant, Antimicrobial, Anti-inflammatory, Antihyperlipidemic
Flavonoids	Antioxidants, Antimicrobial, Cytotoxicity, Anti-inflammatory, Antitumor
Tannins	Antidiarrhoea, Anti-tumor, Anti-inflammatory, Antioxidant
Saponins	Antimicrobial, Antifungal, Antiviral, Anticarcinogenic, Hypoglycaemic
Withanolides	Antihyperglycaemic, Antimicrobial, Immunosuppressive, Antitumour, Heppatoprotective, Anti-inflammatory

2.2 Diabetes mellitus and antidiabetic drugs

2.2.1 Pancreas

Pancreas (Figure 2.2) is not only exocrine gland but also endocrine gland. Enzymes excreted from the exocrine glands of pancreas play a major role in the digestion of food. Pancreatic juice consists of water, salts, bicarbonate, amylase, trypsin and lipase. The secretion of pancreatic juice is controlled by secretin and cholecystokinin (CCK) hormones which are produced by enteroendocrine cells in duodenum and released by the presence of acidic chime, protein and fat. In the case of endocrine glands, islets of Langerhans of pancreas consists of alpha, beta, delta and pancreatic polypeptide cells. Alpha cells produce hormone glucagon, whereas beta cells produce hormone insulin. These hormones have roles in regulating blood glucose levels

and glucose metabolism (the detail of these hormones show in the topic of hormones control blood glucose levels). Delta cells secrete hormone somatostatin, which decreases and inhibits the secretion of glucagon and insulin hormones. Pancreatic polypeptide cells produce hormone pancreatic polypeptides, which inhibits production of pancreatic enzymes and alkaline secretions (Longnecker, 2014).

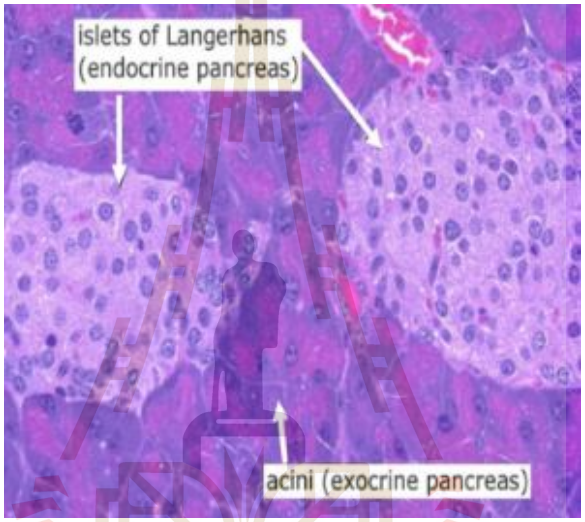

Figure 2.2 The histology of pancreas. The arrows indicate endocrine (islets of Langerhans) and exocrine regions (Longnecker, 2014).

Table 2.2 Isolated compounds from *W. coagulans* and the reported biological activities (Maurya et al., 2010).

No.	**Name of compound**	**Plant part**	**Activity**
1	Coagulin	Whole plant	
2	14,15β-Epoxywithanolide I	Whole plant	
3	17β-Hydroxywithanolide K	Whole plant & fruits	Antihyperglycaemic, Antimicrobial
4	Coagulin B	Whole plant	
5	Coagulin C	Whole plant & fruits	Antihyperglycaemic
6	Coagulin D	Whole plant	
7	Coagulin E	Whole plant	
8	Coagulin F	Whole plant	
9	Coagulin G	Whole plant	
10	Coagulin H	Whole plant	Immunosuppressive
11	Coagulin I	Whole plant	
12	Coagulin J	Whole plant	
13	Coagulin K	Whole plant	
14	Coagulin L	Whole plant & fruits	Antihyperglycaemic
15	Coagulin M	Whole plant	
16	Coagulin N	Whole plant	
17	Coagulin O	Whole plant	
18	Coagulin P	Whole plant	
19	Coagulin Q	Whole plant	
20	Coagulin R	Whole plant	
21	20β-Hydroxy-l-oxo-(22R)-with a-2,5,2,4-trienolide	Whole plant	
22	Withacogulin	Whole plant	

Table 2.2 Isolated compounds from *W. coagulans* and the reported biological activities (Continued).

No.	Name of compound	Plant part	Activity
23	17β-Hydroxy-l-4α,20α-epoxy-l-oxo-(22R)-with a-3,5,2,4-trienolide	Whole plant	
24	Coagulin S	Whole plant	
25	Bispicropodophyllin glucoside	Whole plant	
26	3β-14α,17β,20α_F-Tetrahydroxy-l-oxo-20S,22R-with a-5,24-dienolide	Fruits	Hepatoprotective, Anti-inflammatory, Blood pressure Lowering, Central nervous system depressant
27	Ergosta-5,25-diene-3β,24-diol	Fruits	
28	3β-hydroxy-2,3-dihydrowithanolide H	Fruits	
29	Sitosterol-β-D-glucoside	Fruits	
30	Coagulanolide	Fruits	Antihyperglycemic
31	Withanolide F	Fruits	Antihyperglycemic
32	Withaferin A	Root	Antimicrobial, Immunomodulating, Antitumour, Cytotoxic
33	5,27-Dihydroxy-6α,7α-epoxy-l-oxo-(5α)-with a-2,24-dienolide	Root	
34	Withacoagin	Root	
35	(20R,22R),6α,7α-Epoxy-5α-20-hydroxy-l-oxowitha-2,24-dienolide	Root	
36	(20R,22R),6α,7α-Epoxy-5α-hydroxy-l-oxowitha-2,24-dienolide	Root	Immunosuppressant

Table 2.3 The antihyperglycemic activity of *W. coagulans*.

Pharmacological activity	**Type of the extract**	**Model**	**Dose**	**References**
• Free radical scavenging activity • Antidiabetic activity • Hypoglycemic activity	• Aqueous extract of fruit	• DPPH assay • Streptozotocin-induced diabetic rat • Normal rat	• 2 mg/ml • 1 g/kg	Hemalatha et al. (2004)
• Antidiabetic activity • Antihyperlipiddermic activity	• Isolated compound (Withnolide)	• Streptozotocin induced diabetic rats • C57BL/KsJ-db/db mice	• 100 mg/kg • 50 mg/kg	Maurya et al. (2008)
• Antidiabetic activity	• Room temperature aqueous extract of fruit	• Normal rat • Streptozotocin-induced diabetic rat	• 500-1,250 mg/kg • 1 g/kg	Jaiswal, Rai, and Watal. (2009)
• Hypoglycemic activity • Antidiabetic activity	• Hot ethanol extract of fruit	• Normal rat • Streptozotocin-induced diabetic rats	• 500, 750, 1,000 mg/kg • 750 mg/kg	Jaiswal et al. (2010)
• Antidiabetic activity	• Aqueous extract of flower	• Poloxamer-407-induced diabetic rat	• 150-200 mg/kg	Bharti et al. (2012)

Table 2.3 The antihyperglycemic activity of *W. coagulans* (Continued).

Pharmacological activity	**Type of the extract**	**Model**	**Dose**	**References**
• Antidiabetic activity	• Aqueous extract of fruit	• Nicotinamide/streptozotocin-induced diabetic rat	• 125-500 mg/kg	Shukla et al. (2012)
• Antidiabetic activity	• Hydroalcoholic extract (50% methanol) • Hot water extract • Cold water extract	• Normal rat • Alloxan-induced diabetic rat	• 400 mg/kg	Yasir et al. (2012)
• Antidiabetic activity • Antihyperlipiddermic activity	• Hydroalcoholic extract of fruit	• Streptozotocin induced diabetic rats • Cholesterol-rich diet induced hyperlipidemic rat	• 1 g/kg	Datta et al. (2013)
• α-Glucosidase inhibitory activity • Aldose reductase inhibitory activity • Antidiabetic activity	• Aqueous extract of fruit • Ethanolic extract of fruit	• α-glucosidase inhibitor assay • Aldose reductase inhibitory assay • Streptozotocin-induced diabetic rat	• 0.05-0.5 µg/ml • 100-600 mg/kg	Agrawalet al. (2016)

2.2.2 Hormones that control blood glucose levels

Glucagon and insulin are two major hormones of pancreas that regulate blood glucose levels and glucose mechanism. The effects of insulin to control blood glucose levels are opposite with glucagon (Nirmalan and Nirmalan, 2017). The roles of these hormones are described below.

Glucagon hormone was produced by alpha cells in islets of Langerhans, which is released in response to low levels of glucose in the blood circulation. Glucagon elevates blood glucose levels by breakdown of glycogen, amino acids and fatty acids into glucose to restore normal blood glucose levels (Figure 2.3). The breakdown of glycogen to glucose occurs in liver and skeletal muscle, while the breakdown of fatty acids into glucose occurs in adipose tissue.

Insulin hormone is synthesized by beta cells in islets of Langerhans, the release of this hormone is stimulated by elevated blood glucose levels after meal. Moreover, amino acids, glucagon-like polypeptide (GLP-1), high concentration of fatty acids are stimulants that recognized for insulin secretion. Insulin lowers blood glucose by activating the membrane translocation of glucose transporter in liver, muscle and adipose cells. The increasing of glucose transporter at membrane lead to more glucose uptake of cell. Insulin also accelerates the conversion of glucose into glycogen in liver cells and skeletal muscle. In addition, insulin increased triglyceride synthesis in adipose tissue by the conversion of the excess glucose to triglyceride (Figure 2.3). The effects of insulin on blood glucose levels are opposite to those of glucagon.

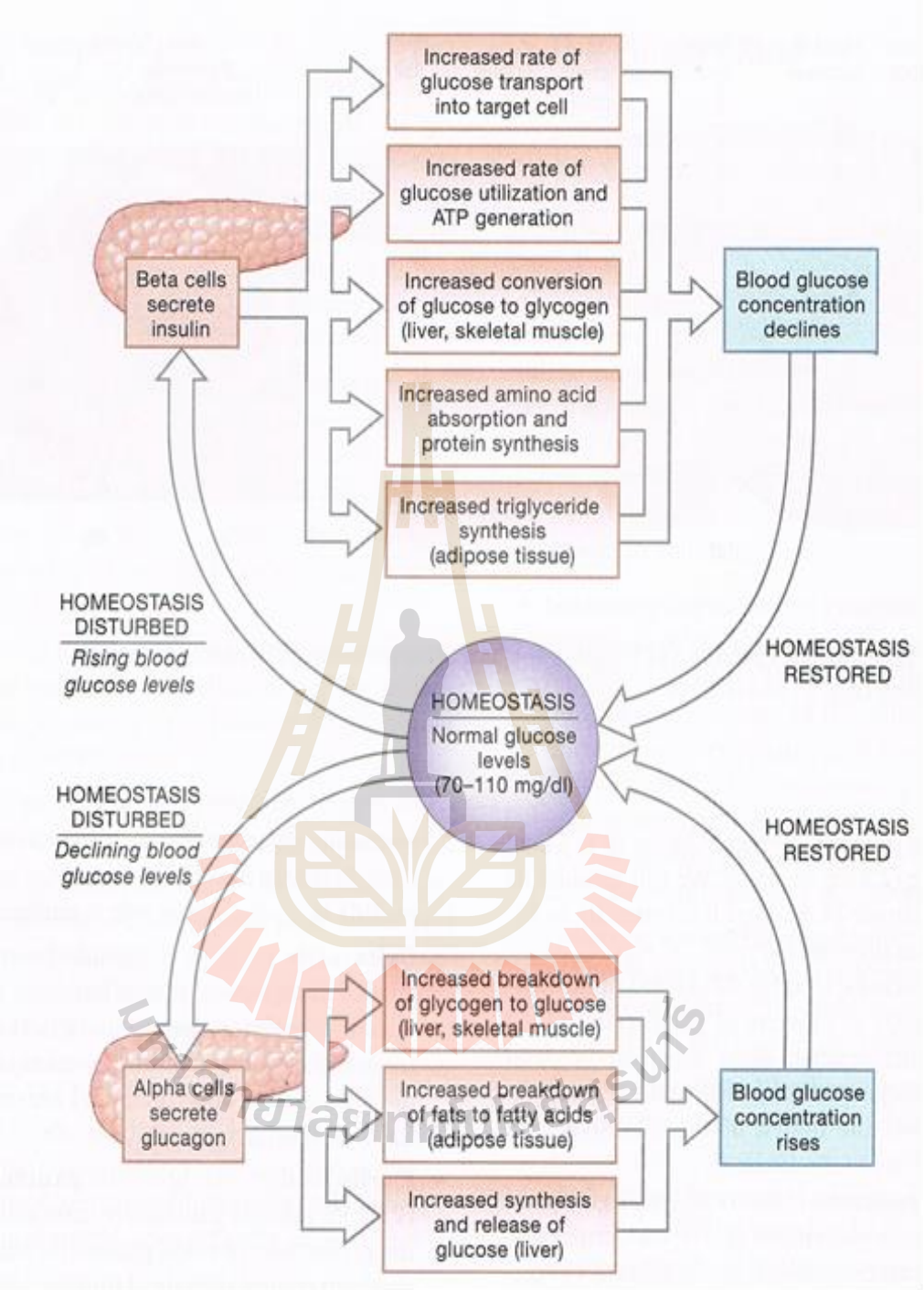

Figure 2.3 The role of insulin in control blood glucose (Martini, Ober, Garrison, Welch, and Hutchings, 2006).

2.2.3 Diabetes mellitus

Diabetes mellitus (DM) is a chronic metabolic disorder characterized by hyperglycemia with disturbances of carbohydrate, fat and protein metabolism (American Diabetes Association, 2011; Bastaki, 2005). These symptoms are resulting from the abnormal of pancreas in producing and secretion insulin and/or the abnormal of peripheral cells in response to insulin action (insulin resistance). Insulin is an important hormone involved in the regulation of the blood glucose level by stimulating removal of glucose from the blood circulation as mentioned earlier (Nirmalan and Nirmalan, 2017). An abnormality of blood glucose concentration leads to many health problems and subsequently to death (Yeo and Sawdon, 2013). Patients with diabetes mostly die from various complications for example cardiovascular diseases, hypertension and nephropathy (American Diabetes Association, 2012; Schlienger, 2013).

2.2.3.1 Type of diabetes mellitus

Diabetes mellitus can be classified into 2 major types as follows :

1. Type 1 diabetes mellitus or Insulin Dependent Diabetes Mellitus is caused from beta-cell damage by autoimmune .The destruction of beta cells makes insulin production decrease .Therefore, these diabetes patients need insulin injections to acquire the normal blood glucose levels .This form of diabetes mellitus, known as a juvenile-onset diabetes, is mostly found in infants and children as age less than 20 years old .The prevalence of type 1 diabetes mellitus is about 5-10% of those with diabetes (American Diabetes Association, 2011)

2. Type 2 diabetes mellitus or Non-Insulin Dependent Diabetes Mellitus is caused from reduction of insulin secretion and/or insulin resistance, which

occurs when cells fail to respond to the normal actions of insulin. Type 2 diabetes mellitus may be caused by genetics, aging or obesity. The prevalence of type 2 diabetes mellitus about 90-95% of those with diabetes. This type of diabetes (adult-onset diabetes) is commonly found in adult as age more than 20 years old (American Diabetes Association, 2012)

2.2.3.2 Symptoms of diabetes mellitus

The symptoms of diabetes mellitus are similar in both types which consist of high blood glucose levels, polyuria, polydipsia, polyphagia and glycosuria (American Diabetes Association, 2012; Olokoba, Obateru, and Olokoba, 2012) .The mechanism underlying these symptoms can be explained as follows:

1. High blood glucose levels: The reduction of insulin secretion and/or insulin resistance leads to the decrease in glucose uptake into the cells and subsequent cellular energy production. Therefore, most of glucose stays in blood circulation, resulting in high blood glucose level.

2. Glycosuria: As the consequence of blood glucose levels which is higher than the capability of the kidneys to reabsorb, the excess blood glucose is excreted to the urine.

3. Polyuria: In diabetes patient, the level of glucose in the blood circulation is abnormally high. Not all of the glucose can be reabsorbed by kidney. The excess glucose from the blood ends up in the urine where it draws more water. This results in unusually large volumes of urine.

2.2.4 Antidiabetic drugs

Antidiabetic drugs are used primarily to save life and alleviate symptoms, but not cure the disease. the medicines also used to prevent the complications, therefore increasing longevity of the patients (Bastaki, 2005). Insulin replacement therapy is the mainstay for patients with type 1 diabetes mellitus while diet, lifestyle modification and oral hyperglycemia drugs are considered for treatment and management of type 2 diabetes mellitus (Bastaki, 2005; Chaudhury et al., 2017; Kennedy and Masharani, 2015). Moreover, insulin was used for type 2 diabetes mellitus patients when blood glucose levels cannot control by diet, exercise and oral hyperglycemia drugs (Bastaki, 2005). The groups of antidiabetic drugs are summarized in Table 2.4 (Chaudhury et al., 2017) and the detail of oral hyperglycemic drugs (Bastaki, 2005; Chaudhury et al., 2017; Kennedy and Masharani, 2015) are explained as the following.

2.2.4.1 Sulfonylureas

Sulfonylureas are insulin secretagogues drug. The sulfonylureas group includes glibenclamide, glipizide and glimepiride. These drugs lower blood glucose levels by increasing the insulin secretion in the pancreas. Sulfonylureas block adenosine triphosphate (ATP) sensitive potassium channels on the plasma membrane of beta cells. The binding of drug with receptor leads to depolarization, calcium influx and subsequently releasing insulin. Hypoglycemia, headache, nausea and weight gain are side effects of sulfonylureas. Moreover, sulfonylurea is also contraindicated in pregnant patients and in patients with hepatic and renal diseases.

2.2.4.2 Dipeptidyl peptidase-IV (DPP-IV) inhibitors

DPP- IV is an enzyme which destroys a group of gastrointestinal hormone called incretins, which stimulate insulin production. The blockade of DPP-IV

enzyme leads to the increase of incretin and insulin level. Sitagliptin, saxagliptin and alogliptin are the example of diabetic drugs in DPP-IV inhibitor group. Nasopharyngitis and headache are side effects of drugs in this group.

2.2.4.3 Insulin sensitizers

Thiazolidinedione (TZDs) is insulin sensitizer drug. Pioglitazone and rosiglitazone is examples in this group. The drugs increase the effectiveness of insulin in the body. They work by binding the peroxisome proliferator activated gamma receptor (PPAR) which plays a role on glucose uptake, glucose metabolism and fat metabolism in liver, adipose tissue and skeletal muscle. The adverse effects are weight gain, hepatotoxicity, osteoporosis, edema and hypoglycamia.

2.2.4.4 α-Glucosidase inhibitors

Acarbose is the example of α-glucosidase inhibitor drug. Drugs in this group work by inhibiting the α-glucosidase enzyme .This enzyme has property in the breakdown of carbohydrates into monosaccharide before absorption. The inhibition on intestinal α-glucosidase would delay the digestion of carbohydrates. Gas production, bloating and diarrhea are the main adverse effects of α-glucosidase inhibitors.

2.2.4.5 Sodium-glucose co-transporter-2 (SGLT-2)

Dapagliflozin is a drug example of SGLT-2. Drugs in this group work by preventing the kidney from reabsorb glucose back to the blood circulation. It causes more glucose to be eliminated in the urine. Side effects of drugs in this group are urinary tract infection and hypoglycaemia.

Table 2.4 Pharmacological agents for glycemic control and their adverse effects (Chaudhury et al., 2017).

Class of antidiabetic medication (route of administration)	Representative agents	Mechanism of action	T1/2 and metabolism	HbA1C reduction (%)	Risk of hypoglycemia	Effect on body weight	Metabolic alterations	Cardiovascular (CV) benefit and risk	Other adverse effects/ additional comments
Biguanide (o)	Metformin	Insulin sensitizer Numerous effects on inhibition of hepatic glucose production	5 h; unmetabolized, renal excretion	1–2	None	Mild weight loss due to anorectic effect	Lactic acidosis (very rare) May cause nausea/vomiting or diarrhea after introduction, which may result in electrolyte or pH alterations	Reduce MI by 39% and coronary deaths by 50% (UKPDS)	Vitamin B12 deficiency, which may cause anemia and neuropathy (risk in elderly) Very safe drug, but stop metformin if creatinine >1.5 mg/dL in males and >1.4 mg/dL in females
Dipeptidyl peptidase 4 (DPP-IV) inhibitor (o)	Sitagliptin Saxagliptin Vidagliptin Linagliptin Alogliptin	Inhibition of degradation of GLP	Excreted by kidneys (except linagliptin) (needs dose reduction in renal failure)	0.5–0.8	Low			Long-term trials to assess CV risk; decreases postprandial lipemia, however, may cause CHF by degradation of BNP	Pancreatitis Upper RTI infection
Sodium-glucose cotransporter (SGLT2) inhibitor (o)	Canagliflozin Dapagliflozin Empagliflozin	Glucosuria due to blocking (90%) of glucose reabsorption in renal PCT; insulin-independent mechanism of action			Low			Positive CV effect due to reduction of sodium and uric acid absorption and reduction of BP	Ketoacidosis (rare) Genital mycosis May increase LDLc Bone fractures
Insulin (p)	Short-acting Regular (R) (Humulin R, Novolin R) Intermediate NPH (N) Long-acting Insulin glargine (Lantus) Insulin determir (Levemir) Insulin degludec (Tresiba) Rapid-acting Humalog (Lispro)	Activation of insulin receptors and downstream signaling in multiple sensitive tissues	30 min-1 r (onset of action) Peak 2–5 h Duration of action 8 h 1.5–4 h (onset of action) Peak 4–12 h Duration of action 24 h 0.8–4 h (onset of action) Peak minimal Duration of action 24 h 10–30 min (onset of action)	1–2.5	Prominent	Weight gain		HF if used in combination with thiazolidinediones (TZD)	Lipoatrophy and lipohypertrophy at sites of injection Allergy to injection components Levemir Food and Drug Administration -approved for gestational diabetes mellitus

Table 2.4 Pharmacological agents for glycemic control and their adverse effects (Continued).

Class of antidiabetic medication (route of administration)	Representative agents	Mechanism of action	T1/2 and metabolism	HbA1C reduction (%)	Risk of hypoglycemia	Effect on body weight	Metabolic alterations	Cardiovascular (CV) benefit and risk	Other adverse effects/ additional comments
	Novolog (Aspart) Glulisine (Apidra) Pre-mixed 75% insulin lispro protamine/25% insulin lispro (Humalog Mix 75/25) 50% insulin lispro protamine/50% insulin lispro (Humalog Mix 50/50) 70% insulin lispro protamine/30% insulin aspart (Novolog 70/30) 70% NPH insulin/30% regular		Peak 30 min–3 h Duration of action 3–5 h 5–15 min (onset of action) Peak dual Duration of action 10–16 h 30–60 min (onset of action) Peak dual Duration of action 10–16 h						
GLP-1 agonists (p)	Liraglutide Exenatide Dulaglutide	Activate GLP1 receptor Increased insulin secretion, decreased glucagon, delayed gastric emptying, increased satiety	24 h 4–6 h (short acting) 7 days (long acting, extended release) 7 days	0.5–1.5	No [risk if used in combination with sulfonylureas (SU)]	Weight loss		Reduce CV risk	Nausea, vomiting, pancreatitis, C cell tumor of thyroid (contraindicated in MEN type 2)
SU (o)	Glimepiride Glipizide Glyburide	Insulin secretion		1–2	Prominent (severe in renal failure)	Weight gain		Increased cardiovascular disease risk, mainly due to hypoglycemia	Use beta-blockers with caution
TZD (o)	Rosiglitazone Pioglitazone	True insulin sensitizer		0.5–1.4		Weight gain		Cardiac failure, pedal edema	Bladder cancer; fractures

O, oral; p, parenteral; iv, intravenous; sc, subcutaneous.

2.3 Diabetes models

2.3.1 Hyperglycemia model

Animal models have been used extensively to obtain different information about various pathological conditions and these models are better suited for observing the overall effects of an experiment. Therefore, many animal models have been created and developed including diabetes model as shown in Table 2.5 (King, 2012; Radenkovic, Stojanovic, and Prostran, 2016). Induction-diabetic, genetic diabetic and miscellaneous models have been established for diabetes experiments. Although, there are several methods can be induced diabetes but chemical method of alloxan-induced diabetes is represented the highly preferable experimental models for type 1 and type 2 diabetes models (Radenkovic et al., 2016). Simultaneously, mice also are generally used in animal experiments with wide range of fields including toxicology, physiology, pathology, immunology and pharmacology (Exner and Christoph, 2016). Mouse hyperglycemia model is one experiment of pharmacology research and have been created and used for antidiabetic activity study (Cefalu, 2006). ICR mice are preferred because they have many advantages. For example, ICR mice have low cost when compared to another animal and have shorter generation intervals. Moreover, ICR mice have small body, so they require small amount of drug (Karthikeyan, Balasubramanian, and Kumar, 2016). Therefore, ICR mice are convenient for studying the chemicals or drugs which have limit of stock.

Table 2.5 Class classification of animal diabetic models (Radenkovic et al., 2016).

1. Method for induction of experimental diabetes mellitus	
1.1 Pancreatectomy in dog	Wahoff et al. (1994)
1.2 Alloxan-induced diabetes	Radenkovic et al. (2013)
1.3 Streptozotocin-induced diabetes	Al-Malki and El Rabey (2015)
1.4 Hormone-induced diabetes	Campbell and Rastogi (1966)
1.5 Virus-induced diabetes	Alkaanani, Hara, Gianani, and Zipris (2004)
1.6 other diabetogenic compounds	Kim et al. (2002)
1.7 Indulin deficiency due to insulin antibodies	Andreev, Strashimirov, Ditzov, and Dashev (1974)
2. Genetically diabetic animals	
2.1 Spontaneously diabetic rats	Miao et al. (2005)
2.2 Spontaneously diabetic mice	Matsumoto, Kobayashi, Ishida, Taguchi, and Kamata (2010)
2.3 Chinese hamsters	Iwashima, Watanabe, and Makino (1990)
2.4 Other species with inherited diabetic sympoms	Kramer (1981)
2.5 Transgenic animals	Streckel et al. (2015)
3. Misellaneous models	
3.1 Invertebrate animal model	Shirazi et al. (2014)
3.2 Diet-induced metabolic dysregulation	Spolding et al. (2014)

2.3.2 Alloxan-induced hyperglycemic model

Alloxan (2,4,5,6- tetraxypyrimidine) is the most prominent diabetogenic chemical agent that is used to induce diabetes in various animal experiments such as rabbits (Alam, Khan, Sirhindi, and Khan, 2005), rats (Raut and Gaikwad, 2006), and mice (Heikkila, 1977). As a hydrophilic compound, alloxan cannot directly penetrate to the lipid bilayer of the plasma membrane of pancreas cell, but enter the cells via GLUT2 glucose transporter (Elsner, Tiedge, Guldbakke, Munday, and Lenzen, 2002) because its chemical structure is similar to glucose (Figure 2.4). After penetrate to beta cells, alloxan induce diabetes by two independent mechanisms, glucokinase inhibition and reactive oxygen species generation (Figure 2.5). Glucokinase inhibition caused by alloxan impedes glucose oxidation and ATP generation process, resulting in the suppression of the ATP-sensitive insulin secretion by beta-cells. For the latter mechanism of action, reactive oxygen species such as superoxide, hydrogen peroxide and hydroxyl radicals are generated and then are ultimately responsible for the death of the beta cells (Lenzen, 2008). The death of the beta cells leads to the decreasing of insulin level and increasing of blood glucose level (hyperglycemia) in animal models, and these symptoms are characteristics of diabetes disease.

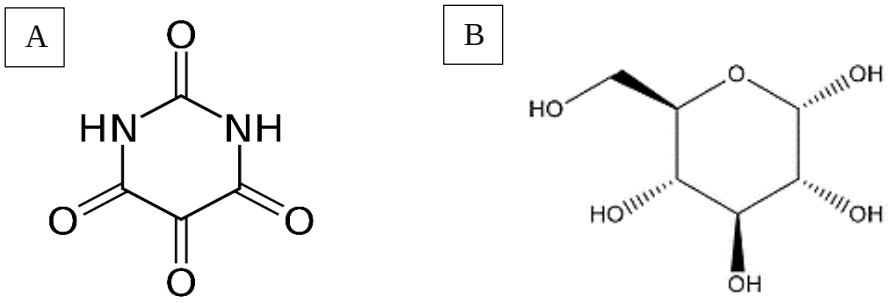

Figure 2.4 Chemical structure of alloxan (A) and glucose (B).

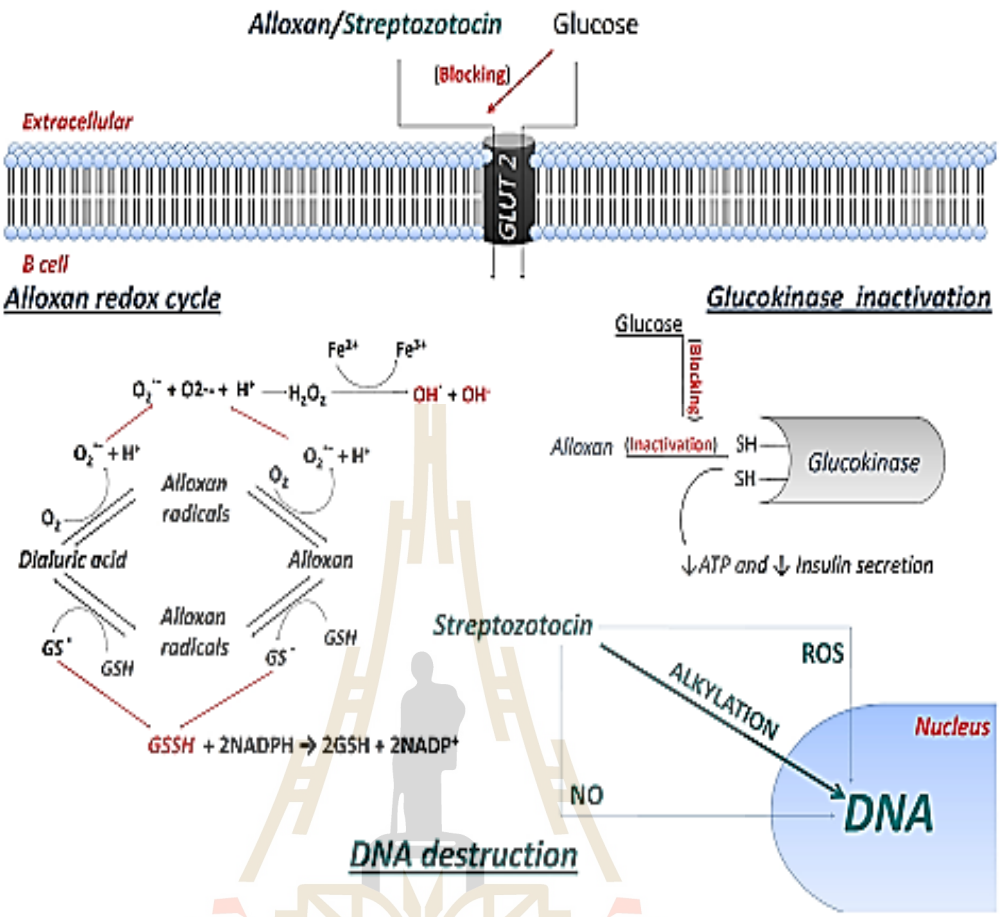

Figure 2.5 Mechanism of action of alloxan on diabetogenic effect (Radenkovic et al., 2016).

2.3.3 α-Glucosidase inhibitory model

α-Glucosidase inhibitory assay, an *in vitro* method, is developed for antidiabetic activity screening and for antidiabetic action study (Dsouza and Lakshmidevi, 2015; Karthikeyan et al., 2016). The α-glucosidase enzyme has property in the breakdown of carbohydrates into monosaccharide before absorption, therefore the inhibition on intestinal α-glucosidase delays the digestion of carbohydrates and

reduces the rate of glucose absorption leading to low blood glucose levels after meal (Clissold and Edwards, 1988).

2.3.4 Insulin secretion model using pancreatic RIN-m5F cells

Insulin secretion assay is *in vitro* method. This assay has been used to explain the antidiabetes action of compounds (Dsouza and Lakshmidevi, 2015; Karthikeyan et al., 2016). This study, RIN-m5F, the pancreatic beta cells of rat (*Rattus norvegicus*) was used which can produce and secrete insulin (American Type Culture Collection, 2017).

2.3.5 Glucose absorption model

Glucose absorption model is *ex vivo* method (Therasa, Thirumalai, Tamilselvan, and David, 2014). This method is used for screening and studying the antidiabetic action similar to insulin secretion and α-glucosidase inhibitory assays. The jejunum from the small intestine is used in this model. Small intestine play a role in absorption nutrition such as glucose, amino acid, mineral, water and nucleotide (Collins and Bhimji, 2017). Therefore, inhibition of glucose absorption at jejunum is one way to decrease blood glucose level in diabetic patient.

2.4 Caco-2 monolayer model

In general, alternative medicines from natural plants are usually used through oral administration. It is known that not all ingredients in the plant extracts can be absorbed by gastrointestinal tract. Some compounds have low oral bioavailability. Flavonoids extracted from plants are considered of low bioavailability (Liu et al., 2015). An

absorption property of chemicals shows direct correlation with their therapeutic efficacy.

Absorption property of compounds can be investigated by Caco-2 monolayer model. Caco-2 monolayer model are generally accepted as a primary intestinal absorption screening and drug transport mechanism tool (Yee, 1997; Hubatsch, Ragnarsson, and Artursson, 2007). Caco-2 cells are derived from human adenocarcinoma colon cells. In this model, Caco-2 cells are grown on permeable filter support and form monolayer of polarized cells pressing function similar to intestinal enterocytes (Figure 2.6). The model will be separated into 2 parts, apical side (AP) as lumen of intestinal and basolateral side (BL) as blood stream. Tested drugs will be added into the AP side. After a suitable incubation period, the solution in the BL side will be collected and analyzed compared to the other side. By this method, absorption property of a compound can be identified.

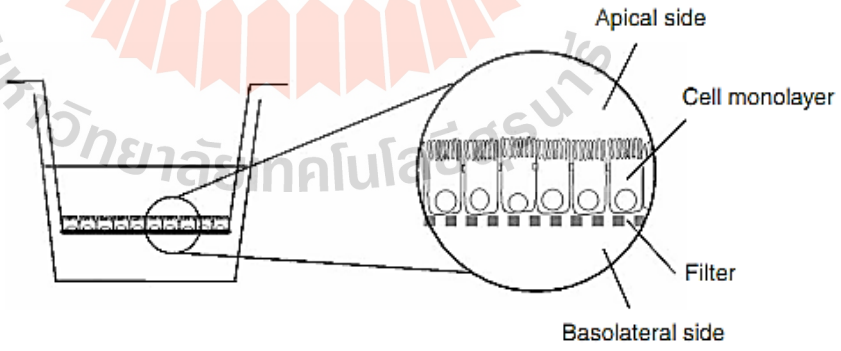

Figure 2.6 Diagram of a Caco-2 monolayer grown on a permeable filter support (Hubatsch et al., 2007).

2.5 Nanocarriers

Nanocarriers which have structures of sizes ranging from 1-100 nanometer are used for transportation of another substance, such as drug, protein, antibody and nutraceutical. These molecules present poor stability, enzyme degradation in gastrointestinal tract and low bioavailability. To solve these problems, many types of nanocarriers, such as polymeric carriers, solid lipid carriers, gold carriers and liposome, have been developed and designed to have a functional protection of substances in gastrointestinal tract, to increase drug solubility and bioavailability or to control drug release (Khodabandehloo, Zahednasab, and Ashrafi, 2016).

Site-specific drug delivery and controlled release can be achieved by using oral nanocarriers. Chitosan nanoparticles (Chnp) have been developed using electrospraying method. Retrograded soluble starch (SS) which is susceptible to digestion by amylases in the small intestine, and retrograded high amylose corn starch (RS) which is susceptible to digestion by enzymes in the colon were used as controlled releasing coatings for gastric protection and targeted delivery of nanoparticles. These enteric coating nanocarriers Chnp+SS and Chnp+RS will be protected in the GIT and can pass through the mucosal lining in the intestine with the size range of 200 nm, thus creating the effective nutrient absorption (Sampathkumar and Loo, 2018). The results demonstrated that Chnp+SS and Chnp+RS were selectively degraded in different parts of gastrointestinal tract, small intestine and colon, respectively. Due to the less efficacy *in vivo* and higher toxicity *in vitro* of the ethyl acetate fraction, the water fraction of *W. coagulans* was suggested to this group of researchers as collaborators to use for encapsulation. *In vitro* safety of the Chnp and their uptake toward Caco-2 cells were

also reported. In this study, two types of targeted delivery nanocarriers, Chnp+SS and Chnp+RS loaded with W. coagulans extract, which were provided by Dr. Loo Say Chye Joachim's Laboratory were tested for its efficiency of antidiabetic activity in diabetic animal model.

CHAPTER III

MATERIALS AND METHODS

3.1 Sample preparations

Water and ethyl acetate fractions of *W. coagulans* fruit and water faction encapsulated with nanoparticles, Chnp, Chnp+SS and Chnp+RS, were provided from Associate Professor Dr. Loo Say Chye Joachim's Laboratory, School of Materials Science & Engineering College of Engineering, Nanyang Technological University, Singapore. The preparation processes are described as follow.

The *W. coagulans* fruits were obtained from a local market in India. The extraction process was performed according to previously reported procedure with slight modifications (Maurya et al., 2008). A known weight of the berries from the plant was crushed mechanically using pestle and mortar and the coarse powder obtained was soaked in a 1:1 mixture of water and ethanol for 24 hours. The extract was collected by filtering out the coarse powder using Whatman filter paper. The hydro alcoholic extract was concentrated using a rotary evaporator. An aliquot of the concentrated extract was mixed with a 1:1 mixture of water and ethyl acetate and extracted to obtain a water soluble fraction and ethyl acetate soluble fraction. The ethyl acetate soluble fraction was subjected to column chromatography over silica gel using a mixture of chloroform and methanol as the mobile phase. The fraction collected from this column was assigned as ethyl acetate fraction (EAF). The water-soluble fraction was concentrated using rotary evaporator and subjected to column

chromatography over silica gel using a mixture of water and methanol as the mobile phase. The fraction collected from this column was assigned as water fraction (WF).

Depend on the safety data and effectiveness found in this study, the water fraction was chosen to load into the nanocarriers for testing their efficiency. The nanocarrier synthesis was conducted using electropraying method as described in the previous report (Sampathkumar and Loo, 2018). The fabricated nanocarriers include the following products.

1. Chitosan nanoparticle loaded with the water fraction (Chnp+WF)
2. Chitosan nanoparticle loaded with the extract coated with retrograded soluble starch (Chnp+SS+WF)
3. Chitosan nanoparticle loaded with the extract coated with slowly digestible or resistant starch (Chnp+RS+WF)

3.2 Chemical analysis by HPLC-MS

Ethyl acetate fraction was dissolved in dimethyl sulfoxide (DMSO) and water fraction was dissolved in water. And then, the fraction solutions were analyzed on an automated HPLC-MS system using an Ultimate 3000 HPLC system (Thermo Scientific) with a column Poroshell 120 EC-C18 (4.6×50 mm, 2.7-micron). The system was coupled with an emitter for nanospray ionization to a MicroTOF-Q mass spectrometer (Bruker). The solvent system was consisted of 2 mobile phase; mobile phase A is water with 0.1% formic acid and mobile phase B is acetonitrile with 0.1% formic acid. The liner gradient is 10% to 40% of mobile phase B within 53 min. Positive ion electrospray ionization (ESI) mass spectrometry was used for the detection and quantification. Scan range was begrimed at 50-1500 m/z.

3.3 Cells and culture conditions

3.3.1 HepG2 cells

HepG2, *Homo sapiens* (Human) liver cell line (Figure 3.1a) was obtained from the American Type Culture Collection (ATCC number: HB-8065). HepG2 cells were cultured in DMEM medium supplemented with 10% fetal bovine serum, 1% antibiotic-antimycotic solution, 1% HEPES, 1% sodium pyruvate and incubated at 37ºC in a humidified atmosphere containing 5% CO_2, as adherent cells in culture flask. The cells were trypsinized with 0.25% trypsin-EDTA and sub-cultured at 70-90 % confluence. HepG2 cells were used in *in vitro* toxicity experiment as described in Sections 3.5.1 and 3.5.2.

3.3.2 RIN-m5F cells

RIN-m5F, *Rattus norvegicus* (Rat) pancreas cell line (Figure 3.1b) was obtained from the American Type Culture Collection (ATCC number: CRL-11605). RIN-m5F cells were cultured in RPMI-1640 medium supplemented with 10% fetal bovine serum, 1% antibiotic-antimycotic solution, 1% HEPES, 1% sodium pyruvate and incubated at 37ºC in a humidified atmosphere containing 5% CO_2. Cell was grown as adherent cells and spread in culture flask. The cells were sub-cultured at 70-90% confluence. The cells were trypsinized with 0.25% trypsin-EDTA. After trypsinized, RIN-m5F cells were used in insulin secretion study (Section 3.8.2).

3.3.3 Caco-2 cells

Caco-2, *Homo sapiens* (Human) colon cell line (Figure 3.1c) was obtained from the American Type Culture Collection (ATCC number: HTB-37). Caco-2 cells were cultured with the procedure similar to HepG-2 cells culture protocol. Caco-2 cells were used in the absorption study as described in Section 3.9.

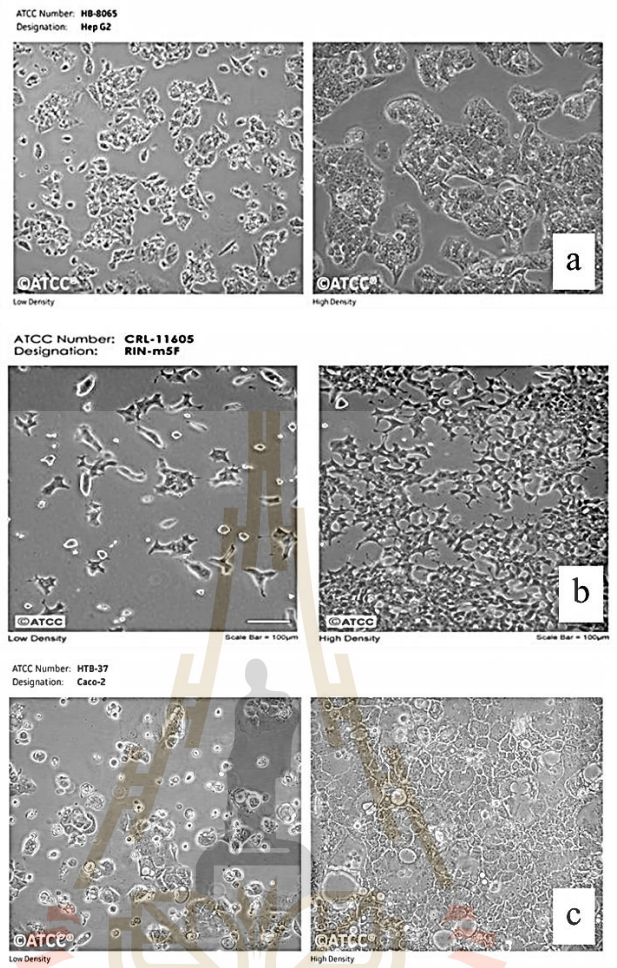

Figure 3.1 Photographs of cells lines used in this study. (a) HepG2, (b) RIN-m5F and (c) Caco-2 cells (American Type Culture Collection, 2017).

3.4 Animals

Male ICR mice (age 5 weeks, weight 28-30 g) and Wistar rat (weight 300-400 g) purchased from Nomura Siam International were housed in stainless steel cages at Laboratory Animal, Suranaree University of Technology. The house temperature was controlled at 25°C, 45%-50% relative humidity and 12 h light/dark cycle. Food and water were given *ad libitum*. Mice were acclimatized for a week. All procedures were

conducted following the guidelines of the Institutional Animal Care and Use Committee, Suranaree University of Technology.

3.5 Investigation of the toxicity

3.5.1 MTT assay

HepG2 cells were seeded in 96-well plates at 4.5×10^4 cells per well and incubated in a humidified incubator containing 5% CO_2 at 37ºC for 16-18 h. After that, cells were treated with various concentrations of WF and EAF at the doses of 0-10,000 µg/ml for 24 h. After treatment, the cells were centrifuged 2,500 rpm at 4ºC for 5 min and the medium was removed. Then, 150 µl of 0.5 mg/ml MTT solution was added for determination of cell viability. After incubation in the dark at 37ºC for 4 h., the cells were centrifuged 2,500 rpm at 4ºC for 5 min. The purple formazan crystals were dissolved with DMSO (50 µl per well), after the culture medium was discarded. The solution was measured at 570 nm using a microplate reader. Results were expressed as percentage of cell viability as the following formula.

$$\%\text{Cell viability} = [\frac{\text{OD}_{\text{sample}}}{\text{OD}_{\text{control}}}] \times 100$$

where $\text{OD}_{\text{sample}}$ is the absorbance of the cell treated with sample

$\text{OD}_{\text{control}}$ is the absorbance of the cell treated with deionized water

3.5.2 Trypan blue exclusion assay

HepG2 cells were prepared for the experiment and treated with the extracts the same as described in the Section 3.5.1. After treatment, the cells were collected by incubating with 0.25% trypsin-EDTA and centrifuging at 1,500 rpm for 3 min. The supernatants were removed and the cell pellets were resuspended in DMEM. Cell

suspension was stained with 0.25% Trypan blue. The number of live cell and dead cells were counted by Automated Cell Counter (Bio-Rad).

3.5.3 Sub-chronic toxicity test

After acclimatization, mice were divided into 4 groups (5 each), including normal control, vehicle control, WF and EAF treated groups. For the treatment groups, mice were received WF and EAF at the dose of 50 mg/kg for 10 days by oral administration and DMSO (10%) is used as a vehicle control. Animal fasting blood glucose levels and body weight were checked every 5 days. At the end of experiment, mice were sacrificed by carbon dioxide inhalation. Blood sample was collected via cardiac puncture for biochemical evaluation of ALT, AST, BUN and creatinine. The liver, kidney and pancreas organs were isolated. And then, the organ weight of liver, kidney and pancreas were checked. After that, the organs were fixed with 10% neutral buffered formaldehyde for histological examination (Section 3.7).

3.6 Determination of antidiabetic activity of the extracts

3.6.1 Study of acute hypoglycemic activity in normal mice

After acclimatization for 7 days, normal mice were divided randomly into 5 groups (6 each) as follow:

1. Normal control group (N+DI) was received deionized water.
2. Vehicle control group (N+DMSO) was received 10% DMSO.
3. WF group (N+WF) was received water fraction (50 mg/kg).
4. EAF group (N+EAF) was received ethyl acetate fraction (50 mg/kg).
5. Drug group (N+Gli) was received glibenclamide (20 mg/kg).

Before starting the experiment, the mice in all groups were fasted for 12-14 h. After receiving the treatments as described above for 30 min by oral administration, hyperglycemic activity was evaluated by oral glucose tolerance test (OGTT). Briefly, the animals were challenged with 2 g/kg glucose solution, and then blood glucose was measured at 0, 30, 60 and 120 min. The results were expressed as blood glucose levels and area under the curve (AUC) value. The AUC was calculated as the following formula.

$$\text{AUC} = \left(\left(\frac{\text{G0} + \text{G30}}{2}\right) \times (30 - 0)\right) + \left(\left(\frac{\text{G30} + \text{G60}}{2}\right) \times (60 - 30)\right) + \left(\left(\frac{\text{G60} + \text{G120}}{2}\right) \times (120 - 60)\right)$$

where G0 is the glucose levels at 0 min

G30 is the glucose levels at 30 min

G60 is the glucose levels at 60 min

G120 is the glucose levels at 120 min

3.6.2 Study of antihyperglycemic activity in alloxan-induced diabetic mice

After fasting food 12- 14 h, mice were induced diabetes by intraperitoneal alloxan injection (120 mg/kg). Blood glucose levels were determined after injection for 3 days. Only mice that have blood glucose $\geq$ 250 mg/dl were used for diabetic groups. The experimental animals were divided into 6 groups (6 each) as follow:

1. Normal control group (N+DI) healthy mice receiving deionized water
2. Diabetes control group (DM+DI) diabetic mice receiving deionized water
3. Vehicle control group (DM+DMSO) diabetic mice receiving 10% DMSO
4. WF group (DM+WF) diabetic mice receiving water fraction (50 mg/kg)
5. EAF group (DM+ EAF) diabetic mice receiving ethyl acetate fraction (50 mg/kg)

6. sPositive control group (DM+Gli) diabetic mice receiving glibenclamide (20 mg/kg)

The mice were received drugs once a day for 10 days by oral administration. Fasting blood glucose levels and body weight were checked every 5 days. At day 10, OGTT was conducted and then mice were sacrificed by carbon dioxide inhalation. Blood samples were collected via cardiac puncture for biochemical evaluation of ALT, AST, albumin, creatinine, LDL, HDL and triglyceride. The pancreases, liver and kidney were isolated. After weighting, the organs were collected and then fixed with 10% neutral buffered formaldehyde for histological examination.

3.7 Histological examination

The liver, kidney and pancreas from the Sections 3.5.3 and 3.6.2 were fixed with 10% neutral buffered formaldehyde for 24 h. After that, 10% neutral buffered formaldehyde was discarded and replaced with 70% ethanol. The organs were dehydrated in 95%, 100% ethanol and infiltrated in xylene by tissue processing automated machine (RVG/2 INTELSINT, Italy). Then, the organs were embedded in paraffin and sectioned into 5 µm thickness slice. The section was fixed on slide. The tissue slide was immersed in xylene and stained with hematoxylin and eosin. The microphotographs of each tissue section were observed under light microscope at 200 magnifications (20X) for liver and kidney and 400 magnifications (40X) for pancreas.

3.8 Investigation of *in vitro* antihyperglycemic action

3.8.1 Investigation of α-glucosidase inhibitory activity

The α-glucosidase inhibitory activity was determined according to the previous reports (Choi et al., 2010; Dong, Li, Zhu, Liu, and Huang, 2012) with some modifications. The reaction mixture consists 10 µl of 0.25 U/ml α-glucosidase enzyme, 50 µl of 0.1 M potassium phosphate buffer pH 6.8 and 20 µl of the test sample (the extracts or acarbose as a positive control). Then, the reaction mixture was mixed and incubated at room temperature for 10 min. After that, 10 µl of 1 mM p-nitrophenyl-α-D-glucopyranoside (PNP-G) was added into the reaction mixture and incubated at room temperature for 30 min. After incubation, the mixture was added with 50 µl of 0.1 M Na_2CO_3 to stop the reaction and the absorbance was measured at 405 nm. Results were shown as IC_{50} (the concentration of inhibitors required for inhibiting 50% for α-glucosidase activity).

$$\%\ \text{Inhibition of}\ \alpha - \text{glucosidase activity} = \frac{[OD_{control} - OD_{sample}]}{OD_{control}} \times 100$$

where $OD_{control}$ is the absorbance of the control reaction

OD_{sample} is the absorbance of sample reaction

3.8.2 Investigation of stimulatory effect on insulin secretion

Firstly, the toxicity of water and ethyl acetate fractions on RIN-m5F cells were evaluated by MTT assay. RIN-m5F cells were seeded to 96-well plates at 2×10^5 cells per well and incubated in a humidified incubator containing 5% CO_2 at 37ºC for 48 h. After incubation, the media was removed and replaced with 200 µl of various concentrations of water and ethyl acetate fractions at the doses of 0-1,000 µg/ml. After incubation for 1 h, cell viability was determined by MTT. The concentrations of EAF

and WF that showed nontoxic on pancreatic cells (100% cell viability) were used in insulin secretion study.

The insulin secretion assay was performed as the previously described method (Keller et al., 2011). Briefly, RIN-m5F cells were seeded in 96 well plates at the concentration of 2×10^5 cells per well and incubated for 48 h. After reaching 70-80% confluence, RPMI media was removed and replaced with Kreb's Ringer buffer. After 60 min of incubation, the cells were washed twice with Kreb's Ringer buffer. Then, cells were treated with water and ethyl acetate fractions at the doses of 100, 250 and 500 μg/ml. After 60 min of incubation, the supernatant was collected for determination insulin secretion by Insulin ELISA kit (Merck). The insulin secretagogue glibenclamide (50 μg/ml) was used as a positive control.

3.8.3 Investigation of inhibitory effect on glucose absorption

Effect on glucose absorption was investigated in rat intestine using method previously described (Krisanapun, Peungvicha, Temsiririrkkul, and Wongkrajang, 2009). The rat was fasting 12-14 h before scarified by chloroform. Rat jejunum was removed immediately after cervical dislocation and immersed in Kreb-Henseleit solution (pH 7.4) and continuously aerated with carbogen. The jejunnun was everted with glass rod. The everted jejunum was cut to several pieces (5 cm each) and tied at one end with cotton thread, then filled with Kreb-Henseleit solution with glucose 140 mg/dl. After tied at the other end, each jejunum sac was incubated in the following solutions: Group I, Kreb-Henseleit solution with glucose 140 mg/dl; Group II, Kreb-Henseleit solution with glucose 140 mg/dl mixed with sodium fluoride (NaF) 0.2 M; Group III, Kreb-Henseleit solution with glucose 140 mg/dl mixed with WF at 0.1 mg/ml and Group IV, Kreb-Henseleit solution with glucose 140 mg/dl mixed with WF at 0.25

mg/ml; Group V, Kreb-Henseleit solution with glucose 140 mg/dl mixed with WF at 0.5 mg/ml; Group VI, Kreb-Henseleit solution with glucose 140 mg/dl mixed with EAF at 0.1; Group VII, Kreb-Henseleit solution with glucose 140 mg/dl mixed with EAF at 0.25 mg/m and Group VIII, Kreb-Henseleit solution with glucose 140 mg/dl mixed with EAF at 0.5 mg/ml. The incubation flasks were shaken at 90 oscillations/min at 37ºC for 30 min. After incubation, the sacs were cut and the concentration of glucose in the sac was measured by using peroxidase-glucose oxidase (PGO) enzyme commercial kit (Sigma). The results were expressed as glucose concentration inside the sacs and % inhibition of glucose absorption. % inhibition of glucose absorption was calculated by the equation below.

$$\%\ \text{Inhibition of glucose absorption} = \frac{[\text{OD}_{control} - \text{OD}_{sample}]}{\text{OD}_{control}} \times 100$$

where $\text{OD}_{control}$ is the absorbance of the control reaction

OD_{sample} is the absorbance of sample reaction

3.9 Investigation of intestinal absorption of water and ethyl acetate fractions by Caco-2 monolayer model

3.9.1 Investigation of toxicity on colon cells

The toxicity of water and ethyl acetate fractions on Caco-2 cells were determined by MTT assay. Caco-2 cells were seeded to 96-well plates at 2×10^4 cells per well and incubated in a humidified incubator containing 5% CO_2 at 37ºC for 72 h. After incubation, the media was removed and replaced with 200 µl of various concentrations of water and ethyl acetate fractions at the doses of 0-10,000 µg/ml. After incubation for 4 h, cell viability was determined by MTT. The highest concentration of

the fraction that showed nontoxic on Caco-2 cells (100% cell viability) was used in the intestinal absorption study.

3.9.2 Caco-2 monolayer model

Caco-2 cells were seeded to insert in 12 well plates at the concentration of 1.13 × 10^5 cells per well and incubated in a humidified incubator containing 5% CO_2 at 37ºC for 21 days. DMEM media, 0.5 and 1.5 ml were changed every day in the apical (AP) and basolateral sides (BL), respectively. At the end of incubation, transepithelial electrical resistance (TEER) value was evaluated using Millicell ERS-2. To further validate monolayer integrity, lucifer yellow (100µM) was added to AP of insert and incubated for 2 h in a control well. The amount of lucifer yellow transported to BL was quantified using a fluorescent microplate reader at EX = 425 nm and Em = 530 nm. Then, the values were used to calculate % lucifer yellow rejection. Only Caco-2 monolayers which had TEER value equal or more than 600 Ω cm^2 and % lucifer yellow rejection equal or more than 99% were used in intestinal absorption study. TEER value and % lucifer yellow rejection were calculated by the equations below.

$$\text{TEER value } (\Omega cm^2) = \left(\text{TEER}_{\text{sample}} - \text{TEER}_{\text{blank}}\right) \times 1.1 \text{ (area ofinsert)}$$

where $\text{TEER}_{\text{sample}}$ is the TEER value of sample

$\text{TEER}_{\text{blank}}$ is the TEER value of blank (empty insert)

$$\%\ \text{Lucifer yellow rejection} = 100\left[1 - \frac{\text{RFU}_{\text{BL}}}{\text{RFU}_{\text{AP}}}\right]$$

where RFU_{BL} is the fluorescent absorption of lucifer yellow in basolateral side of insert

RFU_{AP} is the fluorescent absorption of lucifer yellow in apical side of insert

3.9.3 Intestinal absorption study

Before experiment, media were removed from AP and BL sides of Caco-2 monolayer and washed with Hank's Balanced Salt Solution (HBSS), pH 7.4. Then, 0.5 and 1.5 ml of HBSS were added to AP and BL sides, respectively and incubated for 30 min. The 0.5 ml of 5,000 µg/ml of water fraction and 100 µg/ml of ethyl acetate fraction (the highest of nontoxic concentration) were added to the AP side and continue incubating. After 4 h of incubation, the solution in BL side was collected to the tube. The chemical compositions of water and ethyl acetate fractions were analyzed by HPLC-MS (Section 3.2). TEER value and % lucifer yellow rejection were evaluated at the end of each experiment.

3.10 Determination of antidiabetic activities of drug delivery systems

3.10.1 Inducing diabetes mice

As the results from the section 3.6 showing its higher effectiveness, the water fraction was chosen for encapsulation and tested for the delivery systems. Mice were induced diabetes by intraperitoneal alloxan injection (120 mg/kg) as described in the Section 3.6.2. The animals that had blood glucose $\geq$ 250 mg/dl were used for diabetic groups.

3.10.2 Study of antidiabetic activity of the water fraction-loaded nanocarriers in alloxan-induced diabetic mice

The experimental animals were divided into 6 groups (3 each) as follow:

1. Normal control group (N+ DI), healthy mice receiving deionized water

2. Diabetes control group (DM+DI), diabetic mice receiving deionized water
3. Chnp+WF group (DM+Chnp+WF), diabetic mice receiving chitosan nanoparticle-laoded with the water fraction (50 mg/kg)
4. Chnp+SS+WF group (DM+Chnp+SS+WF), diabetic mice receiving chitosan nanoparticle-laoded with the extract coated with soluble starch (Chnp+SS+WF) (50 mg/kg)
5. Chnp+RS+WF group (DM+Chnp+RS+WF), diabetic mice receiving chitosan nanoparticle-laoded with the extract coated with resistant starch (50 mg/kg)
6. Positive control group (DM+Gli), diabetic mice receiving glibenclamide (20 mg/kg)

The particles were prepared and fed to the animals as the amount of particles to match 50 mg/kg of water fraction. Then, the particles were suspended in DI water and fed to the animals by oral gavage once a day. The mice received drugs consecutively for 5 days. At days 0 and 5, fasting blood glucose levels were measured.

3.10.3 Study of the prolonged effect of the Chnp+SS+WF nanocarriers

Due to the results from the experiment 3.10.2, Chnp+SS+WF was chosen to study the effect of the delivery system. Prolonged effects of water extract encapsulated with chitosan nanoparticle with and without coated with retrograded soluble starch were compared in alloxan-induced diabetes model. After 5 days, the treatment was stopped and the FBG level was monitored for another 5 days.

3.11 Data analysis

Data were expressed as mean ± SEM. Mostly, the comparisons among different groups was performed by analysis of variance (ANOVA) followed by Student-Newman-Keuls (SNK) test. In the case of using other statistical methods, they were indicated in each specific figure legend. *P*-values less than 0.05 were considered as significant difference in all experiments.

CHAPTER IV

RESULTS

4.1 Chemical compositions of the ethyl acetate and water fractions

The chemical compositions of EAF and WF were determined by HPLC-MS. The retention time (R_t) of the extracts were shown in Figure 4.1. Mass spectrum (m/z) of each peak in the EAF and WF were summarized in Table 4.1 and 4.2, respectively. The EAF showed 40 definite peaks in the total ion chromatograms at R_t of 0.2, 20.1, 20.6, 21.3, 21.6, 22.0, 22.9, 23.7, 24.5, 24.7, 25.8, 26.0, 26.7, 27.1, 27.5, 28.2, 28.6, 29.0, 29.4, 29.7, 30.5, 30.8, 31.2, 32.3, 33.7, 34.2, 34.7, 35.0, 35.4, 35.7, 36.0, 36.2, 36.4, 37.1, 37.4, 38.0, 38.4, 38.7, 42.7 and 44.0. The corresponding mass spectrum of EAF showed the fragment ions as m/z 226, 721, 487, 486, 471, 455, 469, 435,406, 267,439, 453, 437, 417, 470, 424, and 421, respectively. While, the numbers of peaks observed in the total ion chromatograms of WF were 25 at R_t of 0.2, 1.5, 1.7, 1.8, 2, 2.3, 2.9, 8.4, 10.8, 13.4, 15.6, 17.5, 17.8, 18.6, 19.0, 19.4, 19.7, 21.6, 22.8, 23.0, 24.2, 24.3, 27.0, 29.5 and 34.3. The mass spectrum of WF showed corresponding fragment ions as m/z 226, 413, 219, 262, 276, 186, 369, 474, 1199, 717, 1035, 471, 608, 507, 633, 617, 621, 453 and 375. Compared to the available database, the presence of withanolides, 17β-Hydroxywithanolide K ($C_{28}H_{38}O_6$, 471), withanolide F ($C_{28}H_{38}O_6$, 471) and coagulin C ($C_{28}H_{36}O_5$, 453) were predicted in both fractions, whereas the presence of Coagulin L ($C_{34}H_{50}O_{12}$, 633) and Coagulin Q ($C_{34}H_{49}O_{10}$, 621) showed only in WF and Coagulanolide ($C_{28}H_{38}O_7$, 487) appeared only in EAF.

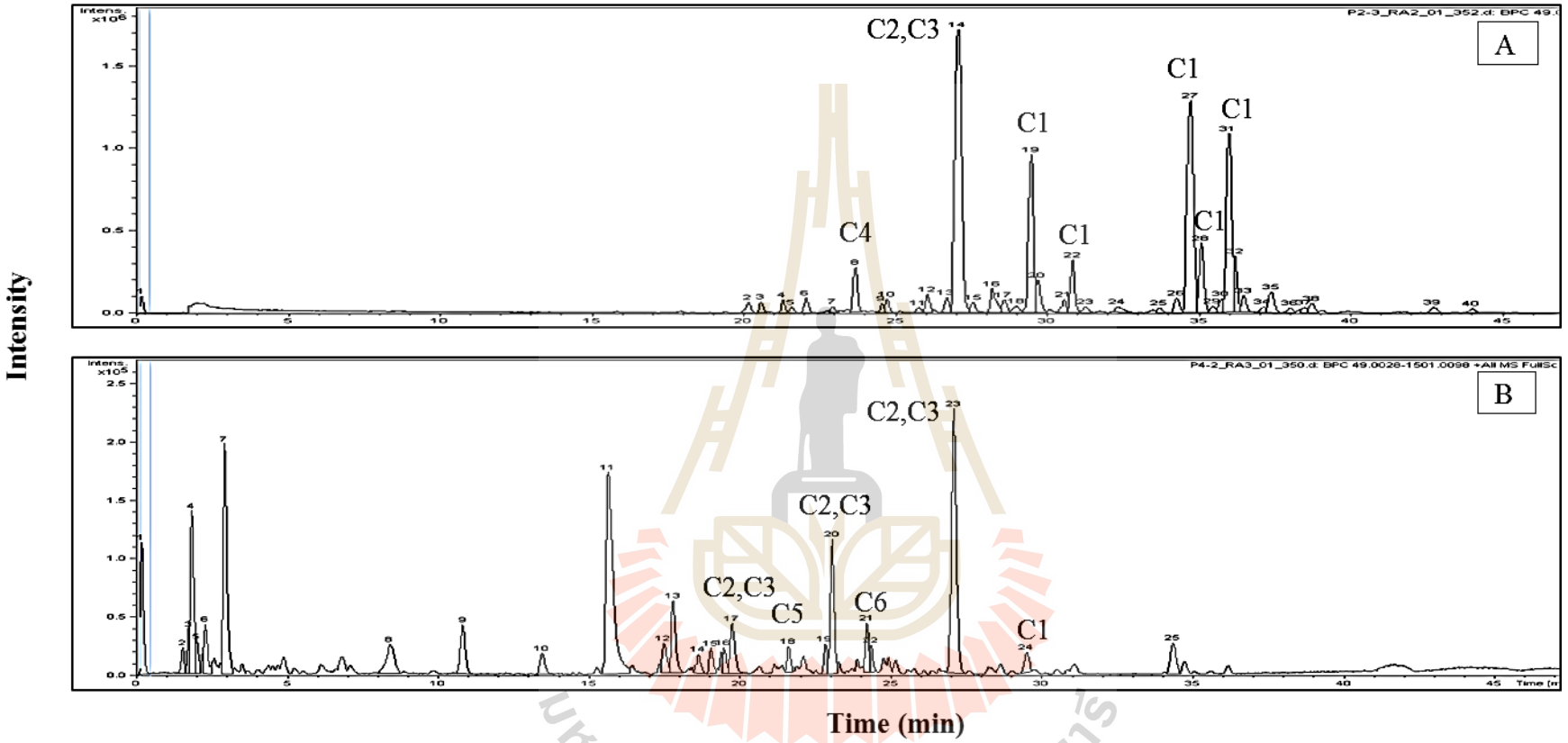

Figure 4.1 Total ion chromatograms and possible withanolides of EAF and WF analyzed by HPLC-MS. Panel A is the chromatogram of ethyl acetate fraction (EAF) and Panel B is the chromatogram of water fraction (WF). The possible withanolides consist of C1-C6. Coagulin C, 17β-Hydroxywithanolide K, Withanolide F, Coagulanolide, Coagulin L and Coagulin Q, respectively.

Table 4.1 The mass spectrum (m/z) of chemical compositions of ethyl acetate fraction (EAF) analyzed by HPLC-MS.

Peak	R_t [min]	Area	m/z	Structure	Possible Withanolide
1	0.2	659596	226.95	-	-
2	20.1	735023	721.32	-	-
3	20.6	488013	487.26	$C_{28}H_{38}O_7$	Coagulanolide
4	21.3	665290	486.26	$C_{28}H_{38}O_7$	Coagulanolide
5	21.6	337944	471.26	$C_{28}H_{38}O_6$	17β-Hydroxywithanolide K, Withanolide F
6	22	899707	471.27	$C_{28}H_{38}O_6$	17β-Hydroxywithanolide K, Withanolide F
7	22.9	370091	487.26	$C_{28}H_{38}O_7$	Coagulanolide
8	23.7	2666189	487.25	$C_{28}H_{38}O_7$	Coagulanolide
9	24.5	376445	486.76	$C_{28}H_{38}O_7$	Coagulanolide
10	24.7	620934	487.26	$C_{28}H_{38}O_7$	Coagulanolide
11	25.8	327192	471.27	$C_{28}H_{38}O_6$	17β-Hydroxywithanolide K, Withanolide F
12	26	1050309	487.26	$C_{28}H_{38}O_7$	Coagulanolide
13	26.7	915422	471.27	$C_{28}H_{38}O_6$	17β-Hydroxywithanolide K, Withanolide F
14	27.1	27413675	471.27	$C_{28}H_{38}O_6$	17β-Hydroxywithanolide K, Withanolide F
15	27.5	708106	455.28	-	-
16	28.2	1770781	469.26	-	-
17	28.6	798101	435.25	-	-
18	29	527917	471.27	$C_{28}H_{38}O_6$	17β-Hydroxywithanolide K, Withanolide F
19	29.4	11063177	453.26	$C_{28}H_{36}O_5$	Coagulin C
20	29.7	1957476	469.26	-	-
21	30.5	825256	406.28	-	-
22	30.8	3123310	453.26	$C_{28}H_{36}O_5$	Coagulin C

Table 4.1 The mass spectrum (m/z) of chemical compositions of ethyl acetate fraction (EAF) analyzed by HPLC-MS (Continued).

Peak	R_t [min]	Area	m/z	Structure	Possible Withanolide
23	31.2	462506	267.17	-	-
24	32.3	599144	453.26	$C_{28}H_{36}O_5$	Coagulin C
25	33.7	337629	469.26	-	-
26	34.2	1070304	439.28	-	-
27	34.7	19407595	453.26	$C_{28}H_{36}O_5$	Coagulin C
28	35	4424427	453.26	$C_{28}H_{36}O_5$	Coagulin C
29	35.4	382501	437.26	-	-
30	35.7	732030	437.26	-	-
31	36	1350224	453.26	$C_{28}H_{36}O_5$	Coagulin C
32	36.2	2499880	437.26	-	-
33	36.4	950694	453.26	$C_{28}H_{36}O_5$	Coagulin C
34	37.1	353029	437.26	-	-
35	37.4	1668368	417.24	-	-
36	38	403318	469.26	-	-
37	38.4	367913	470.29	$C_{28}H_{38}O_6$	17β-Hydroxywithanolide K, Withanolide F
38	38.7	746000	417.24	-	-
39	42.7	502791	424.29	-	-
40	44	298177	421.27	-	-

Table 4.2 The mass spectrum (m/z) of chemical compositions of water fraction (WF) analyzed by HPLC-MS.

Peak	R_t [min]	Area	m/z	Structure	Possible Withanolide
1	0.2	745922	226.95	-	-
2	1.5	156125	413.21	-	-
3	1.7	143125	219.02	-	-
4	1.8	1122771	262.12	-	-
5	2	174411	262.12	-	-
6	2.3	358827	276.14	-	-
7	2.9	1671601	186.09	-	-
8	8.4	470987	369.11	-	-
9	10.8	456100	474.26	-	-

Table 4.2 The mass spectrum (m/z) of chemical compositions of water fraction (WF) analyzed by HPLC-MS (Continued).

Peak	R_t [min]	Area	m/z	Structure	Possible Withanolide
10	13.4	201721	369.11	-	-
11	15.6	2739216	1199.06	-	-
12	17.5	269547	717.39	-	-
13	17.8	625726	1035.41	-	-
14	18.6	163665	471.27	$C_{28}H_{38}O_6$	17β-Hydroxywithanolide K, Withanolide F
15	19	190570	608.28	-	-
16	19.4	164769	507.19	-	-
17	19.7	441064	471.27	$C_{28}H_{38}O_6$	17β-Hydroxywithanolide K, Withanolide F
18	21.6	175329	633.32	$C_{34}H_{50}O_{12}$	Coagulin L
19	22.8	192748	617.332	-	-
20	23	943673	471.27	$C_{28}H_{38}O_6$	17β-Hydroxywithanolide K, Withanolide F
21	24.2	325940	621.36	$C_{34}H_{49}O_{10}$	Coagulin Q
22	24.3	140190	621.36	$C_{34}H_{49}O_{10}$	Coagulin Q
23	27	2455037	471.27	$C_{28}H_{38}O_6$	17β-Hydroxywithanolide K, Withanolide F
24	29.5	184992	453.26	$C_{28}H_{36}O_5$	Coagulin C
25	34.3	344482	376.25	-	-

4.2 Toxicity of the ethyl acetate and water fractions

4.2.1 *In vitro* cytotoxicity of the ethyl acetate and water fractions

The cytotoxicity effects of EAF and WF on HepG2 cells were evaluated by MTT and trypan blue exclusion assays. After treatment with EAF at the doses 0-100 µg/ml for 24 h, the result was shown as Figure 4.2. The MTT result showed that EAF at the concentrations higher than 20 µg/ml significantly decreased the viability of HepG2 cells when compared to control (P<0.05), as show in Figure 4.2A. While, the toxicity effect of EAF on HepG2 cells viability determined by trypan blue exclusion method at the concentrations higher than 80 µg/ml significantly decreased the viability of HepG2 cells (Figure 4.2B). The effect of WF on the viability of HepG2 cells was shown in Figure 4.3. After treated with WF at 0-10,000 µg/ml, the results from trypan blue exclusion method demonstrated that all concentrations of WF did not significantly decrease the cell viability when compared to control (Figure 4.3B). Whereas the results from MTT method showed that the concentration of WF higher than 5,000 µg/ml significantly decreased the viability of HepG2 cells when compared to control (P<0.05), as shown in Figure 4.3A. Since, the cytotoxicity effect of EAF and WF on HepG2 cells showed difference of the toxic dose after determination by MTT and trypan blue exclusion assays. Therefore, the morphological of HepG2 cells after treated with EAF and WF were checked under light microscope as demonstrated in Figure 4.4 and Figure 4.5, respectively. The morphological changes of HepG2 cells after treated with EAF and WF were better correlated with cytotoxicity results determined by MTT method. The vehicle control (0.5% DMSO) did not cause any morphological changes of HepG2 cells or damages in both assays. The half maximal inhibitory concentrations

(IC_{50}) of EAF and WF on HepG2 cells viability by MTT assay were found at 43.60 ± 2.32 and 10,697.86 ± 938.65 µg/ml, respectively.

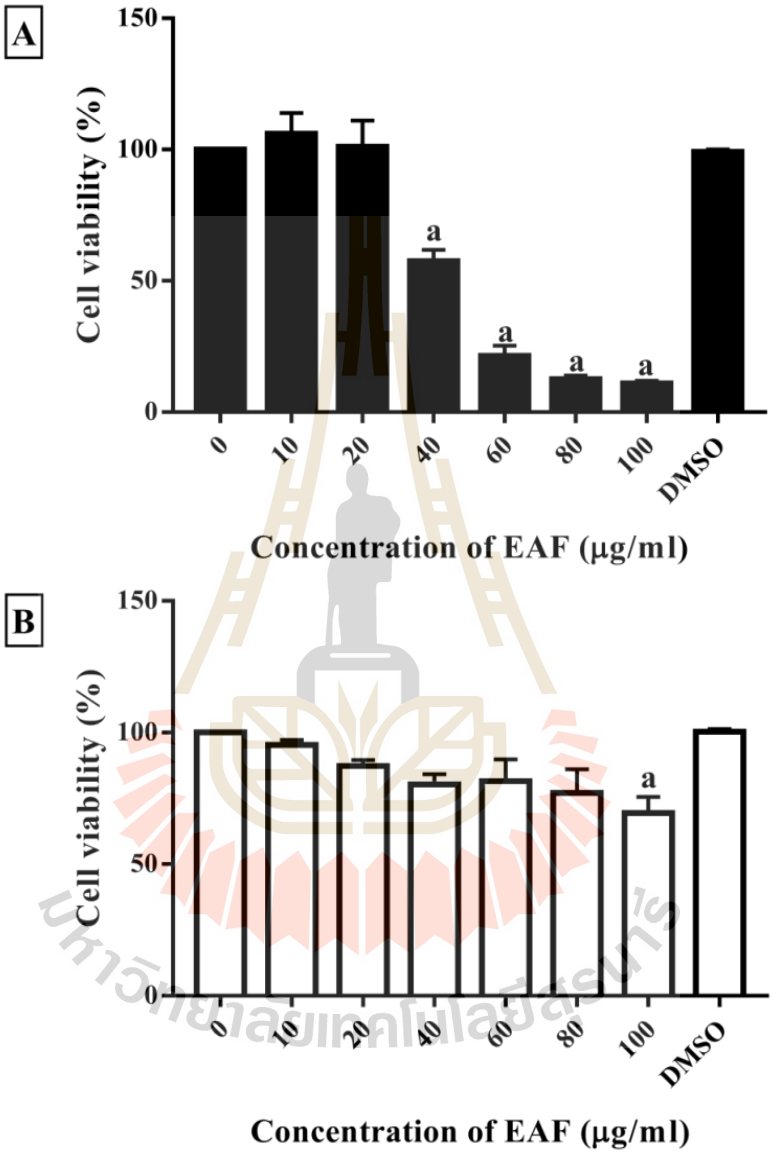

Figure 4.2 Cytotoxicity of ethyl acetate fraction (EAF) on HepG2 cells after treated at various concentrations of EAF. Panels A and B are the cytotoxicity results determined by MTT and trypan blue exclusion methods, respectively. Values are expressed as mean ± SEM (n=4). [a] $P<0.05$; statistically significant difference from control.

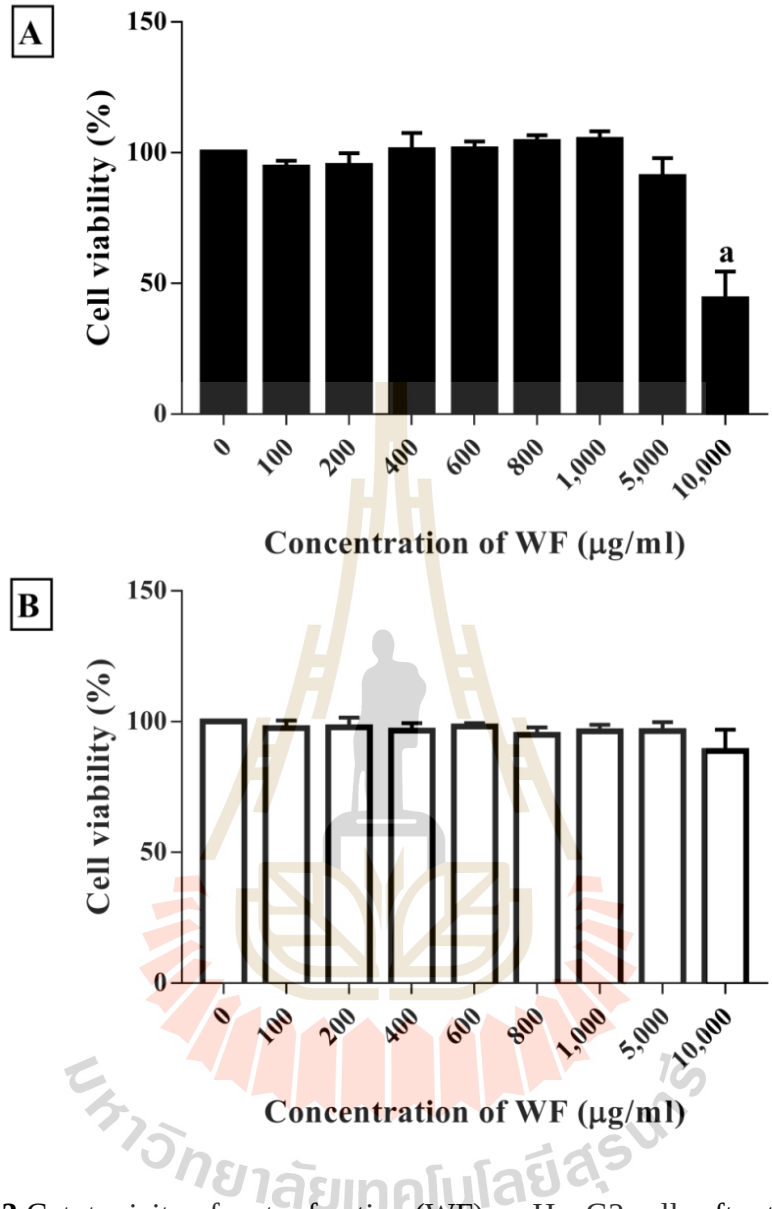

Figure 4.3 Cytotoxicity of water fraction (WF) on HepG2 cells after treated at various concentrations of WF. Panels A is cytotoxicity result determined by MTT method and Panels B is cytotoxicity result determine by trypan blue exclusion assay. Values are expressed as mean ± SEM (n = 4). [a] $P<0.05$; statistically significant difference from control.

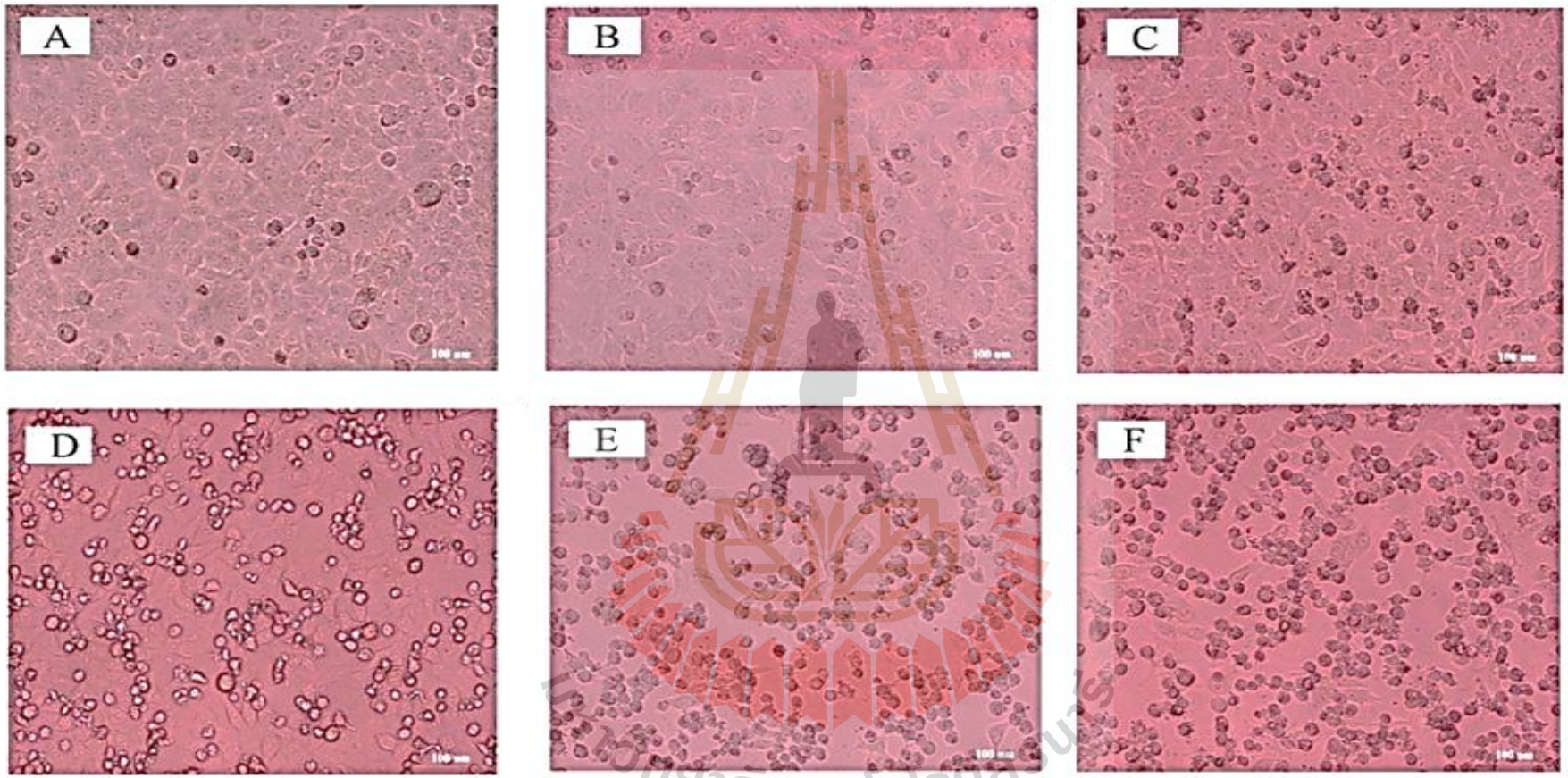

Figure 4.4 The morphology of HepG2 cells under light microscope after treatment for 24 h with various concentrations of ethyl acetate fraction. A = control; B = 10 µg/ml; C = 20 µg/ml; D = 40 µg/ml; E = 60 µg/ml; F = 80 µg/ml; G = 100 µg/ml and H = vehicle control (0.5% DMSO).

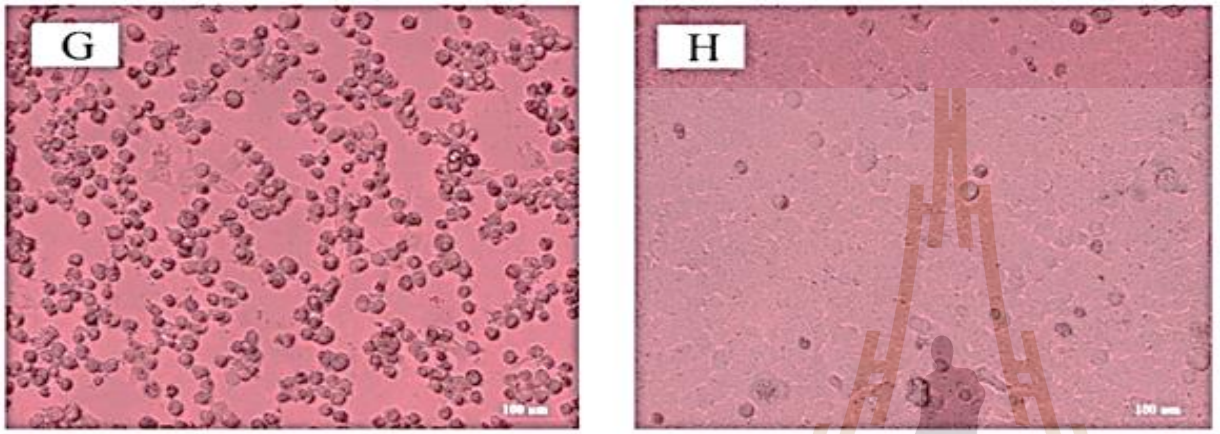

Figure 4.5 The morphology of HepG2 cells under light microscope after treatment for 24 h with various concentrations of ethyl acetate fraction (Continued). A = control; B = 10 µg/ml; C = 20 µg/ml; D = 40 µg/ml; E = 60 µg/ml; F = 80 µg/ml; G = 100 µg/ml and H = vehicle control (0.5% DMSO).

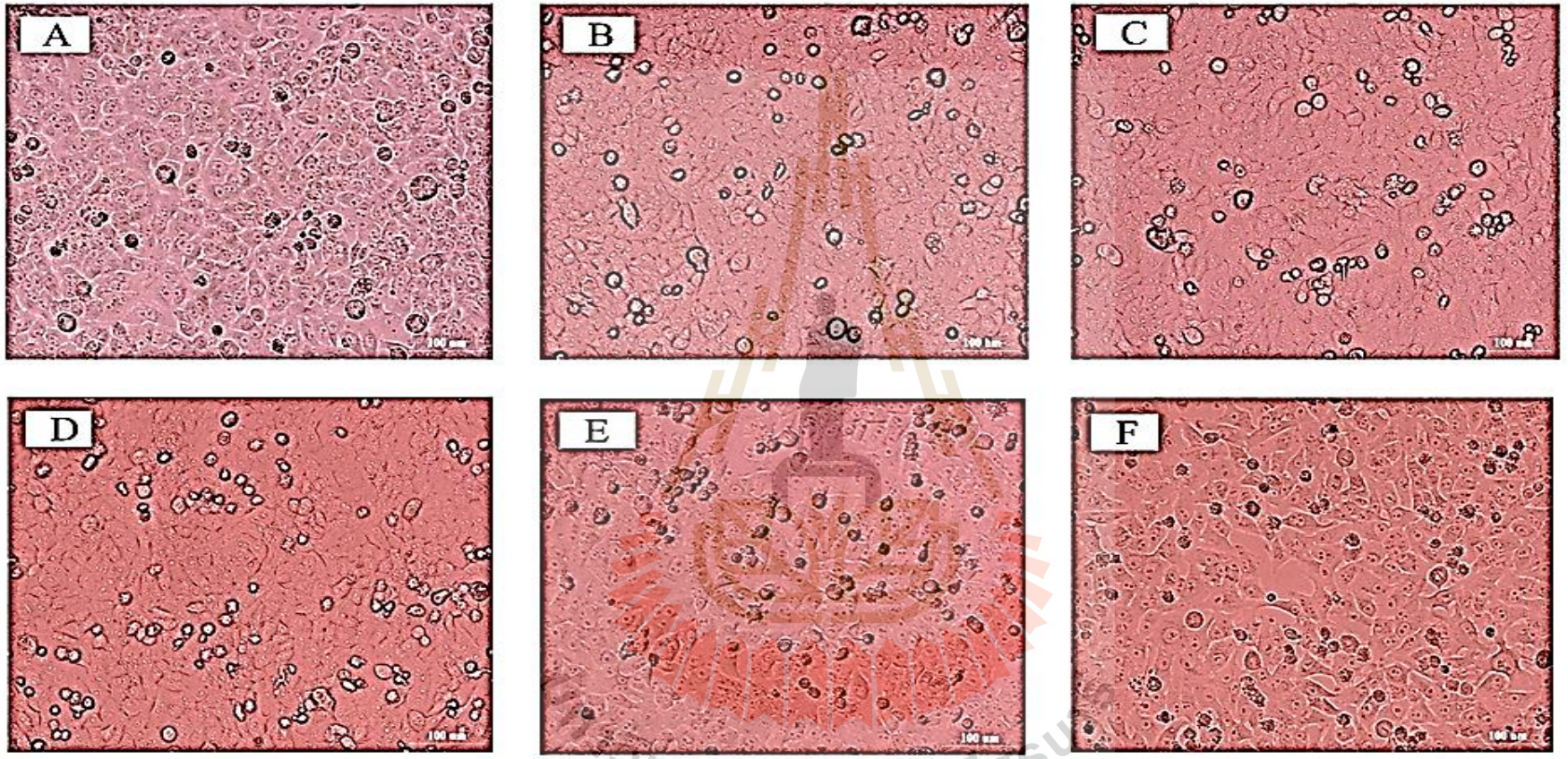

Figure 4.6 The morphology of HepG2 cells under light microscope after treatment for 24 h with various concentrations of water fraction.

A = control; B = 100 µg/ml; C = 200 µg/ml; D = 400 µg/ml; E = 600 µg/ml; F = 800 µg/ml; G = 1,000 µg/ml; H = 5,000 µg/ml and I = 10,000 µg/ml.

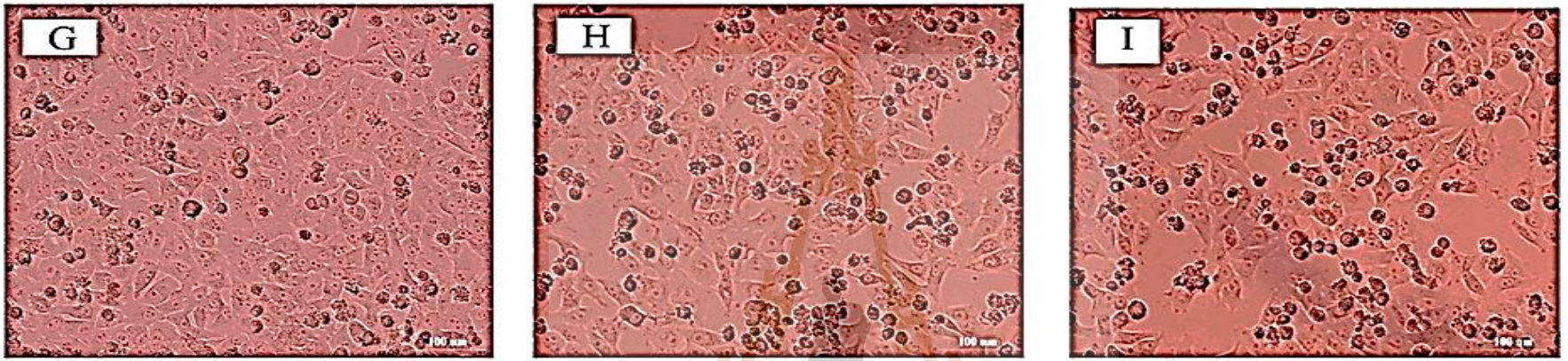

Figure 4.7 The morphology of HepG2 cells under light microscope after treatment for 24 h with various concentrations of water fraction (Continued). A = control; B = 100 µg/ml; C = 200 µg/ml; D = 400 µg/ml; E = 600 µg/ml; F = 800 µg/ml; G = 1,000 µg/ml; H = 5,000 µg/ml and I = 10,000 µg/ml.

4.2.2 Sub-chronic toxicity of the fractions in normal mice

4.2.2.1 Effect of ethyl acetate and water fractions on body weight and blood glucose levels

Sub-chronic administration of EAF and WF at the dose of 50 mg/kg did not induce abnormal behaviours in normal mice and clinical signs of toxicity during 10 days. The body weights and blood glucose levels in all groups were observed and the results are shown in Table 4.3. There were no significant differences when compared with control group (P>0.05).

Table 4.3 Effects of fractions on body weight and blood glucose levels of mice in all groups during experiment.

Treatment	**Body weight (g)**		
	Day 0	**Day 5**	**Day 10**
N+DI	34.20 ± 0.73	34.60 ± 0.81	34.60 ± 0.51
N+DMSO	34.60 ± 0.60	35.60 ± 0.68	34.80 ± 0.58
N+EAF	35.40 ± 0.51	37.60 ± 0.81	36.00 ± 0.55
N+WF	34.60 ± 0.51	35.80 ± 0.58	35.20 ± 0.80
Treatment	**Fasting blood glucose levels (mg/dl)**		
	Day 0	**Day 5**	**Day 10**
N+DI	104.66 ± 6.56	141.20 ± 7.23	102.60 ± 4.50
N+DMSO	97.40 ± 14.70	143.20 ± 11.17	124.80 ± 7.64
N+EAF	97.40 ± 7.70	170.40 ± 12.33	103.80 ± 13.49
N+WF	90.60 ± 5.09	128.00 ± 3.41	101.40 ± 3.49

Values are expressed as mean ± SEM (n=5/group).
N+DI, normal control mice receiving sterile water; N+DMSO, normal mice receiving 10% dimethyl sulfoxide (vehicle control); N+EAF, normal mice receiving ethyl acetate fraction at 50 mg/kg; N+WF, normal mice receiving water fraction at 50 mg/kg. P>0.05; no significant difference when compared with control group.

4.2.2.2 Effects of ethyl acetate and water fractions on organ weights, biochemical parameters and histopathology

At the end of sub-chronic toxicity study, the organ weights (liver, kidney and pancreas), biochemical parameters (AST, ALT, BUN and creatinine) and tissue histology (liver, kidney and pancreas) of normal mice after receiving EAF and WF were evaluated. The results were shown in Tables 4.4-4.5 and Figures 4.6-4.8. All of the biochemical parameters and organ weights, except for BUN value of WF treatment (P<0.05), were not significantly different in all animals treated groups from the control group. Although, the BUN values of WF treated-group showed significant different when compared to control group, the values stayed in the range of BUN standard (shows in Appendix A). Moreover, the histopathological examination results of liver (Figure 4.6), kidney (Figure 4.7) and pancreas (Figure 4.8) in all treated groups showed no differences when compared to normal group. Overall, EAF and WF as well as 10% DMSO (vehicle control) did not induce liver, kidney and pancreas toxicities in normal mice.

Table 4.4 Effects of the *W. coagulans* fractions on organ weights.

Treatment	**Organ weight (g/body weight)**		
	Liver	**Kidney**	**Pancreas**
N+DI	0.042 ± 0.002	0.019 ± 0.001	0.007±0.000
N+DMSO	0.039 ± 0.002	0.017 ± 0.001	0.006±0.000
N+EAF	0.043 ± 0.001	0.018 ± 0.001	0.007±0.000
N+WF	0.039 ± 0.001	0.017 ± 0.001	0.007±0.000

Values are expressed as mean ± SEM. (n=5/group) N+DI, normal control mice receiving sterile water; N+DMSO, normal mice receiving 10% dimethyl sulfoxide (vehicle control); N+EAF, normal mice receiving ethyl acetate fraction at 50 mg/kg; N+WF, normal mice receiving water fraction at 50 mg/kg. P>0.05; no significant difference when compared with control group.

Table 4.5 Effects of the *W. coagulans* fractions on biochemical parameters.

Treatment	Biochemical parameters			
	AST (U/I)	**ALT (U/I)**	**BUN (mg/dl)**	**Creatinine (mg/dl)**
N+DI	97.20 ± 15.29	38.40 ± 1.21	19.34 ± 0.63	0.44 ± 0.05
N+DMSO	122.80 ± 15.54	39.60 ± 1.33	21.72 ± 0.87	0.36 ± 0.04
N+EAF	94.20 ± 6.89	36.60 ± 1.47	21.58 ± 1.91	0.38 ± 0.04
N+WF	116.80 ± 9.55	38.60 ± 2.29	31.18 ± 0.62[a]	0.46 ± 0.04

Values are expressed as mean±SEM. (n=5/group) N+DI, normal control mice receiving sterile water; N+DMSO, normal mice receiving 10% dimethyl sulfoxide (vehicle control); N+EAF, normal mice receiving ethyl acetate fraction at 50 mg/kg; N+WF, normal mice receiving water fraction at 50 mg/kg. [a]$P<0.05$; statistically significant difference from normal control.

4.3 *In vivo* antidiabetic activities of the extracts

4.3.1 Acute hypoglycemia activity on normal mice

4.3.1.1 Effects on oral glucose tolerance test

A single dose of EAF and WF (50 mg/kg), and glibenclamide (20 mg/kg) were orally administered before feeding glucose solution for 30 min. The effects of EAF, WF and glibenclamide (used as positive control) on blood glucose levels at 0-120 min were shown in Figure 4.9A. The initial blood glucose levels of all groups were not significantly different. After 30 min of receiving 2g/kg glucose solution, the blood glucose levels decreased subsequently over the time in all experiment groups. Moreover, the AUC index of WF and glibenclamide, but not EAF, treated groups showed significant differences when compared to control group ($P<0.05$), as illustrated in Figure 4.9B. Therefore, this result indicated that WF had significantly improved glucose tolerance in normal mice similar to the standard drug glibenclamide. It is noted that vehicle control (10% DMSO) did not affect glucose tolerance.

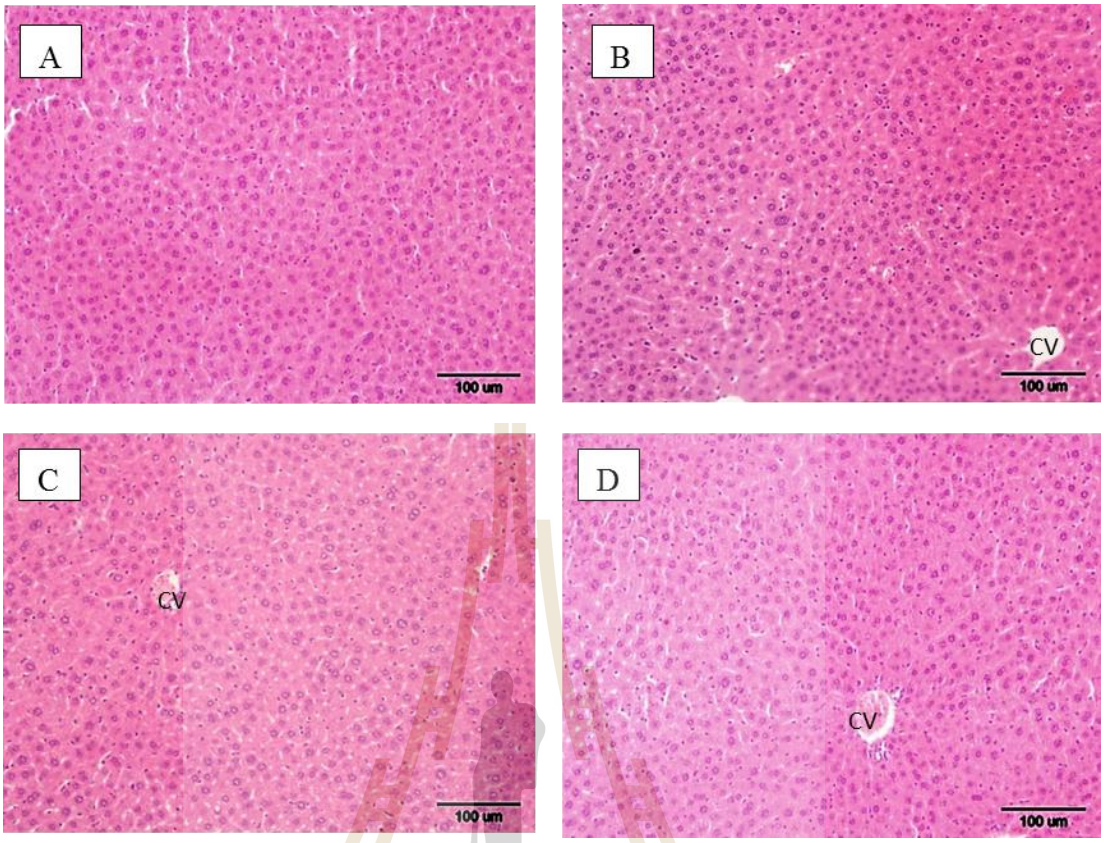

Figure 4.8 Photomicrographs of liver of normal male mice after treated with the extracts. Mice were orally administered with the ethyl acetate and water fractions at 50 mg/kg for 10 days in sub-chronic toxicity experiment. The liver histology showed normality of hepatic cell morphology in all experiment groups. A: N+DI, normal control mice receiving sterile water, B: N+DMSO, normal mice receiving 10% DMSO (vehicle control), C: N+EAF, normal mice receiving the ethyl acetate fraction at 50 mg/kg, D: N+WF, normal mice receiving the water fraction at 50 mg/kg. CV is the central vein in liver. Hematoxylin and eosin staining (200X).

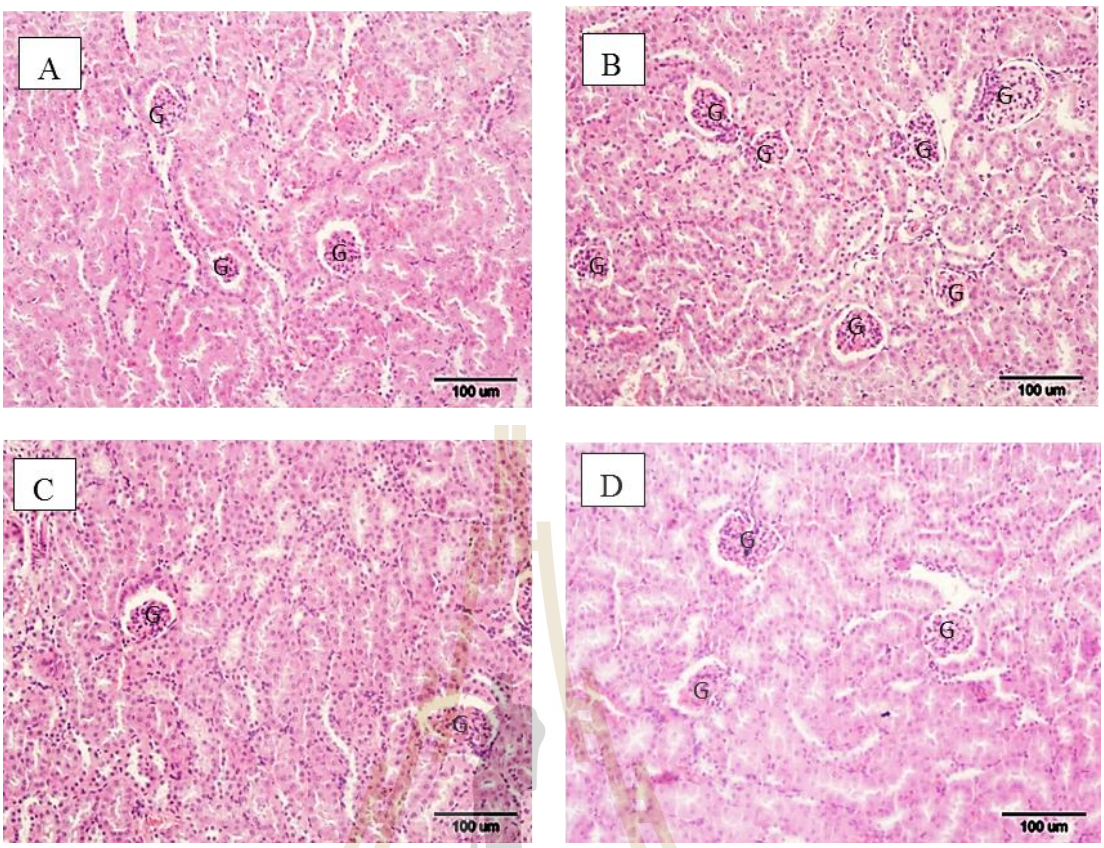

Figure 4.9 Photomicrographs of kidney of normal male mice after treated with the extracts. The kidney histology showed normality of kidney morphology in all experiment groups. A: N+DI, normal control mice receiving sterile water, B: N+DMSO, normal mice receiving 10% DMSO (vehicle control), C: N+EAF, normal mice receiving the ethyl acetate fraction at 50 mg/kg, D: N+WF, normal mice receiving the water fraction at 50 mg/kg. G is glomerulus of kidney. Hematoxylin and eosin staining (200X).

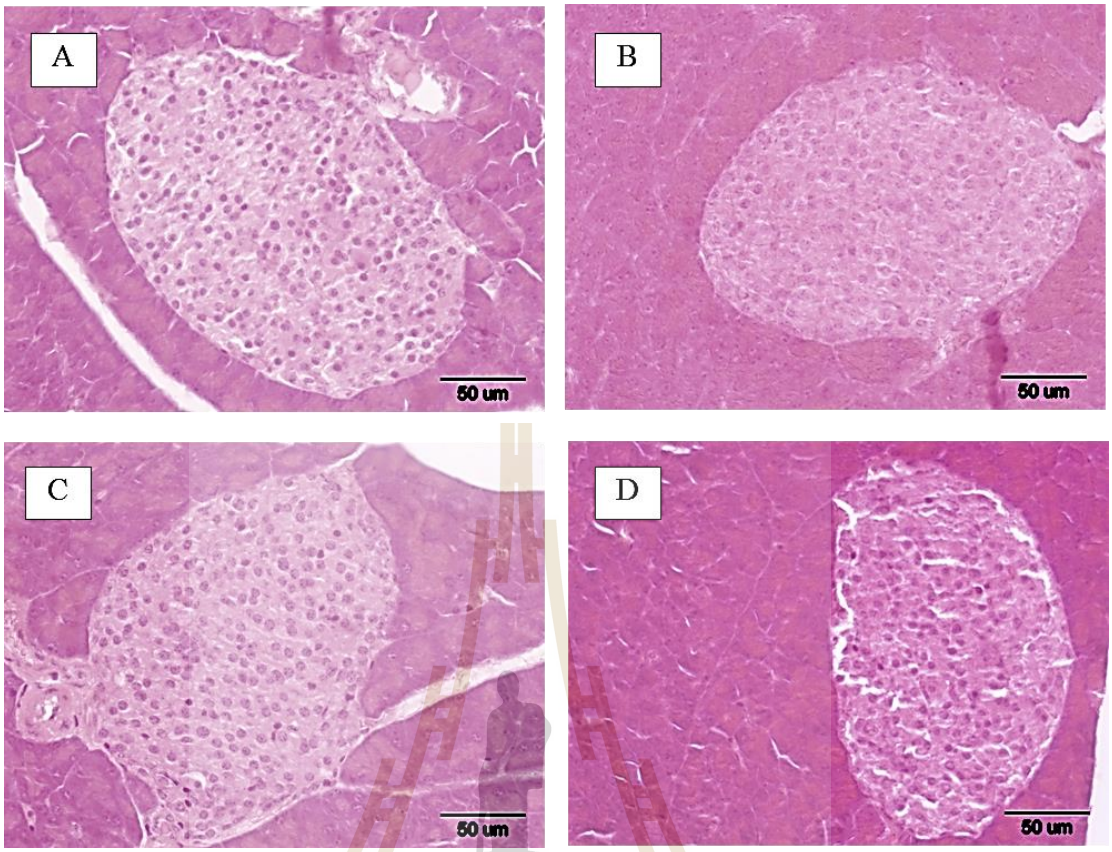

Figure 4.10 Photomicrographs of pancreas of normal male mice after administered with the extracts. The pancreas histological results show normality of size and morphology of ielts of Langerhan in all experiment groups. A: N+DI, normal control mice receiving sterile water, B: N+DMSO, normal mice receiving 10% DMSO (vehicle control), C: N+EAF, normal mice receiving the ethyl acetate fraction at 50 mg/kg, D: N+WF, normal mice receiving the water fraction at 50 mg/kg. Hematoxylin and eosin staining (400X).

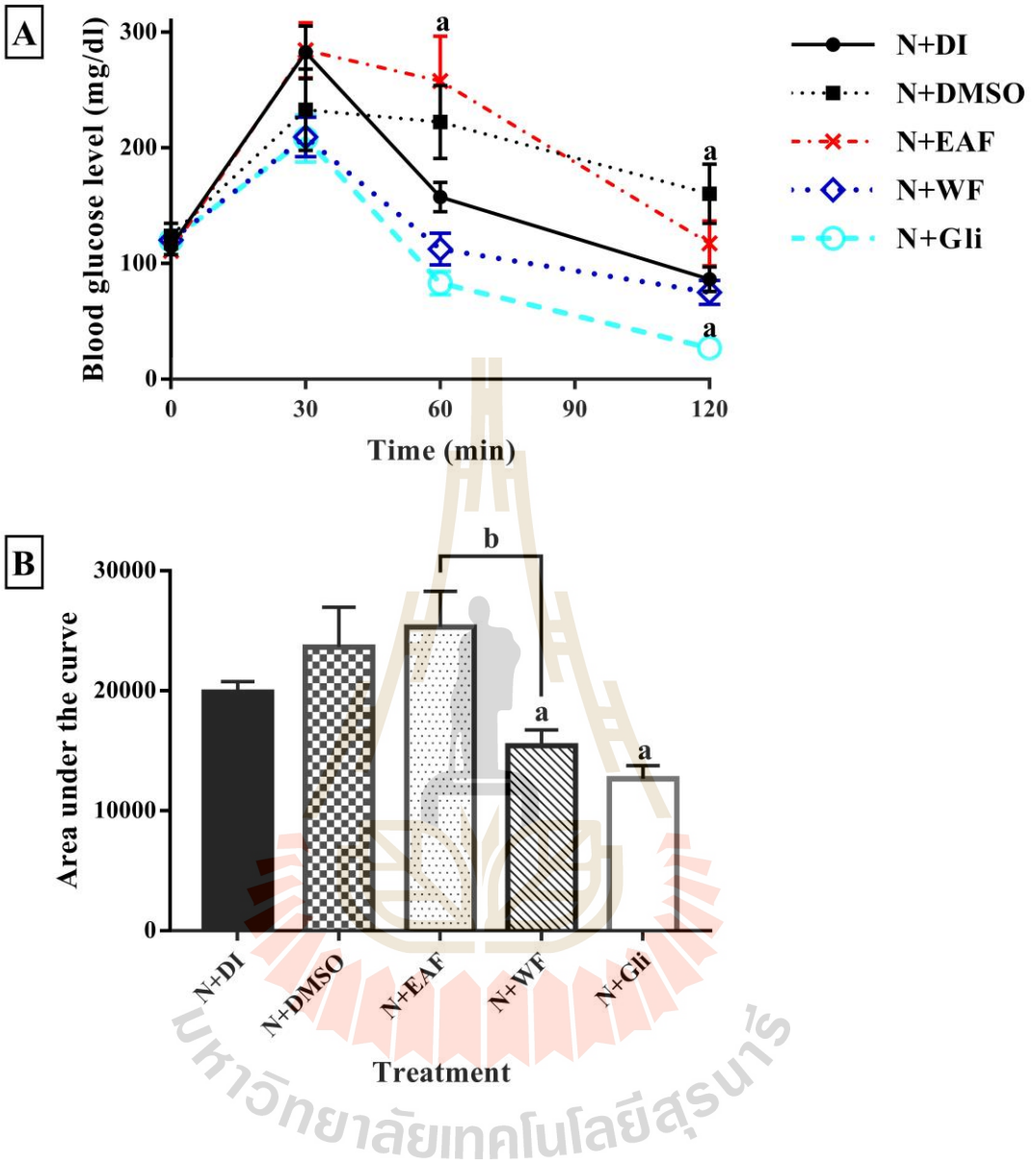

Figure 4.11 The effects of the extracts on oral glucose tolerance test (OGTT) in normal mice. Panel A is blood glucose levels during 0-120 minutes after glucose feeding. Panel B is the area under the curve (AUC), which calculated from blood glucose levels at 0-120 minutes. Values are expressed as mean ± SEM (n=6). [a]*P*<0.05; statistically significant difference from normal control. [b]*P*<0.05; statistically significant difference from water fraction group.

4.3.2 Antihyperglycemic activity in alloxan-induced diabetic mice

4.3.2.1 Effects of ethyl acetate and water fractions on body weight and fasting blood glucose levels

At the initial of experiment, the body weights of diabetic mice induced by alloxan at the dose 120 mg/kg showed significant weight loss in all groups when compared with normal control. After receiving EAF, WF and glibenclamide for 10 days, no animal showed any significant changes in the body weight from the beginning (Table 4.6). Blood glucose levels of the experimental animals were shown in Table 4.6. At the beginning of study, the blood glucose levels in all diabetic groups were significantly higher than normal control group (P<0.05). After receiving drugs for 10 days, blood glucose levels of all treated-groups significantly decreased compared to diabetic control group (P<0.05). The animals which were administered with EAF showed a significant decrease in blood glucose level at day 5, but not at day 10. In contrast, blood glucose levels of diabetic mice treated with WF continuously declined and appeared significantly decreased after receiving WF for 10 days compared to diabetic control group (P<0.05).

4.3.2.2 Effects of the ethyl acetate and water fractions on oral glucose tolerance test

After administered with the sample for 10 days, all of experimental animals were evaluated by oral glucose tolerance test (OGTT). The blood glucose levels at 0-120 min of all experiment groups were shown at Figure 4.10A. The AUC results (Figure 4.10B) indicated that only diabetic mice receiving WF significantly improved glucose tolerance when compared with diabetic control group (P<0.05), similar to

glibenclamide. The vehicle (10% DMSO) did not significant affect glucose tolerance to the animals.

Table 4.6 Body weight and fasting blood glucose of diabetic mice after treated with the extracts for 10 days.

Treatment	**Body weight (g)**		
	0 day	**5 day**	**10 day**
N+DI	34.26 ± 0.52	36.94 ± 0.71	37.93 ± 0.89
DM+DI	26.86 ± 1.08[a]	26.37 ± 0.28[a]	26.24 ± 0.37[a]
DM+DMSO	27.50 ± 1.27[a]	26.54 ± 1.26[a]	27.09 ± 1.11[a]
DM+EAF	28.28 ± 0.73[a]	25.98 ± 1.19[a]	26.09 ± 1.48[a]
DM+WF	27.94 ± 1.43[a]	26.02 ± 2.17[a]	26.08 ± 2.27[a]
DM+Gli	28.47 ± 1.10[a]	26.89 ± 1.05[a]	25.99 ± 1.61[a]
Treatment	**Fasting blood glucose levels (mg/dl)**		
	0 day	**5 day**	**10 day**
N+DI	135.17±2.91[b]	146.50±3.69[b]	116.67±10.63[b]
DM+DI	396.40±41.51[a]	408.60±39.60[a]	489.60±23.24[a]
DM+DMSO	398.20±35.86[a]	356.00±39.88[a]	430.80±54.37[a]
DM+EAF	419.00±35.85[a]	228.50±18.06[ab]	357.00±32.87[a]
DM+WF	402.80±43.02[a]	325.20±66.40[a]	286.20±69.69[ab]
DM+Gli	430.17±39.31[a]	196.00±51.38[b]	292.60±47.01[ab]

Values are expressed as mean ± SEM (n=5-6). N+DI, normal control mice receiving sterile water; DM+DI, diabetic mice receiving sterile water; DM+DMSO, diabetic mice receiving dimethyl sulfoxide; DM+EAF, diabetic mice receiving ethyl acetate fraction at 50 mg/kg; DM+WF, diabetic mice receiving water fraction at 50 mg/kg; DM+Gli, and diabetic mice receiving glibenclamide at 20 mg/kg. [a]$P<0.05$; statistically significant difference from normal control. [b]$P<0.05$; statistically significant difference from diabetic control.

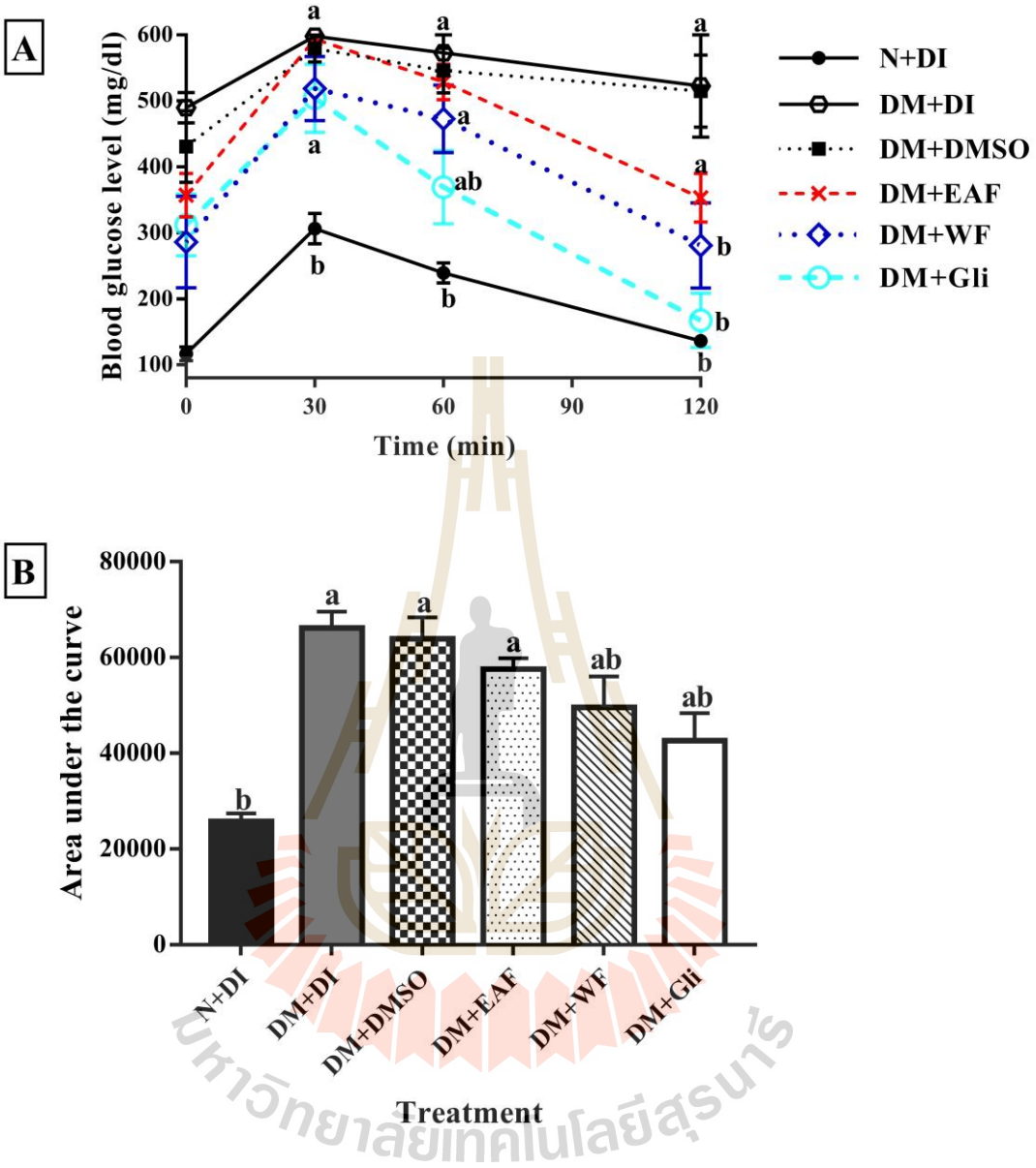

Figure 4.12 The effects of the ethyl acetate and water fractions on oral glucose tolerance test (OGTT) in diabetic mice. Panel A is blood glucose levels during the test, while Panel B is the calculated area under the curve (AUC). Values are expressed as mean ± SEM (n=5-6). [a]*P*<0.05; statistically significant difference from normal control. [b]*P*<0.05; statistically significant difference from diabetic control.

4.3.2.3 Effects of the ethyl acetate and water fractions on organ weight, biochemical parameters and histopathology

The data of organs weight (liver, kidney and pancreas), biochemical parameters (AST, ALT, Albumin, creatinine, LDL, HDL and triglyceride) of all treated groups were summarized in Tables 4.7-4.8, whereas tissue histology (liver, kidney and pancreas) were presented in Figures 4.11-4.13. The results showed that all of the organ weight and biochemical parameters were not significantly different in all treated groups when compared with control (P<0.05). However, the pancreas histology revealed that islets of Langerhan in all diabetic groups had the smaller area than those of normal control group (Figure 4.13). The results from histopathological examination indicated that alloxan induced damages of pancreatic β-cells, but not liver and kidney in this experiment.

Table 4.7 Organs weight of normal mice and diabetic mice after treatments.

Treatment	**Organ weight (g/body weight)**		
	Liver	**Kidney**	**Pancreas**
N+DI	0.042 ± 0.002	0.018 ± 0.001	0.005 ± 0.000
DM+DI	0.052 ± 0.002	0.025 ± 0.001	0.005 ± 0.000
DM+DMSO	0.051 ± 0.002	0.023 ± 0.000	0.006 ± 0.001
DM+EAF	0.053 ± 0.004	0.024 ± 0.002	0.004 ± 0.001
DM+WF	0.056 ± 0.004	0.024 ± 0.001	0.005 ± 0.001
DM+Gli	0.050 ± 0.001	0.027 ± 0.001	0.006 ± 0.001

Values are expressed as mean ± SEM (n=5-6).
N+DI, normal control mice receiving sterile water; DM+DI, diabetic mice receiving sterile water; DM+DMSO, diabetic mice receiving dimethyl sulfoxide; DM+EAF, diabetic mice receiving ethyl acetate fraction at 50 mg/kg; DM+WF, diabetic mice receiving water fraction at 50 mg/kg; DM+Gli, and diabetic mice receiving glibenclamide at 20 mg/kg. P>0.05; no significant difference when compared with control group.

Table 4.8 The biochemical parameters of normal mice and diabetic mice after drug treatments for 10 days.

Treatment	Biochemical parameters						
	AST (U/I)	ALT (U/I)	Albumin (g/dl)	Creatinine (mg/dl)	LDL (mg/dl)	HDL (mg/dl)	Triglyceride (mg/dl)
N+DI	36.50±2.05	44.83±2.36	2.95±0.33	1.37±0.31	25.05±2.65	41.30±2.36	177.83±11.55
DM+DI	37.80±3.44	36.80±3.92	2.52±0.27	0.92±0.09	23.26±1.86	45.38±3.31	175.00±17.34
DM+DMSO	25.00±3.78	44.60±3.03	2.72±0.33	1.32±0.22	25.73±3.09	49.48±4.52	177.40±18.69
DM+EAF	26.33±3.51	47.00±3.19	2.60±0.30	1.10±0.21	23.27±2.32	49.13±3.18	204.50±15.52
DM+WF	27.00±2.31	44.40±3.04	2.60±0.41	1.74±0.25	23.98±3.64	45.84±2.46	170.40±13.67
DM+Gli	30.40±4.01	38.40±4.01	2.66±0.37	1.18±0.35	26.12±3.38	49.42±4.82	186.40±10.56

Values are expressed as mean ± SEM (n=5-6).
N+DI, normal control mice receiving sterile water; DM+DI, diabetic mice receiving sterile water; DM+DMSO, diabetic mice receiving dimethyl sulfoxide; DM+EAF, diabetic mice receiving ethyl acetate fraction at 50 mg/kg; DM+WF, diabetic mice receiving water fraction at 50 mg/kg; DM+Gli, and diabetic mice receiving glibenclamide at 20 mg/kg.
P>0.05; no significant difference when compared with control group.

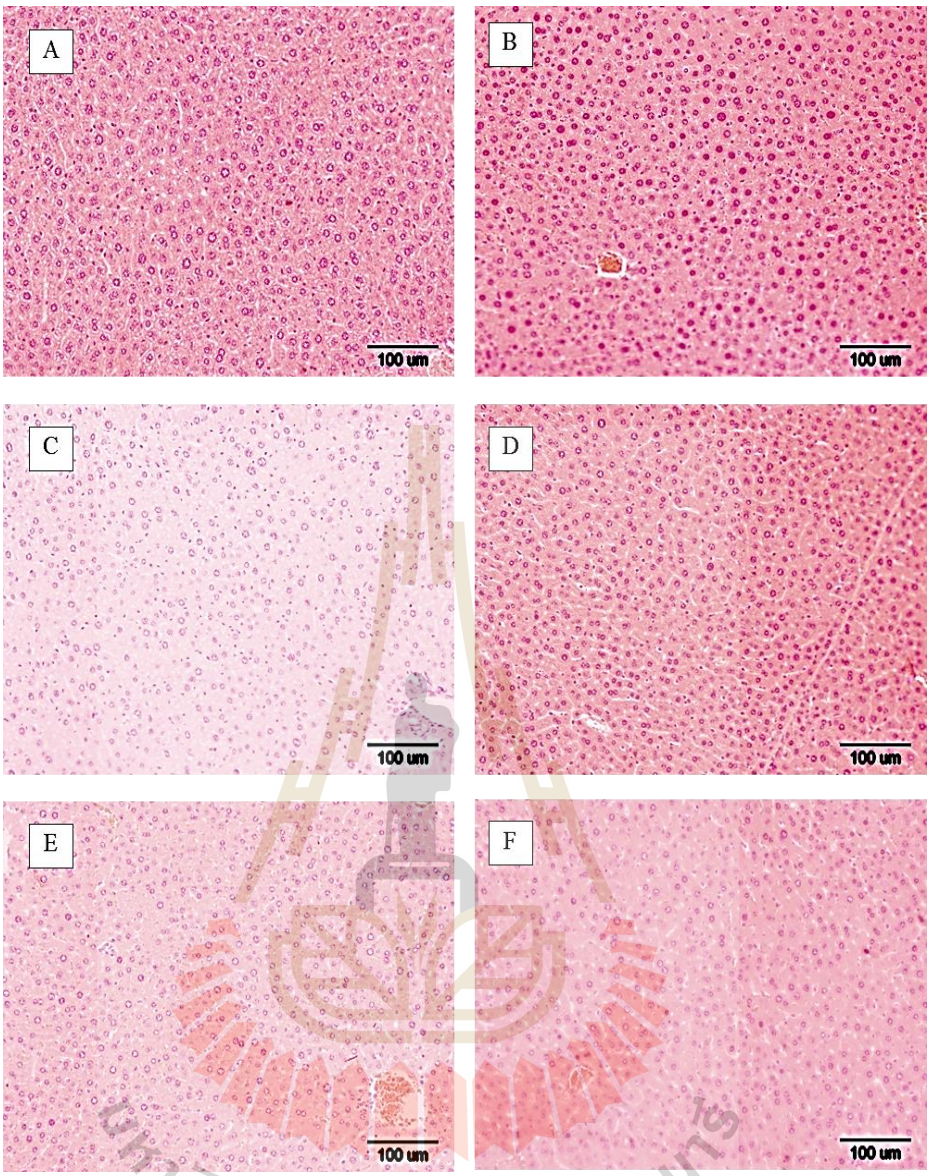

Figure 4.13 Photomicrographs of liver of normal mice and diabetic mice. All drug-treated animals had normal morphology of hepatic cells. A: N+DI, normal control mice receiving sterile water, B: DM+DI, diabetic mice receiving sterile water, C: DM+DMSO, diabetic mice receiving 10% dimethyl sulfoxide (vehicle control), D: DM+EAF, diabetic mice receiving ethyl acetate fraction at 50 mg/kg, E: DM+WF, diabetic mice receiving water fraction at 50 mg/kg, and F: DM+Gli, diabetic mice receiving glibenclamide at 20 mg/kg. Hematoxylin and eosin staining (200X).

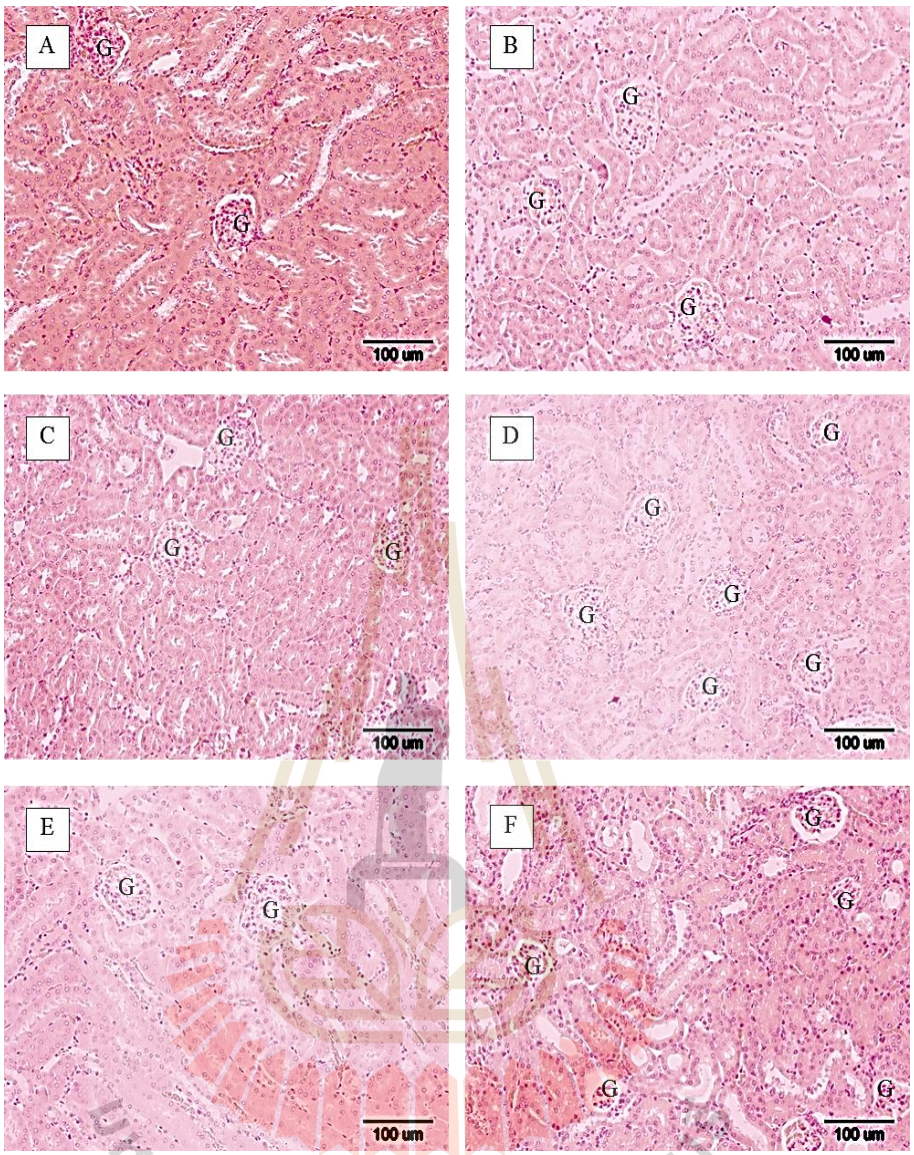

Figure 4.14 Photomicrographs of kidney of normal mice and diabetic mice. The kidney histology showed normality of kidney morphology in all experiment groups. A: N+DI, normal control mice receiving sterile water, B: DM+DI, diabetic mice receiving sterile water, C: DM+DMSO, diabetic mice receiving 10% dimethyl sulfoxide (vehicle control), D: DM+EAF, diabetic mice receiving ethyl acetate fraction at 50 mg/kg, E: DM+WF, diabetic mice receiving water fraction at 50 mg/kg, and F: DM+Gli, diabetic mice receiving glibenclamide at 20 mg/kg. G is glomerulus of kidney. Hematoxylin and eosin staining (200X).

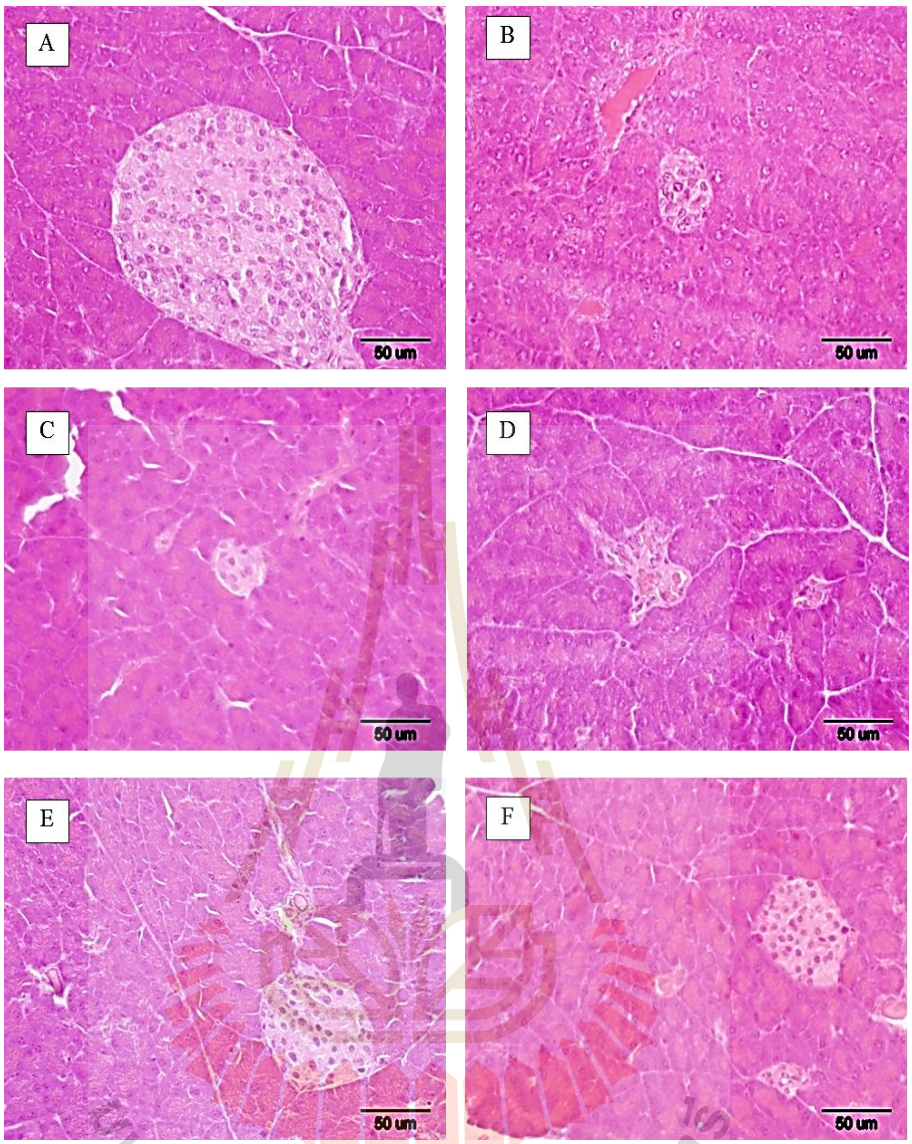

Figure 4.15 Photomicrographs of pancreas of normal mice and diabetic mice. The pancreas histology results showed smaller size of islets of Langerhan in all diabetic groups. A: N + DI, normal control mice receiving sterile water, B: DM+DI, diabetic mice receiving sterile water, C: DM+DMSO, diabetic mice receiving 10% dimethyl sulfoxide (vehicle control), D: DM+EAF, diabetic mice receiving ethyl acetate fraction at 50 mg/kg, E: DM+WF, diabetic mice receiving water fraction at 50 mg/kg, and F: DM+Gli, diabetic mice receiving glibenclamide at 20 mg/kg. Hematoxylin and eosin staining (400X).

4.4 *In vitro* antihyperglycemic action

4.4.1 Inhibitory effect of ethyl acetate and water fractions on α-glucosidase activity

The α-glucosidase inhibition curves of EAF and acarbose are shown in Appendix B. In the case of WF, its α-glucosidase inhibition curve was not included in the report because WF showed no inhibitory effect on α-glucosidase enzyme with even very high concentration (5,000 µg/ml). The IC_{50} value of acarbose, a positive control, and EAF were 226.99 ± 9.58 and 115.33 ± 14.58 µg/ml, respectively.

4.4.2 Stimulatory effects of the extracts on insulin secretion

Only the concentrations of the extracts that showed nontoxic on pancreatic cells were used in this experiment. The concentration response curve of EAF and WF on RIN-m5F cells were evaluated by MTT assay (Appendix C). WF shows nontoxic to pancreas cells at all tested concentrations when compared to control (P<0.05). However, EAF at the concentration higher than 250 µg/ml significantly decreased cell viability (P<0.05). Therefore, the concentration at 100 and 250 µg/ml of EAF and 100, 250 and 500 µg/ml of WF were selected for insulin secretion study.

After treatment, both EAF and WF increased insulin concentration in the medium dose-dependently (Figure 4.14). The vehicle (0.5% DMSO) showed no effect on insulin secretion, whereas glibenclamide (positive control) significantly increased insulin concentration in the medium when compared with control (P<0.05). Note that EAF produced stronger insulin stimulatory effect than WF *in vitro*.

4.4.3 Inhibitory effects of the extracts on glucose absorption

Inhibition of intestinal glucose absorption by EAF, WF and NaF were examined by everted intestinal sacs method. As presented in Table 4.9, glucose concentrations inside the sacs incubated with the fractions and NaF (positive control) significantly decreased when compared to untreated control (P<0.05). The optimal concentration of EAF and WF to inhibit glucose absorption were 2.5 mg/ml which produced 47.24 ± 3.58 % and 66.55 ± 13.03 % inhibition, respectively. The inhibitory effects of these extracts of *W. coagulans* fruits were comparable to 0.2 M NaF (47.12 ± 3.64%).

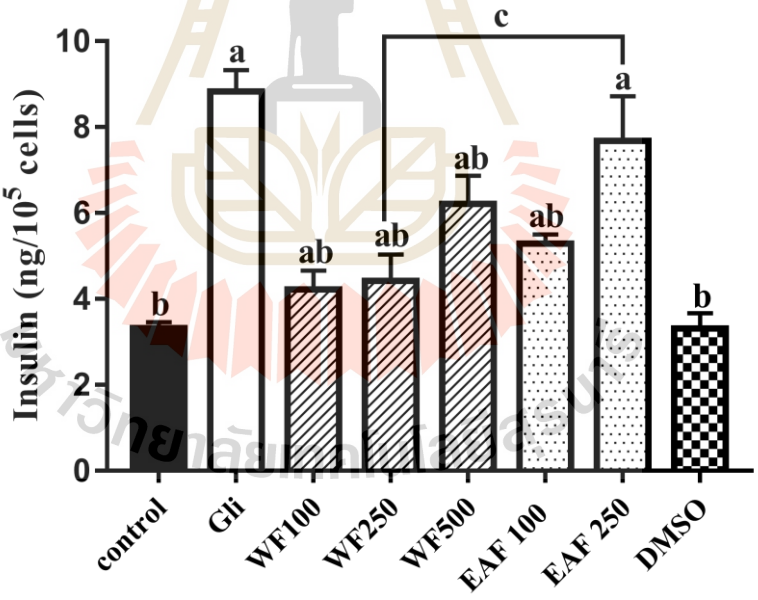

Figure 4.16 Effects of ethyl acetate and water fractions on insulin secretion. Values are expressed as mean ± SEM (n=3). [a]P<0.05; statistically significant difference from control. [b]P<0.05; statistically significant difference from glibenclamide. [c]P<0.05; statistically significant difference from water fraction at the same concentration.

Table 4.9 Inhibitory effects of ethyl acetate and water fractions on glucose absorption.

Treatment	Glucose concentration inside the sacs (mg/dl)	%inhibition
Control	260.46 ± 7.26	0.00 ± 2.79
EAF 0.1 mg/ml	192.07 ± 22.66[a]	26.26 ± 8.70[a]
EAF 0.25 mg/ml	137.41 ± 5.41[a]	47.24 ± 2.08[ab]
EAF 0.5 mg/ml	181.76 ± 15.46[a]	30.22 ± 5.93[a]
WF 0.1 mg/ml	185.20 ± 14.10[a]	28.90 ± 5.41[a]
WF 2.5 mg/ml	87.13 ± 19.60[a]	66.55 ± 7.52[a]
WF 0.5 mg/ml	193.94 ± 18.19[a]	25.54 ± 6.98[a]
NaF 0.2 M	137.73 ± 5.47[a]	47.12 ± 2.10[a]
1.25% DMSO	262.02 ± 1.53	0.00 ± 0.72

Values are expressed as mean ± SEM (n=3). [a]$P<0.05$; statistically significant difference from control. [b]$P<0.05$; statistically significant difference from water fraction at the same concentration.

4.5 Intestinal absorption of the extracts in Caco-2 monolayer model

The doses of the fractions used in this experiment were based on cell viability data. The survival rates of Caco-2 cells treated with EAF and WF at concentration 0-10,000 μg/ml for 4 h are exhibited in Appendix D. The highest concentrations that showed no toxicity to Caco-2 cells were 100 μg/ml and 5,000 μg/ml for EAF and WF, respectively.

After seeding Caco-2 cells to the insert, the monolayer integrity was evaluated by transepithelial electrical resistance (TEER) value and Lucifer yellow (LY) assay (shown in Appendix E). TEER values of the monolayer developed in this study increased steadily over time and was above 600 Ωcm^2 on day 21. % LY rejection of monolayer show higher than 99% in both of pre-test and post-test of experiment.

The absorbability of EAF and WF through Caco-2 monolayer was present in Figures 4.15-4.16 and summarized in Tables 4.10-4.11. The EAF showed 9 peaks in the total ion chromatograms at R_t of 0.2, 1.5, 1.7, 1.9, 26.8, 30.5, 34.2, 34.5 and 35 with the corresponding mass spectrum (m/z) at 226, 234, 261, 239, 471, 453, 376, 453 and 493. While, the numbers of peaks observed in the total ion chromatograms of WF were 13 at R_t of 0.2, 1.5, 1.5, 1.7, 2, 2.3, 26.0, 26.8, 30.4, 33.8, 34.2, 34.5 and 35.0. The mass spectrum of WF showed fragment ions at m/z of 226, 177, 262, 261, 277, 261, 243, 471, 493, 333, 376, 453 and 493. This result indicated that there were three major compounds from both fraction including Coagulin C ($C_{28}H_{36}O_5$, 453), 17β-Hydroxywithanolide K ($C_{28}H_{38}O_6$, 471) and Withanolide F ($C_{28}H_{38}O_6$, 471) and (C1-C3, respectively) could be absorbed through Caco-2 monolayer.

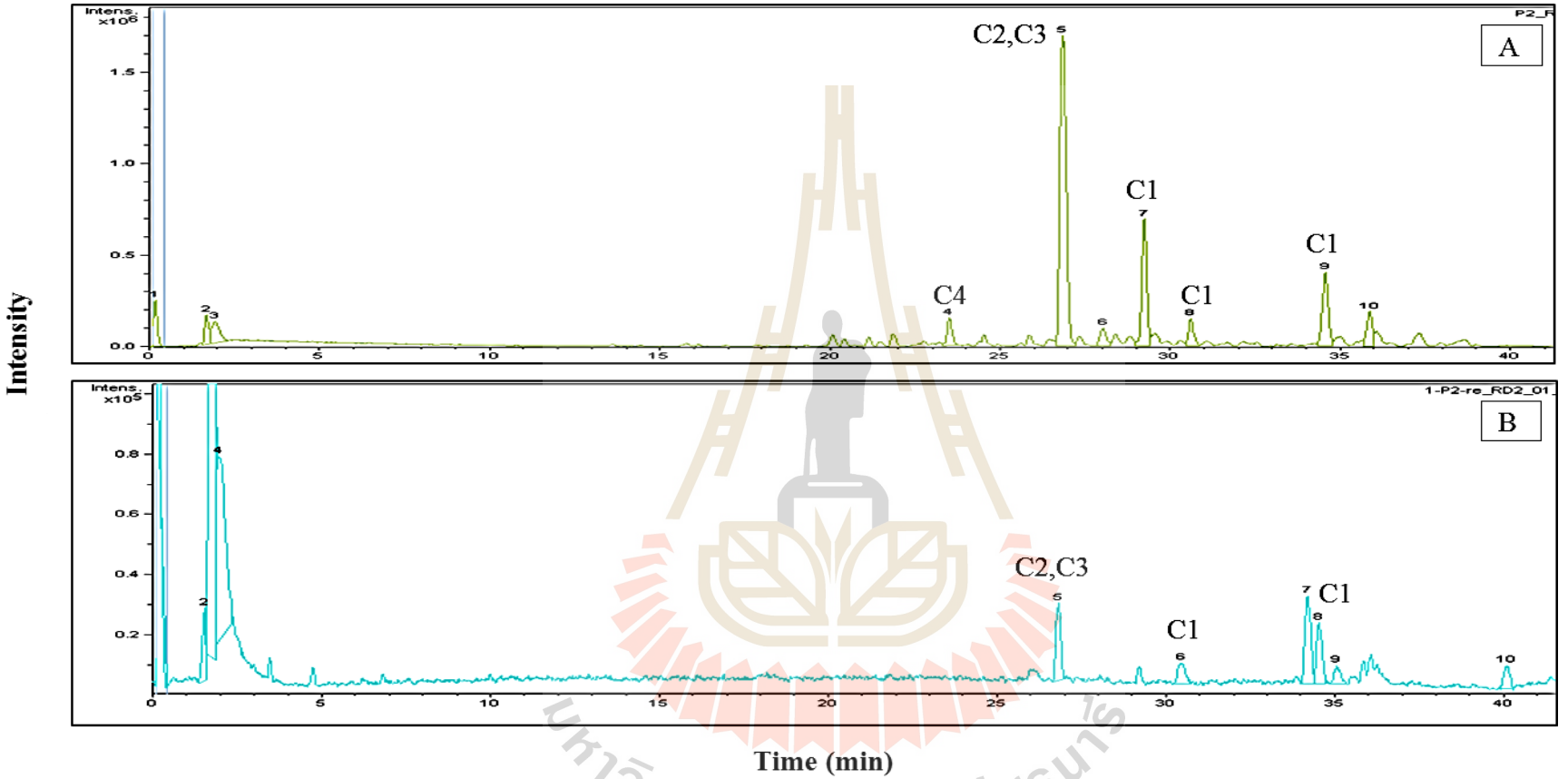

Figure 4.17 Total ion chromatograms of possible withanolides in EAF. Panel A is the HPLC-MS chromatogram of EAF at the ‘concentration of 100 µg/ml and Panel B is that of EAF after passing through Caco-2 monolayer. The possible withanolides consisted of C1-C6, Coagulin C, 17β-Hydroxywithanolide K, Withanolide F, Coagulanolide, Coagulin L and Coagulin Q, respectively.

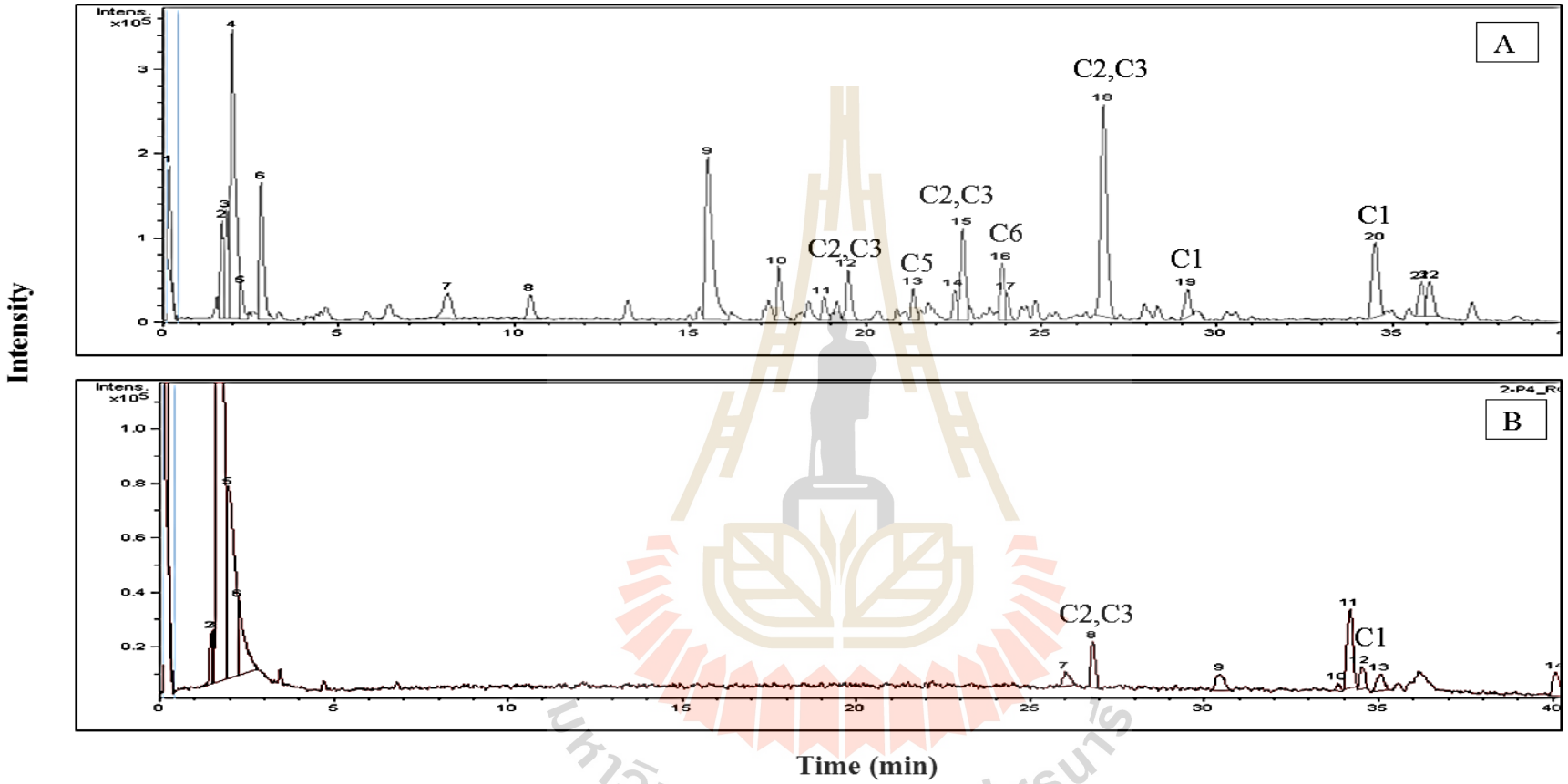

Figure 4.18 HPLC-MS chromatograms and predicted withanolides of WF. Panels A and B are the chromatogram of WF control (5,000 µg/ml) and WF after passing Caco-2 monolayer. The predicted withanolides consisted of C1-C6, Coagulin C, 17β-Hydroxywithanolide K, Withanolide F, Coagulanolide, Coagulin L and Coagulin Q, respectively.

Table 4.10 The mass spectrum (m/z) of EAF control and EAF after passing Caco-2 monolayer.

EAF control					
Peak	**R_t [min]**	**Area**	**m/z**	**Structure**	**Possible Withanolide**
1	0.2	1672667	226.9514	-	-
2	1.7	1405000	261.0884	-	-
3	1.9	1890195	239.1064	-	-
4	23.5	1464248	487.2678	$C_{28}H_{38}O_7$	Coagulanolide
5	26.8	21835688	471.2760	$C_{28}H_{38}O_6$	17β-Hydroxywithanolide K, Withanolide F
6	28	1263712	469.2595	-	-
7	29.2	7264636	453.2642	$C_{28}H_{36}O_5$	Coagulin C
8	30.6	1557142	453.2642	$C_{28}H_{36}O_5$	Coagulin C
9	34.5	4767312	453.2647	$C_{28}H_{36}O_5$	Coagulin C
10	35.8	2161047	493.2565	-	-

EAF after passing Caco-2 monolayer					
Peak	**RT [min]**	**Area**	**m/z**	**Structure**	**Possible Withanolide**
1	0.2	746642	226.9515	-	-
2	1.5	161325	234.9612	-	-
3	1.7	2364087	261.0883	-	-
4	1.9	1070131	239.1064	-	-
5	26.8	249926	471.2732	$C_{28}H_{38}O_6$	17β-Hydroxywithanolide K, Withanolide F
6	30.5	106322	453.2621	$C_{28}H_{36}O_5$	Coagulin C
7	34.2	354143	376.2601	-	-
8	34.5	223068	453.2633	$C_{28}H_{36}O_5$	Coagulin C
9	35	76199	493.2549	-	-

Table 4.11 The mass spectrum (m/z) of WF control and WF passing Caco-2 monolayer model analyzed by HPLC-MS.

WF control					
Peak	**R_t [min]**	**Area**	**m/z**	**Structure**	**Possible Withanolide**
1	0.2	602080	226.9514	-	-
2	1.7	798527	261.0879	-	-
3	1.8	798395	262.1309	-	-
4	2	3419482	215.0163	-	-
5	2.2	214920	276.1448	-	-
6	2.8	1354953	186.0919	-	-
7	8.1	474173	369.1176	-	-
8	10.4	307243	474.2592	-	-
9	15.5	2720124	1199.0602	-	-
10	17.5	557470	717.3950	-	-
11	18.8	241246	608.2890	-	-
12	19.5	591787	471.2734	$C_{28}H_{38}O_6$	17β-Hydroxywithanolide K, Withanolide F
13	21.3	321887	633.3285	$C_{34}H_{49}O_{11}$	Coagulin L
14	22.5	297922	617.3317	-	-
15	22.7	978357	471.2747	$C_{28}H_{38}O_6$	17β-Hydroxywithanolide K, Withanolide F
16	23.9	572340	621.3637	$C_{34}H_{52}O_{10}$	Coagulin Q
17	24	204895	617.3318	-	-
18	26.8	3139160	471.2750	$C_{28}H_{38}O_6$	17β-Hydroxywithanolide K, Withanolide F
19	29.1	349110	453.2636	$C_{28}H_{36}O_5$	Coagulin C
20	34.5	1147975	453.2636	$C_{28}H_{36}O_5$	Coagulin C
21	35.8	422556	493.2570	-	-
22	36	502023	477.2603	-	-

Table 4.11 The mass spectrum (m/z) of WF control and WF passing Caco-2 monolayer model analyzed by HPLC-MS (Continued).

WF after passing Caco-2 monolayer					
Peak	**R_t [min]**	**Area**	**m/z**	**Structure**	**Possible Withanolide**
1	0.2	640455	226.9514	-	-
2	1.5	84711	177.0073	-	-
3	1.5	67738	262.9925	-	-
4	1.7	3108798	261.0882	-	-
5	2	1010689	277.0616	-	-
6	2.3	337459	261.088	-	-
7	26	32830	243.1447	-	-
8	26.8	161010	471.2734	$C_{28}H_{38}O_6$	17β-Hydroxywithanolide K, Withanolide F
9	30.4	103076	493.2572	-	-
10	33.8	22460	333.1671	-	-
11	34.2	345536	376.3596	-	-
12	34.5	81875	453.2636	$C_{28}H_{36}O_5$	Coagulin C
13	35	92115	493.2554	-	-

4.6 Antihyperglycemic activity in alloxan-induced diabetic mice of water fraction-loaded nanocarriers

4.6.1 Effect of water fraction-loaded nanocarriers on fasting blood- glucose levels

Blood glucose levels of all treated groups were shown in Figure 4.17A. At the beginning of experiment, the blood glucose levels in all diabetic groups were significantly higher than normal control group ($P<0.05$). After receiving the treatments for 5 days, only DM mice in glibenclamide group showed a significant decrease in fasting blood glucose when compared to diabetic control ($P<0.05$). Diabetic mice treated with Chnp+SS+WF showed tendency to lower blood glucose level, whereas Chnp+WF and Chnp+RS+WF did not exhibit any decrease in blood sugar. Therefore, Chnp+SS+WF was used for studying the prolonged effect in the next experiment.

4.6.2 Prolonged effect of water fraction-loaded Chitosan nanoparticles coated with retrograded soluble on fasting blood glucose levels

Similar to the result observed in Figure 4.17A, after DM mice receiving treatment for 5 day, Chnp+SS+WF significantly lowered the FBG values compared to diabetic control group ($P<0.05$). Interestingly, even after five days of treatment withdrawal, the animals in the nanocarrier-treated diabetic mice showed a significant decrease in FBG compared to untreated group as seen in Figure 4.17b, indicating the ability of the delivery system to prolong the release of water fraction over an extended period of time.

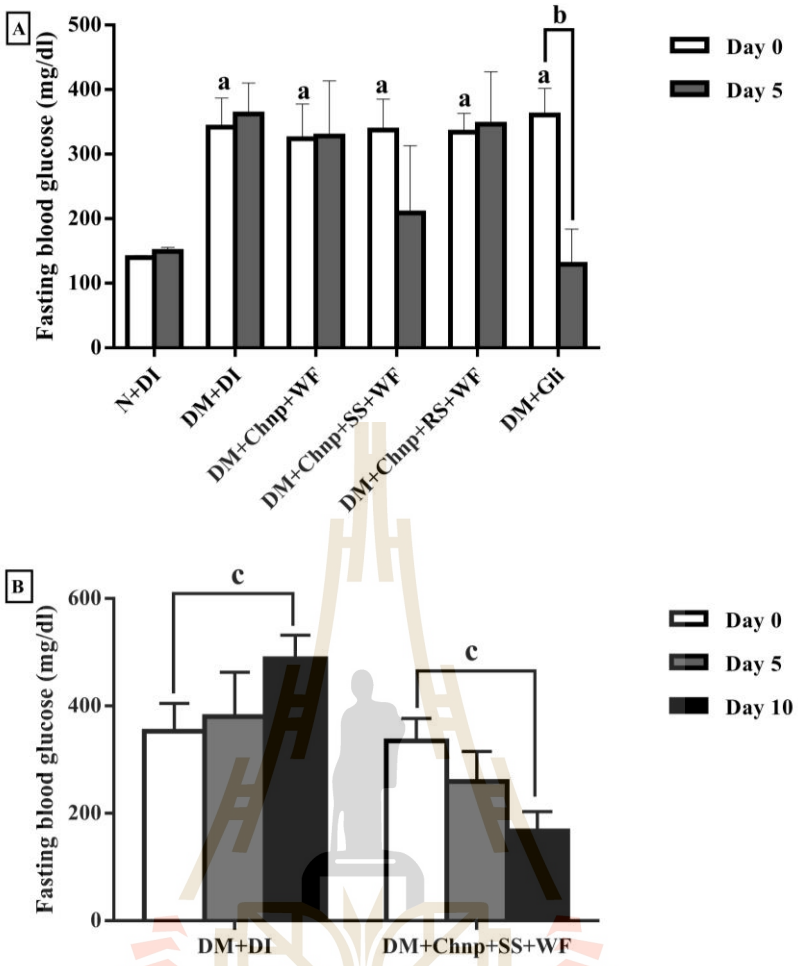

Figure 4.19 Effects of water fraction-loaded nanocarriers on fasting blood glucose in DM mice. Panels A is the antihyperglycemic effects of nanocarriers. DM mice after receiving glibenclamide showed a significant decrease in blood sugar level. Chnp+SS +WF, but not Chnp+WF, and Chnp+RS+WF, had a trend to lower fasting blood sugar. Panels B is a prolonged effect of Chnp+SS+WF on DM mice after drug termination for 5 days. Values are expressed as mean ± SEM (n=3-4). $^{a}P<0.05$; compared to normal control analyzed by one-way ANOVA, $^{b}P<0.05$; compared to the initial level of the same treatment analyzed by paired t-test and $^{c}P<0.05$; compared to blood glucose at day 0 of the same treatment analyzed by one-way ANOVA repeated measures followed by SNK.

CHAPTER V

DISCUSSION AND CONCLUSION

Nowadays, the technology brings about the knowledge and understanding in human diseases, especially diabetes mellitus. Many risk factors leading to diabetes disease have been reported (Dendup, Feng, Clingan, and Astell, 2018). The prevalence of this disease for all age groups has been predicted to be double in 2020 (Shaw, Sicree, and Zimmet, 2010). Diabetes mellitus is not only a major public health problem worldwide but also causes 5% of all deaths globally each year (Joshi and Shrestha, 2010). Eventually, the patients with diabetes mellitus mostly die from various complications for example cardiovascular diseases, hypertension and nephropathy (American Diabetes Association, 2012; Schlienger, 2013). These complications can develop whenever normal blood glucose levels cannot be controlled for a long time.

Insulin, insulin secretagogues, dipeptidyl peptidase IV (DPP IV) inhibitors, glucagon-like peptide-1 (GLP-1), insulin sensitizers, α-glucosidase inhibitors and sodium-glucose co-transporter-2 (SGLT-2) drugs are the hyperglycemia drugs and used to prevent the complications, save life, alleviate symptoms and increase longevity (Bastaki, 2005; Chaudhury et al., 2017). However, these synthetic drugs show some serious side effects such as hypoglycemia, kidney complication, diarrhea, liver complication and urinary tract infection (Bastaki, 2005). Therefore, the natural products from plants are searched as alternative medicines for diabetes mellitus

treatment (Gurjeet and Gloria, 2010; Wang et al., 2010) because they have been accepted to cause fewer side effects than synthetic chemicals (Blasa, Gennari, Angelino, and Ninfali, 2010; Wang et al., 2010). Moreover, they are not expensive and available in most areas (Gaddipati et al., 2004; Gautam et al., 2009; Thakur, Chauhan, Bhargava, and Dixit, 2009; Ven Murthy, Ranjekar, Ramassamy, and Deshpande, 2010).

Withania coagulans commonly known as Indian cheese maker, vegetable pennet or vegetable paneer. It is a traditional medicinal plant that has been used in Indian Ayurvedic and indigenous medicine for more than 3,000 years (Gupta, 2012; Mishra et al., 2013). Many parts of *W. coagulans* are used in the prevention and treatment of various diseases including diabetic mellitus. The antidiabetic property of the aqueous and alcoholic extracts of *W. coagulans* have been reported in several *in vivo* models including normal rat, streptozotocin-, alloxan- and poloxamer-induced diabetic rats. In contrast to these previous studies, crude extract was not included in this study. In general, crude extracts contain many compounds and are difficult to identify the active ingredients that are responsible for their pharmacological actions. Moreover, only α-glucosidase inhibitory activity of *W. coagulans* extract has been demonstrated (Agrawal et al., 2016). So, it is worth evaluating more possible mechanisms of action which are account for the antidiabetic effect of *W. coagulans*.

In the present study, water (WF) and ethyl acetate (EAF) fractions of *W. coagulans* fruit were provided from Associate Professor Dr. Loo Say Chye Joachim's Laboratory. WF was water soluble, while EAF needed to be dissolved in dimethyl sulfoxide (DMSO) due to its hydrophobic property. However, it is worth noting that DMSO at all concentrations used to improve the solubility of EAF was tested and it appeared to have no effect in all experiments.

In the previous phytochemicals studies, carbohydrates, saponin, flavonoids, glycoside, steroids and oil were presented in both of methanolic and hydro-alcoholic extracts of *W. coagulans* fruits (Mathur, Agrawal, and Shrivastava, 2013; Shendkar, Chaudhari, and Shendkar, 2014). Moreover, withanolides have been isolated from the whole plant of *W. coagulans*. Thus, this group of major compounds are proposed to be responsible for preventing disease and promoting health. In the present study, firstly the constituents of the extracts were examined by HPLC-MS. As seen in Figure 4.1, fewer components were found in WF compared to EAF. At least two peaks (as m/z 471 and 453) appeared in chromatograms of both fractions. Based on available library data, the peak of m/z at 471 could be 17β-Hydroxywithanolide K ($C_{28}H_{38}O_6$) or withanolide F ($C_{28}H_{38}O_6$), whereas it is likely that the peak of m/z at 453 was coagulin C ($C_{28}H_{36}O_5$). Moreover, the data showed that coagulin L ($C_{34}H_{50}O_{12}$, 633) and coagulin Q ($C_{34}H_{49}O_{10}$, 621) was present only in WF, while the peak of coagulanolide ($C_{28}H_{38}O_7$, 487) appeared only in EAF. These compounds are derivatives of withanolides which were reported by a previous study of *W. coagulans* (Maurya et al., 2010).

The toxicity studies of the extracts were conducted in both *in vitro* and *in vivo* experiments. First, hepatic toxicity of the fractions was tested in HepG2 cells. Since liver plays many essential roles in maintaining normal physiology and it is the first organ encounter of meal, toxicants and drugs, liver functions can be adversely affected by their acute or chronic exposure (Klaassen, Amdur, and Doull, 2007). Therefore, the liver is one of the primary organs in drug and chemical safety evaluation. The cytotoxicity results showed that WF had less toxicity to HepG2 cells than EAF. After treated with the WF at the concentrations up to 5,000 μg/ml for 24 h. In contrast, after exposure of EAF at the concentrations higher than 20 μg/ml, cell death increased

significantly. Next, *in vivo* toxicity of the fractions was accessed via sub-chronic toxicity examination in mice at dose 50 mg/kg for 10 days. Time and dose of the fractions used in this study were based on the previous study as shown in Table 2.3 (Maurya, Singh, and Srivastava, 2008) and preliminary data. The toxic effects of the fractions on liver, kidneys and pancreas were mainly focused in this experiment. The administration of the fractions at dose 50 mg/kg for 10 days did not induced mortality, signs of morbidity, and any significant changes in body weight, organ tissues and biochemical parameters (as shown in Tables 4.3-4.5 and Figures 4.6-4.8). These indicated that EAF and WF did not induce liver, kidney and pancreas toxicities in normal mice. Moreover, the result of blood glucose level implied that EAF and WF not produced hypoglycemia which is an important side effect of oral hyperglycemia drugs (Bastaki, 2005).

Antidiabetic activities of both fractions were evaluated in both of normal and diabetic mice. First, acute hypoglycemia effect of the extracts was investigated using an oral glucose tolerant test (OGTT). OGTT is a diagnostic method for diabetic screening (Phillips, 2012). After normal mice receiving the treatment and oral glucose, blood sugar levels decreased subsequently over the time in all groups as shown in Figure 4.9. When the AUC index is considered, the result indicated that WF had significantly improved glucose tolerance in normal mice, similar to the insulin secretagogue glibenclamide, a positive control (Chaudhury et al., 2017).

Antihyperglycemia activities of the fractions were determined in diabetic mice as well. Diabetic mice were induced by intraperitoneal alloxan injection at the dose 120 mg/kg. This concentration was based on preliminary experiment and a previous report (Radenkovic et al., 2016). Alloxan is diabetogenic chemical agent that is widely used

to induce diabetes in animal experiments. Alloxan cannot directly penetrate to the lipid bilayer of the plasma membrane of pancreas cell, but enter the cells via GLUT2 glucose transporter (Elsner, Tiedge, Guldbakke, Munday, and Lenzen, 2002) because its chemical structure is similar to glucose. After penetrating to beta cells, alloxan induce diabetes by two independent mechanisms, glucokinase inhibition and reactive oxygen species generation (Lenzen, 2008). The death of the beta cells leads to the decreasing of insulin level and increasing of blood glucose level (hyperglycemia) in animal models. Therefore, diabetic mice showed high blood glucose level and had smaller area of islets of Langerhans than normal control. These symptoms are characteristics of diabetes disease which inducing by alloxan. Moreover, all of diabetic mice presented body weight loss because insulin cannot function efficiently, and the glucose consequently cannot be used as a primary source of energy. Therefore, the body shifts to use fat and protein as an energy source (American Diabetes Association, 2012). The data in Table 4.6 showed that the administration of EAF and WF for 10 days reduced blood glucose levels in alloxan-induced diabetic mice. EAF showed significant decrease blood glucose level at day 5, but not at day 10. In contrast, blood glucose level of diabetic mice treated with WF continuously declined and significantly decreased after receiving WF at days 5 and 10.

Since the previous report has been proposed that the antidiabetic activity of the *W. c*oagulans extract is probably caused by its antioxidant activity and α-glucosidase inhibitory activity (Agrawal et al., 2016; Hemalatha et al., 2004). More possible mechanisms underlying the antidiabetic activity, including stimulation of insulin secretion and inhibitory effect on glucose absorption, were elucidated in this study. The α-glucosidase enzyme has property in the breakdown of carbohydrates into

monosaccharide before absorption, therefore the inhibition on intestinal α-glucosidase delays the digestion of carbohydrates and reduces the rate of glucose absorption, which lowering blood glucose levels after meal (Clissold and Edwards, 1988). Small intestine plays a role in absorption of nutrition such as glucose, amino acids, minerals, and nucleotides (Collins and Bhimji, 2017). Therefore, inhibition of glucose absorption at jejunum is one way to decrease blood glucose level in diabetic patients. The results in Figure 4.14 and Table 4.9 indicated that both WF and EAF possessed insulin secretion stimulatory effect and glucose absorption inhibitory activity, respectively. Interestingly, α-glucosidase inhibitory activity presented only in EAF as seen in Appendix B. There was one interesting point from pancreas histology examination group. It was revealed that the areas of islets of Langerhan in WF group were bigger than that of EAF and diabetic control group (Figure 4.14). This probably could be the result of antioxidant activity of the WF (Hemalatha et al., 2004).

Generally, alternative medicines from natural plants are administered by oral route. However, not all ingredients in the plant extracts can be absorbed by gastrointestinal tract. The absorption property of compounds shows direct correlation with their therapeutic efficacy. Therefore, the absorption properties of both fractions were evaluated. The absorbability of EAF and WF through Caco-2 monolayer was presented in Figures 4.15-4.16. The results indicated that there were two major compounds from both fractions including Coagulin C ($C_{28}H_{36}O_5$, 453) and 17β-Hydroxywithanolide K ($C_{28}H_{38}O_6$, 471) or Withnolide F ($C_{28}H_{38}O_6$, 471) which corresponding to peaks C1-C3, respectively could be absorbed through Caco-2 monolayer.

Due to the constituent analysis of the absorbed compounds in Caco-2 monolayer model (Figures 4.15-4.16) and insulin secretion stimulatory activity of both fractions,

it was suggested that 17β-Hydroxywithanolide K, Withanolide F and Coagulin C may be responsible for the stimulation of insulin secretion of WF and EAF because before reaching pancreatic β-cells, chemicals must be absorbed through gastrointestinal tract after oral administration. These compounds have been previously reported to process antidiabetic activity (Maurya, Singh, and Srivastava, 2008).

Since WF showed no α-glucosidase inhibitory activity, it is suggested that the chemical components presented in WF, including 17β-Hydroxywithanolide K, Withanolide F and Coagulin C, may not be the active ingredients that responsible for this activity. In the case of glucose absorption, the results from OGTT demonstrated that blood glucose peak of WF-treated group at 30 min was lower (but not significant) than that of EAF-treated group in both normal and alloxan-induced diabetic mice. Along with the stronger inhibitory effect of WF compared to EAF shown in Table 4.9, it is likely that the chemical compositions of WF that were not absorbed through Caco-2 monolayer and not presented in EAF were responsible for the glucose absorption inhibition of WF, impeding the initial glucose elevation in OGTT. However, further investigation to confirm the active compounds of *W. coagulans* is needed.

Depend on the safety data and effectiveness found in this study, the water fraction of *W. coagulans* fruits which appeared more effective and less toxic effect was chosen for developing nanocarriers to improve its oral bioavailability and duration of action. Two types of targeted delivery nanocarriers, Chnp+SS and Chnp+RS, which were provided by Dr. Loo Say Chye Joachim's Laboratory were tested for its efficiency of antidiabetic activity in diabetic animal model. The results showed that Chnp+SS+WF had more potential to decrease fasting blood glucose compared to Chnp+WF and Chnp+RS+WF. These results suggested that Chnp+SS was a better drug delivery

system developed for WF of *W. coagulans*. The explanation would be because the soluble sugar coating in Chnp+SS formulation provided functional protection of substances in gastrointestinal tract and selectively degraded in small intestine and improved intestinal absorption (Sampathkumar and Loo, 2018). Therefore, the prolonged effect of Chnp+SS+WF was further investigated. As seen in Figure 4.17b, after five days of treatment withdrawal, the nanocarrier-treated diabetic mice showed a significant decrease in blood glucose level, indicating the ability of the delivery system to prolong the release of water fraction over an extended period of time. In addition, the result also proves that the Chnp+SS+WF delivery system not only delays premature release of the drug but also enables the extract to be absorbed systemically to exert an antidiabetic effect.

In conclusion, the present study has demonstrated that there were two major compositions found in both EAF and WF by HPLC-MS at m/z 471 and 453, which could be 17β-Hydroxywithanolide K ($C_{28}H_{38}O_6$) or Withanolide F ($C_{28}H_{38}O_6$) and Coagulin C ($C_{28}H_{36}O_5$), respectively. EAF produced more toxic effects than WF on HepG2 cell viability. However, the sub-chronic toxicity study in normal mice indicated that neither EAF nor WF induced any toxic effect to liver, kidney and pancreas. The antidiabetic activity *in vivo* presented in both fractions of *W. coagulans* fruits, but WF showed more effective than EAF. The obtained data indicated that EAF exerted its antihyperglycemic effects through all three mechanisms of action tested in this study, including insulin secretion stimulatory effect, glucose absorption inhibitory possessed only insulin secretion stimulation and glucose absorption inhibition. It is proposed in the present study that 17β-Hydroxywithanolide K, Withanolide F or Coagulin C could be one of the active compounds that are responsible for the stimulation of insulin

release. Finally, the drug delivery system Chnp+SS+WF, that has been developed by a joint research laboratory from NTU, Singapore, was demonstrated to provide a sustained release of the *W. coagulans* water extract *in vivo*. Therefore, this synthesized nanocarriers may be useful for encapsulating a plant extract which is damaged in gastrointestinal tract and has low bioavailability as drug delivery system.

REFERENCES

REFERENCES

Agrawal, O. P., Jain, S. K., Sharma, P., Ghule, S., Kumar, I., and Zubair, A. (2016). *In-vitro* α-glucosidase and aldose reductase activity and *in-vivo* antidiabetic activity.of.*Withania coagulans*. **Asian Journal of Ethnopharmacology and Medicinal Foods.** 3: 17-21.

Ahmad, R., Fatima, A., Srivastava, A. N., and Khan, M. A. (2017). Evaluation of apoptotic activity of *Withania coagulans* methanolic extract against human breast cancer and vero cell lines. **Journal of Ayurveda and Integrative Medicine.** 8(3): 177-183.

Alam, S. A., Khan, A. H., Sirhindi, G. A., and Khan, S. (2005). Alloxan induced diabetes in rabbits. **Pakistan Journal of Pharmacology.** 22(2: 41-45).

American Diabetes Association. (2012). Diagnosis and classification of diabetes mellitus. **Diabetes Care.** 35(1): 64-71.

American Type Culture Collection. (2017). **HepG2 cells.** [On-line]. Available: http://www.atcc.org/products/all/HB-8065.aspx#characteristics.

American Type Culture Collection. (2017). **Caco-2 cells.** [On-line]. Available: https://www.atcc.org/Products/All/HTB-37.aspx.

American Type Culture Collection. (2017). **RIN-m5F cells.** [On-line]. Available: https://www.atcc.org/Products/All/CRL-11605.aspx#characteristics.

Awortwe, C., Fasinu, P. S., and Rosenkranz, B. (2014). Application of Caco-2 cell line in herb-drug interaction studies: current approaches and challenges.

Journal of Pharmacy and Pharmaceutical Sciences. 17(1): 1-19

Bastaki, S. (2005). Diabetes mellitus and its treatment. **International Journal of Diabetes and Metabolism.** 13: 111-134.

Bharti, S. K., Kumar, A., Sharma, N. K., Krishnan, S., Gupta, A. K., and Padamdeo, S. R. (2012). Antidiabetic effect of aqueous extract of *Withania coagulans* flower in Poloxamer-407 induced type 2 diabetic rats. **Journal of Medicinal Plants Research.** 6(45): 5706-5713.

Blasa, M., Gennari, L., Angelino, D., and Ninfali, P. (2010). **Bioactive Foods in Promoting Health.** San Diego: Academic Press.

Budhiraja, R. D., Garg, K. N., Sudhir, S., and Arora, B. (1986). Protective effect of 3-β-Hydroxy-2,3-dihydrowithanolide F against CCl_4-induced hepatotoxicity. **Planta Medica.** 52(1): 28-29.

Cefalu, W. T. (2006). Animal models of type 2 diabetes: clinical presentation and pathophysiological relevance to the human condition. **Institute for Laboratory Animal Research Journal.** 47(3): 186-198.

Chaudhury, A., Duvoor, C., Reddy Dendi, V. S., Kraleti, S., Chada, A., Ravilla, R., and Mirza, W. (2017). Clinical review of antidiabetic drugs: implications for type 2 diabetes mellitus management. **Frontiers in Endocrinology.** 8(6).

Choi, C. W., Choi, Y. H., Cha, M. R., Yoo, D. S., Kim, Y. S., Yon, G. H., and Ryu, S. Y. (2010). Yeast alpha-glucosidase inhibition by isoflavones from plants of Leguminosae as an in vitro alternative to acarbose. **Journal of Agricultural and Food Chemistry.** 58(18): 9988-9993.

Clissold, S. P., and Edwards, C. (1988). Acarbose. a preliminary review of its pharmacodynamic and pharmacokinetic properties, and therapeutic potential. **Drugs.** 35(3): 214-243.

Collins, J., and Bhimji, S. (2017). **Anatomy, Abdomen, Small Intestine.** [On-line] Available: https://www.ncbi.nlm.nih.gov/books/NBK459366/.

Datta, A., Bagchi, C., Das, S., Mitra, A., Pati, A. D., and Tripathi, S. K. (2013). Antidiabetic and antihyperlipidemic activity of hydroalcoholic extract of *Withania coagulans* Dunal dried fruit in experimental rat models. **Journal of Ayurveda and Integrative Medicine.** 4(2): 99-106.

Dendup, T., Feng, X., Clingan, S., and Astell, B. T. (2018). Environmental risk factors for developing type 2 diabetes mellitus: a systematic review. **International Journal of Environmental Research and Public Health.** 15(1): 78.

Diabetes Mellitus Management. **Frontiers in Endocrinology.** 8(6): 1-12.

Dong, H. Q., Li, M., Zhu, F., Liu, F. L., and Huang, J. B. (2012). Inhibitory potential of trilobatin from *Lithocarpus polystachyus* Rehd against α-glucosidase and α-amylase linked to type 2 diabetes. **Food Chemistry.** 130(2): 261-266.

Dsouza, D., and Lakshmidevi, N. (2015). Models to study *in vitro* antidiabetic activity of plants: a review. **Internationnal Journal of Pharma and Bio Sciences.** 6(3): 732-741.

Elsner, M., Tiedge, M., Guldbakke, B., Munday, R., and Lenzen, S. (2002). Importance of the GLUT2 glucose transporter for pancreatic beta cell toxicity of alloxan. **Diabetologia.** 45(11): 1542-1549.

Exner, C., and Christoph, L. (2016). **Animal Experimentation in Research.** Germany: Deutsche Forschungsgemeinschaft.

Gaddipati, J. P., Rajeshkumar, N. V., Thangapazham, R. L., Sharma, A., Warren, J., Mog, S. R., and Maheshwari, R. K. (2004). Protective effect of a polyherbal preparation, *Brahma rasayana* against tumor growth and lung metastasis in rat prostate model system. **Journal of Experimental Therapeutics and Oncology.** 4(3): 203-212.

Gautam, M., Saha, S., Bani, S., Kaul, A., Mishra, S., Patil, D., and Patwardhan, B. (2009). Immunomodulatory activity of *Asparagus racemosus* on systemic Th1/Th2 immunity: implications for immunoadjuvant potential. **Journal of Ethnopharmacology.** 121(2): 241-247.

Gupta, C. P. (2012). *Withana Coagulans* - an overview. **International Journal of Pharmaceutical Sciences Review and Research.** 12(2).

Gurjeet, B. S., and Gloria, Y. (2010). Complementary and alternative medicine therapies for diabetes: a clinical review. **Clinical Diabetes.** 28: 147-155.

Heikkila, R. E. (1977). The prevention of alloxan-induced diabetes in mice by dimethyl sulfoxide. **European Journal of Pharmacology.** 44(2): 191-193.

Hemalatha, S., Wahi, A., Singh, P., and Chansouria, J. (2004). Hypoglycemic activity of *Withania coagulans* Dunal in streptozotocin induced diabetic rats. **Journal of Ethnopharmacology.** 93(2): 261-264.

Hemalatha, S., Wahi, A. K., Singh, P. N., and Chansouria, J. P. (2006). Hypolipidemic activity of aqueous extract of *Withania coagulans* Dunal in albino rats. **Phytotherapy Research.** 20(7): 614-617.

Hoda, Q., Ahmad, S., Akhtar, M., Najmi, A. K., Pillai, K., and Ahmad, S. J. (2010). Antihyperglycaemic and antihyperlipidaemic effect of poly-constituents, in aqueous and chloroform extracts, of *Withania coagulans* Dunal in experimental

type 2 diabetes mellitus in rats. **Human and Experimental Toxicology.** 29(8): 653-658.

Hubatsch, I., Ragnarsson, E. G., and Artursson, P. (2007). Determination of drug permeability and prediction of drug absorption in Caco-2 monolayers. **Nature Protocols.** 2(9): 2111-2119.

Huanga, C. F., Lei, M., Sunb, L. J., Alic, M., Arfanc, M., Liu, J. W., and Hu, L. H. (2009). Immunosuppressive withanolides from *Withania coagulans*. **Chemistry and Biodiversity.** 6: 1415-1426.

Jaiswal, D., Rai, P. K., and Watal, G. (2009). Antidiabetic effect of *Withania coagulans* in experimental rats. **Indian Journal of Clinical Biochemistry.** 24(1): 88-93.

Jaiswal, D., Rai, P. K., and Watal, G. (2010). Hypoglycemic and antidiabetic effects of *Withania Coagulans* fruit ethanolic extract in normal and streptozotocin-induced diabetic rats. **Journal of Food Biochemistry.** 34(4): 764-778.

Joshi, S. K., and Shrestha, S. (2010). Diabetes mellitus: a review of its associations with different environmental factors. **Kathmandu University Medical Journal.** 8(21): 109-115.

Karthikeyan, M., Balasubramanian, T., and Kumar, P. (2016). *In-vivo* Animal models and *in-vitro* techniques for screening antidiabetic activity. **Journal of Developing Drugs.** 5(2).

Keller, A. C., Ma, J., Kavalier, A., He, K., Brillantes, M. B., and Kennelly, E. J. (2011). Saponins from the traditional medicinal plant *Momordica charantia* stimulate insulin secretion in vitro. **Phytomedicine.** 19(1): 32-37.

Kennedy, S. M., and Masharani, U. (2015). Pancreatic hormones & antidiabetic drugs. In Katzung, B. G., and Trevor, A. J. (Eds.), **Basic & Clinical Pharmacology** (p.997-1007). New York: McGraw-Hill Medical.

Khodabandehloo, H., Zahednasab, H., and Ashrafi, H. A. (2016). Nanocarriers usage for drug delivery in cancer therapy. **Iranian Journal of Cancer Prevention**. 9(2): 3966.

King, A. J. (2012). The use of animal models in diabetes research. **British Journal of Pharmacology.** 166(3): 877-894.

Klaassen, C., Amdur, M., and Doull, J. (2007). **Casarett and Doull's Toxicology: the Basic Science of Poison** (8th ed.). New York: McGraw Hill Profesional.

Krisanapun, C., Peungvicha, P., Temsiririrkkul, R., and Wongkrajang, Y. (2009). Aqueous extract of *Abutilon indicum* Sweet inhibits glucose absorption and stimulates insulin secretion in rodents. **Nutrition Research.** 29(8): 579-587.

Lenzen, S. (2008). The mechanisms of alloxan-and streptozotocin-induced diabetes. **Diabetologia.** 51(2): 216-226.

Liu, L., Guo, L., Zhao, C., Wu, X., Wang, R., and Liu, C. (2015). Characterization of the intestinal absorption of seven flavonoids from the flowers of *Trollius chinensis* using the Caco-2 cell monolayer model. **PLOS ONE**. 10(3): e0119263.

Longnecker, D. (2014). Anatomy and histology of the pancreas. **Pancreapedia: Exocrine Pancreas Knowledge Base.** 1: 1-14.

Machin, R. P., Veleiro, A. S., Nicotra, V. E., Oberti, J. C., and Padron, M. J. (2010). Antiproliferative activity of withanolides against human breast cancer cell lines. **Journal of Natural Products.** 73(5): 966-968.

Martini, F. H., Ober, W. C., Garrison, C. W., Welch, K., and Hutchings, R. T. (2006). **Fundamentals of Anatomy and Physiology** (7th ed.). San Francisco: Dary Fox.

Mathur, D., Agrawal, R. C., and Shrivastava, V. (2013). Phytochemical screening and determination of antioxidant potential of fruits extracts of *Withania coagulans*. **Recent Research in Science and Technology.** 3(11): 26-29.

Maurya, R., Akanksha, and Jayendra. (2010). Chemistry and pharmacology of *Withania coagulans*: an Ayurvedic remedy. **Journal of Pharmacy and Pharmacology.** 62(2): 153-160.

Maurya, R., Singh, A. B., and Srivastava, A. K. (2008). Coagulanolide, a withanolide from *Withania coagulans* fruits and antihyperglycemic activity. **Bioorganic and Medicinal Chemistry Letters.** 18(24): 6534-6537.

Mishra, J., Dash, A. K., Mishra, S. N., and Gupta, A. K. (2013). *Withania coagulans* in treatment of diabetics and some other diseases: a review. **Research Journal of Pharmaceutical Biological and Chemical Sciences.** 4(2): 125-128.

Nirmalan, N., and Nirmalan, M. (2017). Hormonal control of metabolism: regulation of plasma glucose. **Anaesthesia and Intensive Care Medicine.** 18(10): 502-507.

Olokoba, A. B., Obateru, O. A., and Olokoba, L. B. (2012). Type 2 diabetes mellitus: a review of current trends. **Oman Medical Journal.** 27(4): 269-273.

Phillips, P. J. (2012). Oral glucose tolerance testing. **Australian Family Physician.** 41(6): 391-393.

Prasad, S. K., Kumar, R., Patel, D. K., and Hemalatha, S. (2010). Wound healing activity of *Withania coagulans* in streptozotocin-induced diabetic rats. **Pharmaceutical Biology.** 48(12): 1397-1404.

Radenkovic, M., Stojanovic, M., and Prostran, M. (2016). Experimental diabetes induced by alloxan and streptozotocin: the current state of the art. **Journal Journal of Pharmacological and Toxicological Methods.** 78: 13-31.

Raut, N. A., and Gaikwad, N. J. (2006). Antidiabetic activity of hydro-ethanolic extract of *Cyperus rotundus* in alloxan induced diabetes in rats. **Fitoterapia.** 77(7): 585-588.

Sampathkumar, K., and Loo, S. C. J. (2018). Targeted gastrointestinal delivery of nutraceuticals with polysaccharide-based coatings. **Macromolecular Bioscience.** 18(4): e1700363.

Saxena, M., Jyoti, S., Rajeev, N., Dharmendra, S., and Abhishek, G. (2013). Phytochemistry of medicinal plants. **Journal of Phrarmacognosy and Phytochemistry.** 1(6): 168-182.

Schlienger, J. L. (2013). Complications fo diabete type 2. **La Presse Medicale.** 42(5): 839-848.

Shaw, J. E., Sicree, R. A., and Zimmet, P. Z. (2010). Global estimates of the prevalence of diabetes for 2010 and 2030. **Diabetes Research and Clinical Practice.** 87(1): 4-14.

Shendkar, A. K., Chaudhari, S. G., and Shendkar, Y. K. (2014). Analgesic activity of *Withania coagulans* Dunal fruit extracts in experimental animal models. **International Journal of Pharmaceutical Sciences.** 6(2): 602-605.

Shukla, K., Dikshit, P., Shukla, R., and Gambhir, J. K. (2012). The aqueous extract of *Withania coagulans* fruit partially reverses nicotinamide/streptozotocin-induced diabetes mellitus in rats. **Journal of Medicinal Food.** 15(8): 718-725.

Thakur, M., Chauhan, N. S., Bhargava, S., and Dixit, V. K. (2009). A comparative study on aphrodisiac activity of some ayurvedic herbs in male albino rats. **Archives of Sexual Behavior.** 38(6): 1009-1015.

Therasa, S. V., Thirumalai, T., Tamilselvan, N., and David, E. (2014). *In-vivo* and *ex-vivo* inhibition of intestinal glucose uptake: a scope for antihyperglycemia. **Journal of Acute Diseas.** 3(1): 36-40.

Ven, M. R., Ranjekar, P. K., Ramassamy, C., and Deshpande, M. (2010). Scientific basis for the use of Indian ayurvedic medicinal plants in the treatment of neurodegenerative disorders: ashwagandha. **Central Nervous System Agents in Medicinal Chemistry.** 10(3): 238-246.

Wang, L., Zhang, Y., Chen, S., Chen, J., Zhuang, Y., and Chen, J. (2010). Association of metabolic syndrome and IgA nephropathy. **Journal of Clinical Pathology.** 63(8): 697-701.

Yasir, M., Shrivastava, R., Jain, P., and Das, D. (2012). Hypoglycemic and antihyperglycemic effects of different extracts and combinations of *Withania coagulans* Dunal and *Acacia arabica* lamk in normal and alloxan induced diabetic rats. **Pharmacognosy Communications.** 2(2): 61-66.

Yee, S. (1997). *In vitro* permeability across Caco-2 cells (colonic) can predict *in vivo* (small intestinal) absorption in man-fact or myth. **Pharmaceutical Research.** 14(6): 763-766.

Yeo, R., and Sawdon, M. (2013). Hormonal control of metabolism: regulation

of plasma glucose. **Anaesthesia and Intensive Care Medicine.** 14(7): 296-300.

APPENDICES

APPENDIX A

BIOCHEMICAL PARAMETERS OF NORMAL MICE

The biochemical of ICR mice in each age period (http://www.clea-japan.com/en/animals/animal_e/e_06.html).

Jcl:ICR

Age in weeks	Sex	n		GPT U/l	GOT* U/l	ALP U/l	Glu* mg/dl	T.C mg/dl	T.P g/dl	Ca mg/dl	Cl mmol/dl	BUN mg/dl	CRE mg/dl
5	Male	5	Mean	43	115	201	126	142	5.8	10.5	116	30.0	0.53
			SD	6	26	51	23	19	0.3	0.2	2	2.4	0.04
	Female	5	Mean	30	56	179	146	98	6.4	10.9	111	31.8	0.47
			SD	6	9	35	19	18	0.2	0.2	4	3.1	0.06
31	Male	5	Mean	33	49	79	169	84	6.4	9.3	119	28.9	0.31
			SD	7	5	15	23	14	0.3	0.2	2	2.6	0.03
	Female	5	Mean	28	44	72	154	49	6.5	9.6	117	22.9	0.36
			SD	6	5	19	15	13	0.3	0.1	3	7.5	0.06
52	Male	5	Mean	25	42	62	170	80	6.6	9.3	118	30.8	0.30
			SD	5	7	24	34	12	0.3	0.1	1	2.5	0.06
	Female	5	Mean	27	42	69	150	136	6.2	9.4	119	27.6	0.34
			SD	8	4	25	19	93	0.6	0.6	3	7.0	0.03

*Measured in plasma (heparinized)

APPENDIX B

α-GLUCOSIDASE INHIBITORY ACTIVITY

B.1 α-glucocidase inhibitory activity of ethyl acetate fraction

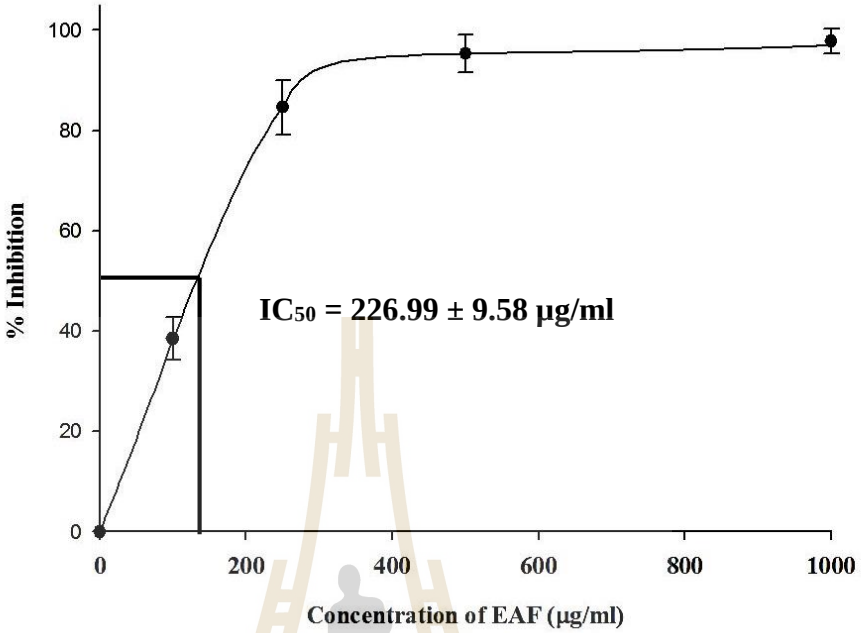

B.2 α-glucocidase inhibitory activity of acarbose

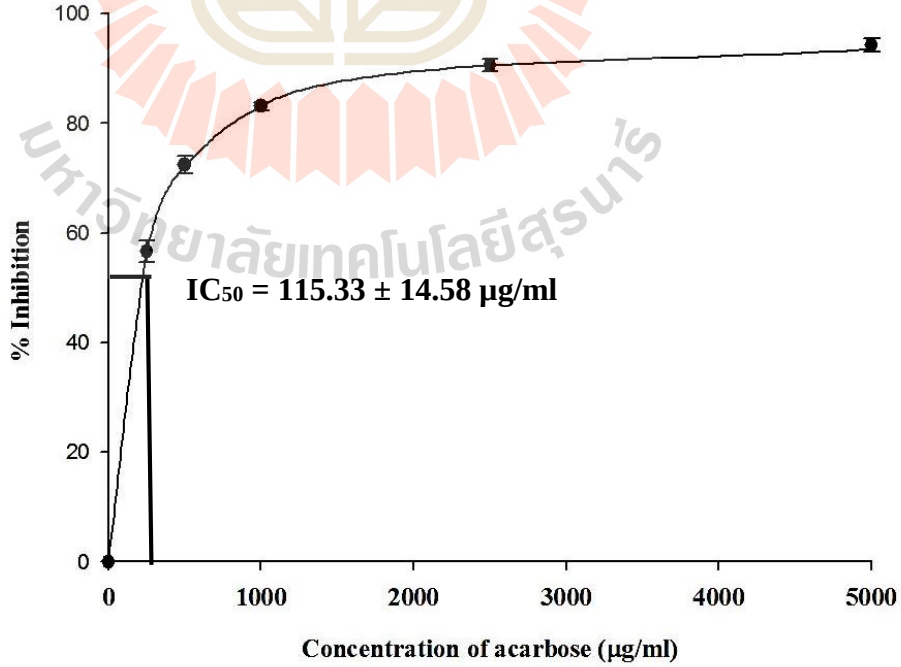

APPENDIX C

TOXICITY OF ETHYL ACETATE AND WATER FRACTIONS ON RINM-5F CELLS FOR INSULIN SECRETION EXPERIMENT

C.1 Toxicity of ethyl acetate fraction on RINm-5F cells

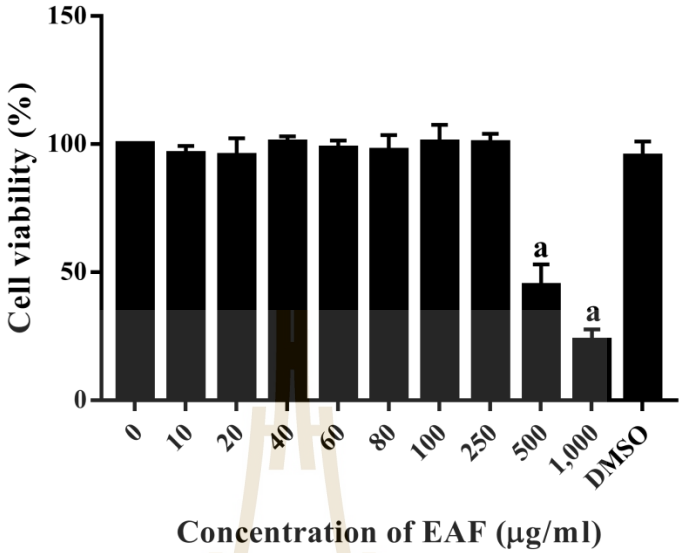

C.2 Toxicity of water fraction on RINm-5F cells

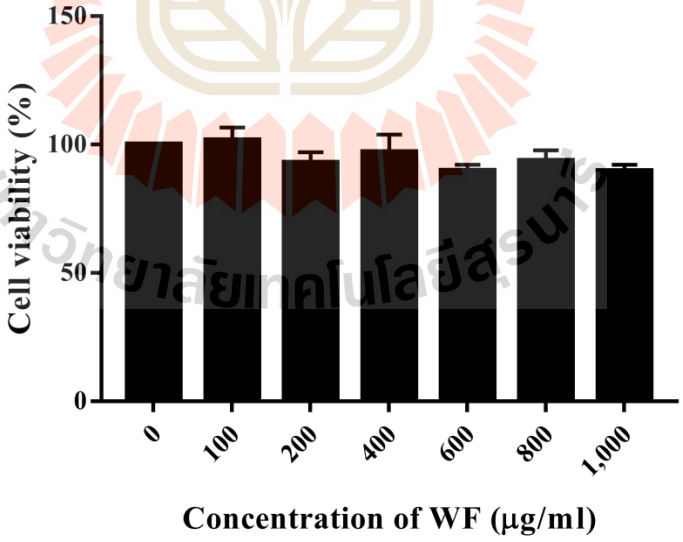

APPENDIX D

TOXICITY OF ETHYL ACETATE AND WATERFRACTIONS ON CACO-2 CELLS FOR INTESTINAL ABSORPTION EXPERIMENT

D.1 Toxicity of ethyl acetate fraction on Caco-2 cells

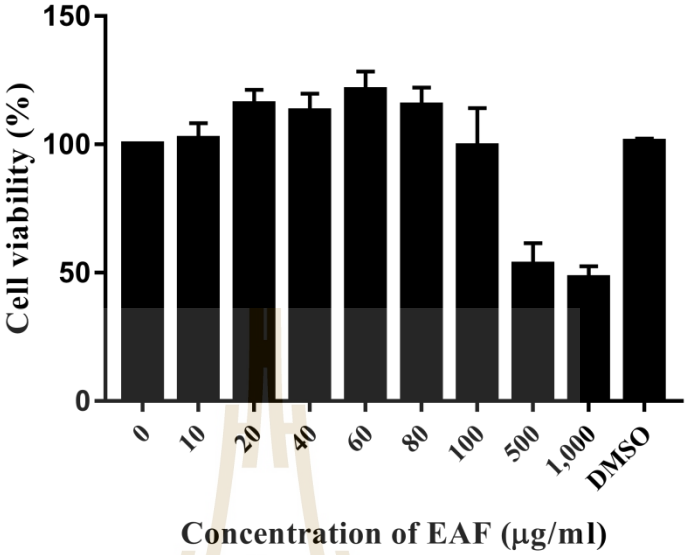

D.2 Toxicity of water fraction on Caco-2 cells

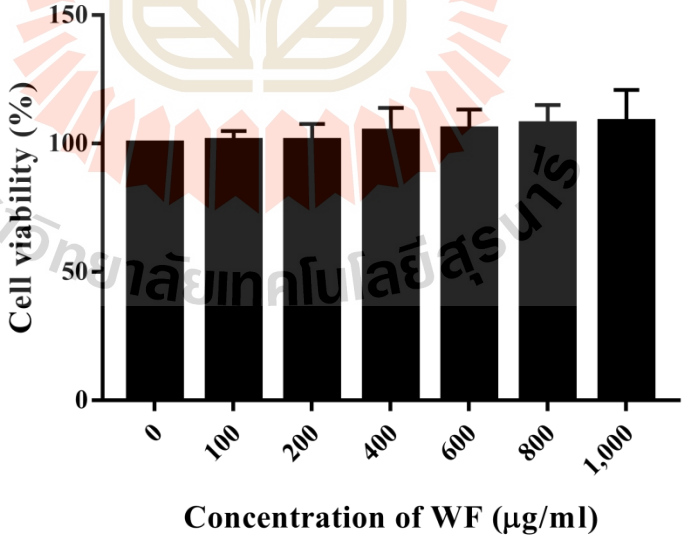

APPENDIX E

TRANSEPITHELIAL ELECTRICAL RESISTANCE (TEER) AND % LUCIFER YELLOW REJECTION VALUES OF CACO-2 MONOLAYER MODEL FOR INTESTINAL ABSORPTION EXPERIMENT

TEER and % lucifer yellow rejection values of Caco-2 monolayer before and after experiments

Insert	Test	TEER value (Ωcm^2)		% Lucifer yellow rejection	
		Before	After	Before	After
1	EAF	1876.97	1705.37	93.63	99.87
2		2508.73	2050.77	99.79	99.88
3		2295.70	1938.93	99.83	99.84
4		2360.60	2050.40	99.72	99.83
5		2293.13	2041.23	99.81	99.84
6	WF	2316.60	1893.47	99.78	99.87
7		2029.50	2087.07	99.85	99.85
8		2000.53	2121.90	99.81	99.82
9		2102.47	1682.63	99.87	99.88
10		2441.63	2255.00	99.85	99.85
Blank		0.00	0.00	84.52	83.46

CURRICULUM VITAE

NAME: Miss Siriporn Riyajan

DATE OF BIRTH: December 29, 1989

PLACE OF BIRTH: Udonthani, Thailand

EDUCATION: Walailak University, 2013, Bachelor of Science Program in Computational Science, Second Class Honors

Suranaree University of Technology, 2015, Master of Science Program in Biomedical Sciences

SCHOLARSHIP: The Science Achievement Scholarship of Thailand (SAST), 2013

PUBLICATIONS:

Riyajan, S., Yentua, W., and Phinchongsakuldit, J. Low cost DNA moleculaer weight marker: primer-directed synthesis from pGEM-T easy vector (2011). **Walailak Journal.** 8(2): 187-92.

Riyajan, S., Yusook, K., Kumkrai, P., and Chudaponges, N. Phytochemical screening and antioxidant activity of hexane, chloroform and aqueous extracts of *Derris reticulata* stem. (2015, March). **Proceeding of the 34th the National Graduate Research Conference. Symposium conducted at the meeting of Khon Kaen University, Thailand.**

Doan, H. V., Riyajan, S., Iyara, R., and Chudapongse, N. (2018). Antidiabetic activity, glucose uptake stimulation and α-glucosidase inhibitory effect of *Chrysophyllum cainito* L. stem bark extract. **BMC Complementary and Alternative Medicine.** 18(267): 1-10.

Sampathkumar, K., Riyajan, S., Tan, C. K., Demokritou, P., Chudapongse, N., Chye, S., & Loo, J. (2019). Small-intestine-specific delivery of antidiabetic extracts from *Withania coagulans* using polysaccharide-based enteric-coated nanoparticles. **ACS Omega.** 4: 12049–12057.